

OASIS

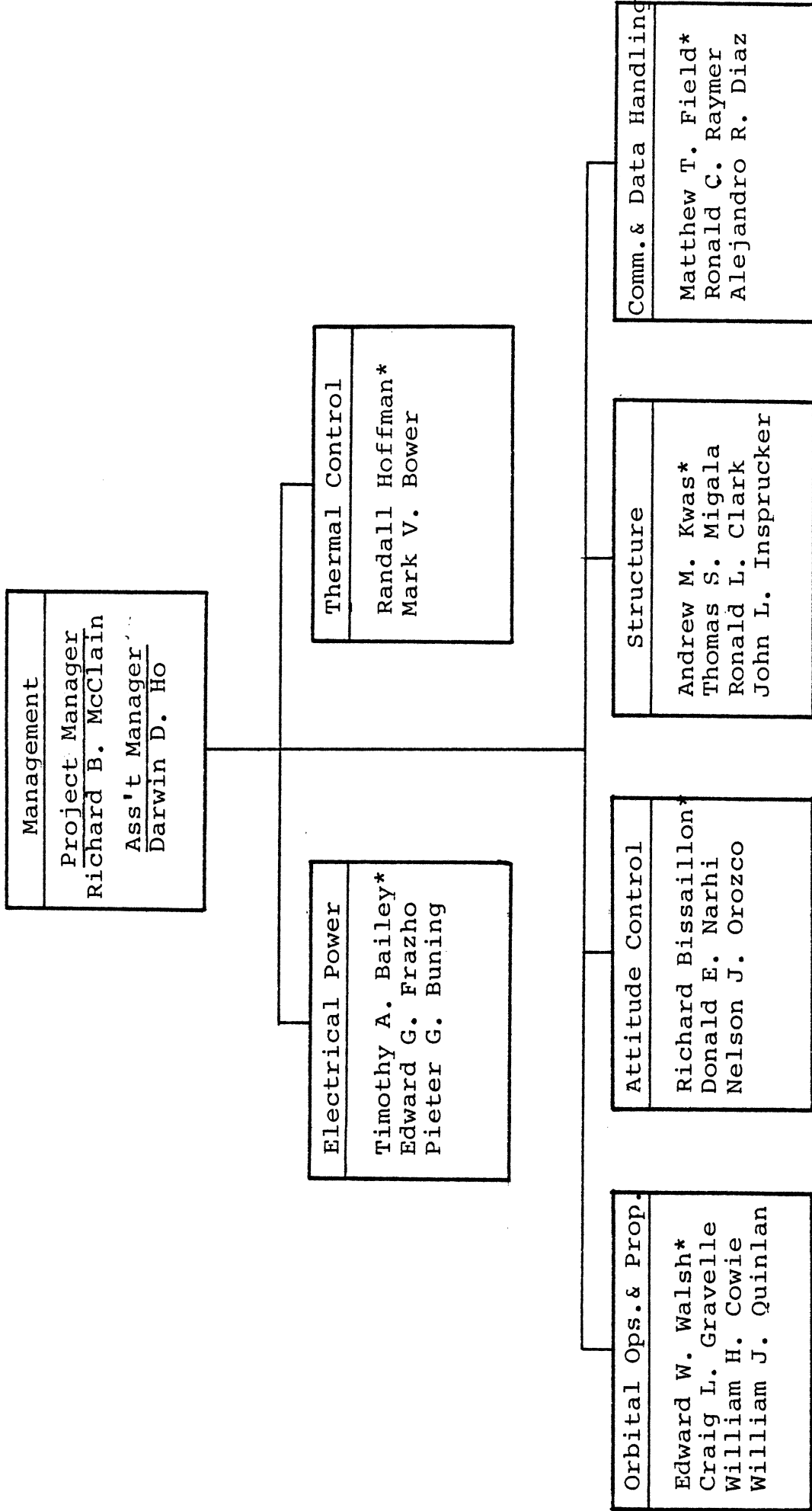
Orbiter Assistance Satellite with Integrated Services

A Student Design Project  
Department of Aerospace Engineering  
The University of Michigan  
Winter Term 1978

Cover drawn by Miss Lynn M. Wegner



# PROJECT PERSONNEL



\*group leader



## FOREWORD

A preliminary design study was undertaken to develop a satellite which has the capability to provide essential services to the Shuttle Orbiter and its payload. The primary services are electric power, cooling, and attitude control. Although it is visualized that the services can also be extended to other free flying payloads the study dealt primarily with interaction with the orbiter.

OASIS, Orbiter Assistance Satellite with Integrated Services, is launched into orbit as a single shuttle payload. Before being left in space certain aspects of its construction are to be carried out in space by astronauts in extra-vehicular activity (EVA). A propulsion and an attitude control system allow OASIS to carry out orbital maneuvers to facilitate rendezvous with future Orbiters it is to serve. Occasionally refuelled propulsion units are to be brought up to maintain this capability. This replacement is also carried out in EVA.

The students of the senior Aerospace System Design course are organized into a management group and several engineering teams, one for each of the major subsystems.

Technical assistance is obtained through cooperation from engineering faculty members as well as in consultation with technical and management staff members in Government and Industry. The approximate 10 weeks' work of each group was integrated into the overall report at hand.

Professor Harm Buning  
April 1978



## TABLE OF CONTENTS

PROJECT PERSONNEL	ii
FOREWORD	iii
Chapter 1 INTRODUCTION	1
1.1 Introduction	1
1.2 Summary & Conclusions	1
1.3 References	1
Chapter 2 MISSION OBJECTIVES, REQUIREMENTS AND BENEFITS	3
2.1 Objectives	3
2.2 Requirements	3
2.3 Benefits	4
2.4 References	5
Chapter 3 POWER	6
3.1 Introduction	6
3.2 Summary and Conclusions	6
3.3 Solar Cells	10
3.4 Physical Characteristics of Solar Cells	13
3.5 Solar Cell Array Design	14
3.6 Battery System	20
3.7 Power Conditioning and Distribution	23
3.8 System Performance	26
3.9 References	30
Chapter 4 THERMAL CONTROL	32
4.1 Introduction	32
4.2 Summary and Conclusions	32
4.3 Discussion	33
4.4 References	39
Chapter 5 PROPULSION	41
5.1 Introduction	41
5.2 Summary	41
5.3 Mission Constraints and Considerations	41
5.4 Design Constraints and Considerations	42
5.5 Component Description of the Propulsion Unit	44
5.6 Performance	49
5.7 Other Systems Considered	52
5.8 References	53

Chapter 6 ORBITAL OPERATIONS	54
6.1 Introduction	54
6.2 Summary and Conclusions	54
6.3 Orbital Operations	54
6.4 References	63
Chapter 7 ATTITUDE CONTROL	64
7.1 Introduction	64
7.2 Summary and Conclusions	64
7.3 Definition of Axis	64
7.4 Primary Attitude Control Unit	67
7.5 Desaturation of Momentum Wheels	71
7.6 Attitude Sensing	73
7.7 Data Handling	75
7.8 Modes of Operation	75
7.9 References	76
Chapter 8 STRUCTURES	78
8.1 Introduction	78
8.2 Summary and Conclusions	78
8.3 Support Tube	83
8.4 Internal Structure	83
8.5 Solar Array	85
8.6 Heat Rejection Systems	87
8.7 Access and Docking	88
8.8 Propulsion Substructure	89
8.9 Component Weight and Center of Gravity	91
8.10 Areas of Further Study	93
8.11 References	94
Chapter 9 COMMUNICATIONS AND DATA HANDLING	96
9.1 Introduction	96
9.2 Summary	96
9.3 Advantages of Utilizing the NASA Standard C&DH Subsystem	98
9.4 C&DH Subsystem Description	98
9.5 Ground Communications Systems	102
9.6 Tracking	104
9.7 References	104
Chapter 10 PROGRAM COST AND DEVELOPMENT	106
10.1 Introduction	106
10.2 Summary and Conclusions	106
10.3 Discussion	107
10.4 References	113



APPENDIX A	114
APPENDIX B	121
APPENDIX C	126
APPENDIX D	128
APPENDIX E	129
APPENDIX F	132
APPENDIX G	141
ACKNOWLEDGMENTS	145



1  
INTRODUCTION

### 1.1 INTRODUCTION

The Shuttle Transportation System (STS) will significantly decrease the costs and complexity involved in delivering payloads to space. NASA has estimated that the benefits made possible by Space Shuttle use in the 12 years from 1980 through 1991 will average more than \$1 billion per year (Reference 4). The Space Transportation System could become even more efficient if on orbit stay times of the Orbiter are increased beyond the nominal 7 day limit. This limitation in the operational capability of the Orbiter is determined by its available expendables for electric power and attitude control. This problem may be overcome by the use of an orbiting service satellite with "plug-in" utilities.

Project OASIS is the result of a feasibility study of a satellite that can provide solar-generated electric power, heat rejection, and attitude control to the Orbiter and certain free-flying payloads. The purpose of this report is to describe OASIS and to show that the utilization of such a system will significantly increase the operational capability of the STS/Spacelab program. This project was inspired by initial studies of such a system carried out by NASA Marshall Space Flight Center and reported in Reference 2.

Certain constraints were applied to the system design. In order to minimize cost and complexity, it was decided to use only one Orbiter launch for orbital insertion of OASIS, and to make use of existing hardware wherever possible. Also, the utilization of extravehicular activity (EVA) is stressed in the OASIS design. It is necessary for the construction of certain parts of the spacecraft as well as for routine maintenance operations. The use of EVA here simplifies the design considerably, and thus is thought to be cost effective. OASIS is designed for an on orbit lifetime of five years before overhaul. Furthermore it will be self-propelled to reduce the necessity for alterations in the Orbiter flight plan if rendezvous is desired.

### 1.2 SUMMARY AND CONCLUSIONS

It has been determined that the construction and operation of OASIS is feasible. Also, OASIS can increase the efficiency of the STS/Spacelab, and thereby prove to be cost effective. The satellite can be ready for launch in 1983 and the cost of two (one operational and one for backup) is estimated to be approximately \$316 million for the five year mission lifetime.

### 1.3 REFERENCES

1. Astronautics & Aeronautics, "Next Step in Space Transportation and Operations," Disher, John H., January 1978.

2. "25 kW Power Module Preliminary Def. ," NASA Marshall Space Flight Center, Alabama, September 1977.
3. Space Station System Analysis Study, Part 3: Volume 1, Executive Summary McDonnell Douglas.
4. Space Shuttle Transportation System, Rockwell International, Space Division, September 1976.

## MISSION OBJECTIVES, REQUIREMENTS AND BENEFITS

## 2.1 OBJECTIVES

In the design of OASIS several mission objectives were considered. The first is to provide the Space Transportation System with greater flexibility and endurance in space. Secondly, the OASIS satellite should support free-flying payloads detached from the Orbiter (e.g. Spacelab). Further studies will have to determine how best to employ this free-flying potential. The third objective is to provide an evolutionary buildup to a large scale (or advanced) power module. The average power level of 39 kW provided by OASIS falls well short of expected needs for a number of applications projected for 1984 and later in areas such as advanced communications, experimental evaluation of solar power satellite (SPS) parameters, materials processing, and advanced space propulsion (Reference 1).

## 2.2 REQUIREMENTS

Various design requirements must be satisfied if the mission objectives are to be fulfilled. These are discussed below.

2.2.1 Services

The services required to extend the duration and capability of Orbiter missions include:

a. Electrical Power - OASIS can produce approximately 39 kW average power. This is the greatest amount of power the satellite can provide and still stay within the design constraint of a one shot launch. The basic Orbiter with its fuel cells can produce approximately 8 kW of power for 30 days. However, its additional cryo-tanks substantially reduce payload volume and subtract about 16,000 lbs (7,257.6 kg) from Orbiter payload for this mode of operation (Reference 1). With OASIS connected and the Orbiter fuel cells idling at approximately 1 kW (this is necessary to keep the fuel cells warm), the satellite can provide about 22 kW average power to Orbiter payloads on board the Orbiter for 60 or more days after which food, water, and other crew consumables become the limiting factor.

b. Thermal Control - The OASIS thermal control system increases the capabilities of the Orbiter by providing heat rejection service in addition to that carried out by the Orbiter itself. This enables the Orbiter to carry payloads that generate large amounts of heat and to absorb heat generated by the additional power available.

c. Attitude Control - Attitude control of the Orbiter is normally limited to approximately 7 days by the amount of fuel carried in the Reaction Control System (RCS). This can be increased with fuel kits, but not without a payload penalty. Therefore, OASIS was designed to provide supplementary attitude hold capability to the Orbiter for extended duration missions.

### 2.2.2 Orbital Operations and Propulsion

Consideration must be given to orbital operations for launch, recovery, orbit transfer, rendezvous, and calculation of shade times.

The onboard propulsion system enables OASIS to have an increased mission potential by providing the capability of executing various orbital maneuvers.

### 2.2.3 Weight and Structural Limitations

OASIS is designed to provide its services in any orbital inclination that the Orbiter might use. Since the OASIS satellite will be placed in orbit by just one Orbiter launch, the satellite's maximum weight is restricted by the Orbiter's payload limit. This varies from 65,000 lbs (29,484 kg) for a Kennedy Space Center launch down to 32,000 lbs (14,515 kg) for a Vandenburg launch to a maximum inclination of  $104^{\circ}$ . Since sun-synchronous orbits by definition, have no shade time, this weight reduction can be achieved by eliminating part of the batteries and reducing solar array size, and will have little or no effect on the average power production.

Structural limitations are determined by accelerations, Orbiter cargo bay dimensions, the docking mechanism, and other factors.

### 2.2.4 Communications and Data Handling

The purpose of communications and data handling is to provide command and telemetry uplinks and downlinks to a command facility. It also provides onboard evaluation of various subsystem inputs to allow for autonomous operation.

## 2.3 BENEFITS (Reference 2)

### 2.3.1 More Efficient Use of the STS/Spacelab

a. OASIS can increase the on orbit stay time of the Orbiter (without payload penalty), resulting in a reduction of the number of necessary launches, and therefore a reduction in cost/day on orbit.

b. Mission planning will be simplified because:

1. a reduction in the number of launches will relax timelines,
2. the increase in electrical power available to payloads will allow simultaneous, rather than sequential operation of certain instruments.

### 2.3.2 Benefits to Payloads

The following fields of study will benefit from extended duration missions and/or increased electrical power.

- a. Astronomy
- b. Solar Physics
- c. Atmospheric and Magnetospheric Physics
- d. Space Processing
- e. Earth Observations
- f. Life Sciences

### 2.4 REFERENCES

1. Astronautics and Aeronautics, "Next Step in Space Transportation and Operations" Disher, John H., January 1978.
2. "25 kW Power Module Preliminary Definition" NASA Marshall Space Flight Center, Alabama, September 1977.
3. Smith, William L., NASA, Washington, D. C. Personal Communication.

3  
POWER

### 3.1 INTRODUCTION

OASIS will provide electrical power to the Orbiter system and payloads vital to prolong their orbit stay times. This electrical power is obtained by the use of a solar cell array. During the sunlit periods of orbit, the solar array will provide power to the user systems and battery chargers. The batteries will provide an equivalent amount of power to the user systems during the dark periods of orbit.

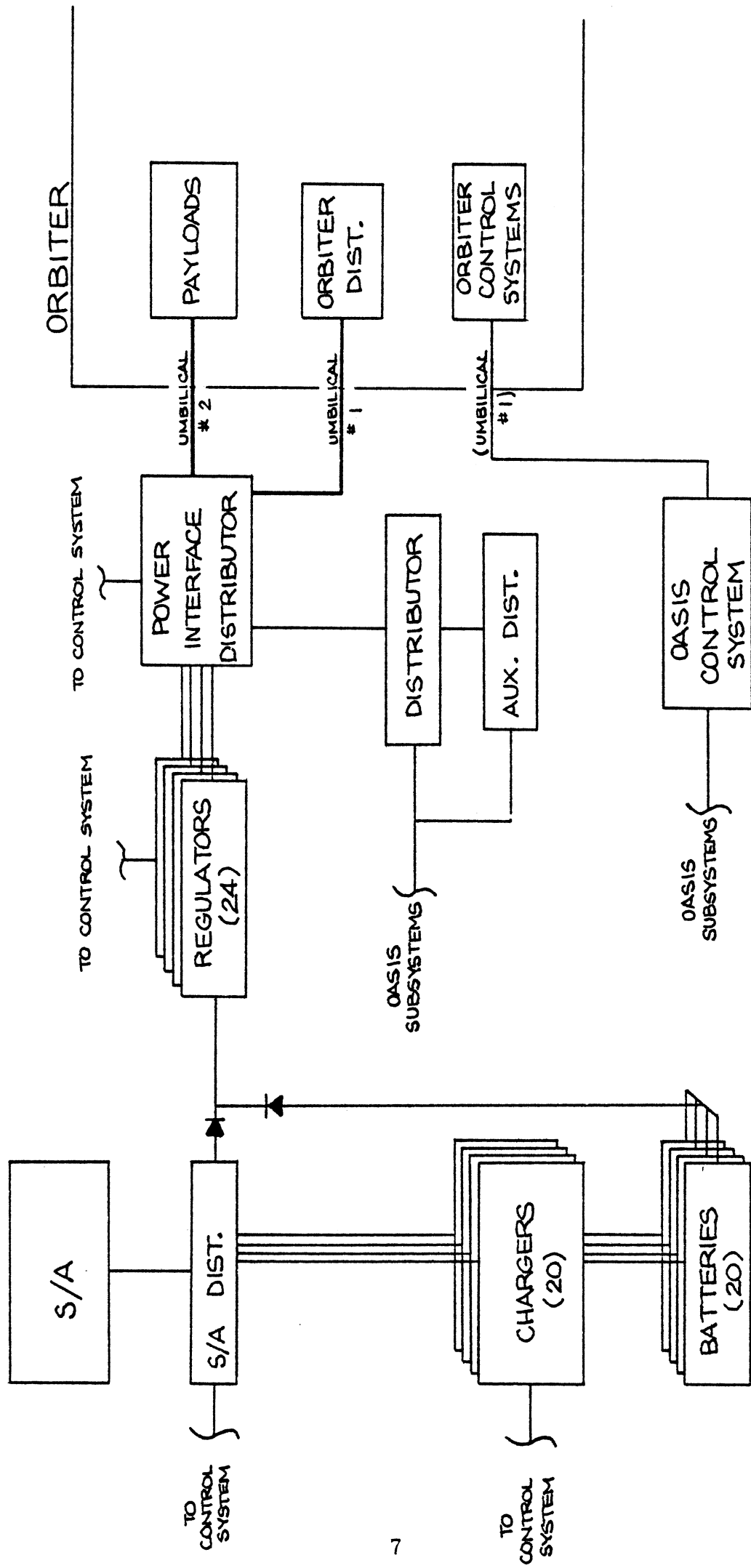
There are basically two modes of operation for the satellite array system. When docked to the Orbiter system, the solar array will be fully deployed to supply maximum power. For the periods when not docked to the Orbiter, the satellite array system will operate in a "standby mode" in which the array will be only partially extended to power only the satellite subsystems.

### 3.2 SUMMARY AND CONCLUSIONS

The electrical power system consists of a 2-degree of freedom solar array, batteries, regulators, and a power distribution system. External power will be supplied through two Orbiter buses and two payload buses. A system block diagram is given in Figure 3.1. Power transmitted directly from the solar array is 88% efficient, while battery system efficiency is 65.6% (see Figure 3.2). Overall system efficiency, somewhat dependent on the orbit, is better than 78%. For a sun synchronous orbit where the use of batteries is minimized, the system efficiency approaches 88%.

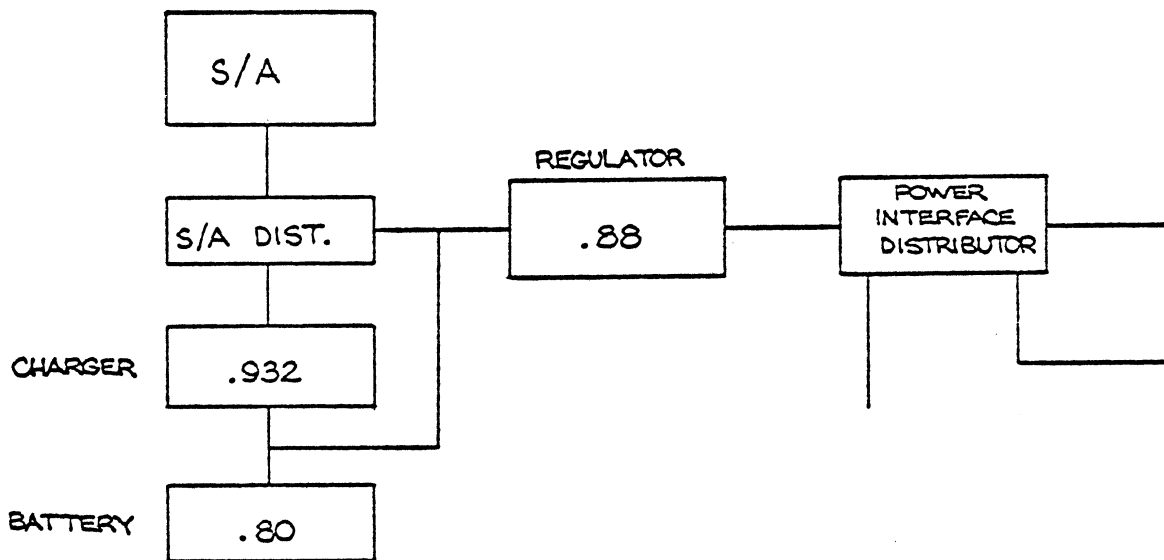
The solar array system uses silicon solar cells mounted on 2 deployable/retractable "wings." Each wing measures 23.9' (7.28m) by 236.7' (72.15m) and together supply a total of 84.75 KW. A degradation rate of 8.0% occurs over the 5-year lifetime of the satellite array system, reducing the power available to 77.97 KW. This loss of 6.78 KW of power is due to radiation degradation of the solar cells. A summary of the mission power requirements is given in Table 3.1. Note that the reduction in power over 5 years is subtracted from the payloads value. The power supplied to the Orbiter (14 KW) and OASIS subsystems (2.76 KW) are kept constant throughout the entire mission.





POWER SYSTEM BLOCK DIAGRAM

FIGURE 3.1



SIMPLIFIED BLOCK DIAGRAM  
FOR POWER TRANSMISSION EFFICIENCY

FIGURE 3.2

Table 3.1 Mission Power Requirements (KW)

	<u>BOM*</u>	<u>EOM*</u>
I. Communications	0.200	0.200
Attitude & control	1.300	1.300
Propulsion	0.160	0.160
Structures	0.100	0.100
Thermal control	<u>1.000</u>	<u>1.000</u>
Total OASIS Subsystems Power	2.76	2.76
II. Battery Recharge (during sunlit period)	40.7	37.45
III. Orbiter	14.0	14.0
Payloads (spacelab, experiments, etc.)	22.0	18.91
IV: Power transmission losses (88% power conditioning & distribution efficiency)	5.29	4.85
Total Avg. Power Supplied	84.75	77.97

\*BOM - beginning of mission

\*EOM - end of mission ( 5 years)

The OASIS battery system consists of 20 batteries and 20 chargers. Each battery weighs 680 lbs (308 kg) and is rated at 6.96 KW-h. This provides a useable energy of 27.8 KW-h at 20% depth-of-discharge. The battery recharge fraction (A-h in/A-h out) is estimated at 1.25, reflected in the 80% battery efficiency. Battery/charger pairs can be remotely switched off on failure, and are connected in parallel, supplying 140 volts.

The solar array distributor divides power between the battery chargers and the regulators. 10 regulators provide a fixed output voltage of between 28 and 32 volts to the OASIS subsystems and the Orbiter. The remaining 14 regulators provide a variable output voltage, up to the input of 140 or 211 volts. These can be remotely set to supply required voltage to the Spacelab and/or other payloads. Each regulator can be individually switched between several buses for better load sharing. This is done in the power interface distributor.

Electrical connections between OASIS and the Orbiter are through two umbilicals. Umbilical #1 carries 14 KW average/24 KW peak to the Orbiter and provides control system connection. Power to payloads is supplied through umbilical #2, rated at 22 KW average, 30 KW peak.

When the satellite is not docked to an Orbiter, it is in standby mode, and supplies power only to its own subsystems. In this mode the array will be extended to approximately 8% of its fully deployed area.

Array pointing is accomplished using a 2-degree of freedom system, providing full solar power for any spacecraft orientation. Solar power will be transferred to the solar array distributor through slip-rings. This allows full 360° rotation in either degree of freedom.

A special sun synchronous mission was also examined. Satellite system changes involve the removal (prior to launch) of 18 of the 20 battery/charger pairs and a reduction of the solar array size by 46%. These provide a satellite weight reduction of 14895 lb (6756 kg).

In addition to solar cells, nuclear energy was also considered as a possible source of electrical power. After careful consideration nuclear power was eliminated due to the complex problems associated with it. Some of the problems are as follows:

#### Nuclear reactor power system

- . Extra shielding needed to protect Orbiter crew presents a weight problem
- . Reliability of space nuclear reactors not well established
- . Heat rejection of a system capable of producing approximate 40 KW (electrical) becomes a critical problem
- . No system presently exists which produces the large output (~ 40 KWe) desired for the power system

## Radioisotope

- . Much more flexible than the above system, however, existing radioisotope systems are still in the test stages (i. e. reliability not established)
- . Fuel costs are extremely high
- . This system provides continuous power; since high power needed only when docked with the Orbiter, system is not practical

Although radioisotope power generation is extremely useful in lower level power production (less than 10 KWe) it is not useful in the case of OASIS.

### 3.3 SOLAR CELLS

#### 3.3.1 Solar Cell Type

The conventional single crystal N/P silicon solar cell was chosen for the solar array design. This type of cell is the leading candidate for space photovoltaic power systems due to their availability and proven reliability.

Two other types of solar cells were considered for our solar array but were not as attractive as the silicon cell. First, the gallium arsenide cell has a higher resistance to radiation degradation than does the silicon cell, however, applications are limited because of gallium availability and fabrication processes. The cadmium sulfide cell also has a greater radiation resistance (vs the silicon cell) in addition to reduced weight, but present technology has been unable to manufacture this cell with feasible (11-14%) efficiencies.

#### 3.3.2 Environmental Effects

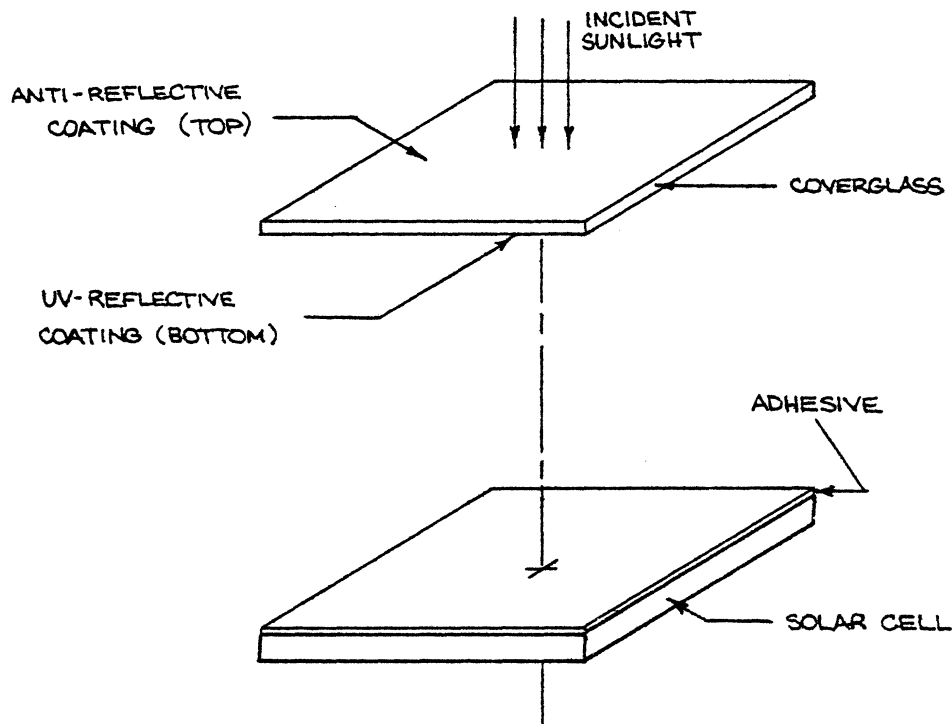
The space environment produces effects on the silicon solar cells and array that can severely limit its normal operating characteristics. Basically there are 4 main effects due to the environment: (1) particle radiation from the Van Allen radiation belt, (2) ultraviolet radiation, (3) effects due to temperature and (4) micrometeoroid bombardment.

##### 1) Particle radiation

The satellite will be in a 300 nm orbit which will subject the solar cell array to particle radiation due to the Van Allen belt. This radiation belt is made up of two concentric belts, the inner belt and the outer belt. The inner belt ranges from 162 nm to 3456 nm which includes the 300 nm orbit of our satellite. Although the maximum intensity occurs in the 1560-1730 nm range, the radiation will still produce a significant reduction in the solar cell's energy conversion efficiency. At the satellite orbit of 300 nm and inclination angle of 50°, it was found that a degradation rate of 5.5% would occur (Reference 13). This assumes that the arrays will be operating a total of 1 year out of the 5-year on-orbit operation time.

## 2) Ultraviolet radiation

Ultraviolet radiation has been found to cause a darkening of the solar cell covers and coverslide adhesives. This darkening effect causes a reduction in sunlight transmission to the solar cell thereby lowering the cell's efficiency. This warrants the need of a coverglass with a reflecting filter. Coverglasses with reflecting filters are coated on both sides (see Figure 3.3). The outer "exposed" side has an anti-reflective coating which is designed to enhance the transmission of sunlight through the coverglass. However, a transmission efficiency of 81% (percent of sunlight that is transmitted through the cover and into the cell) will still occur. The "inner" side of the cover has an ultraviolet (UV) reflective coating to prevent darkening of the coverglass adhesive. The array design will use silicon monoxide (SiO) for the anti-reflective coating and a blue-red reflecting filter with a cut-on wavelength of 400 n meter (located on the inner surface).



SOLAR CELL & COVERGLASS

FIGURE 3.3

A degradation rate of 2.5% for UV radiation damage will be used (Reference 10). This value of 2.5% plus the value of 5.5% for particle radiation degradation combines to give a total of 8.0% degradation. This degradation value will produce a decrease of power of 8.0% at the end of the 5-year mission.

### 3) Effects due to temperature

The major effects of temperature (due to incident sunlight) are electrical and mechanical in nature:

1. Electrical effects - The solar cell output power decreases with increasing temperature and therefore lowers the cell's efficiency. The steady-state operating temperature of the array was found to be approximately 200°F (92°C) with the addition of concentrators (Refer to Appendix A. 1 for temperature analysis). This increase in temperature (due to the addition of concentrators) has the following effect on the cell's efficiency (see Appendix A. 3). It was assumed that 13.5% efficient cells (at 28°C) would exist by 1983, the estimated time of OASIS launch.

<u>Approx temp of cell</u>	<u>Estimated efficiency of cell</u>	<u>Condition</u>
81°F (28°C)	13.5%	Room temp
139°F (60°C)	11.5%	w/o concentrator
200°F (93°C)	10.0%	with concentrator

Note that the above estimates are conservative.

The use of concentrators has the desirable effect of increasing the Solar Constant from 135.3 mW/cm<sup>2</sup> to a figure of 215 mW/cm<sup>2</sup> (see Appendix A. 2). However, as was shown, the increase in temperature causes the efficiency to drop from 11.5% to 10%. This tradeoff is desirable however because an increase in power of 24.6% is gained at the loss of 15% in efficiency (see Section 3.5.3).

2. Mechanical effects - Exposure of the array to many cycles of alternating high and low temperatures causes cyclic stress variations. These stress variations may lead to eventual fatigue failures of the array supporting structure, electrical components, coverglass material, adhesive bonds, and soldered and welded joints on the structure. However, since it is expected that the steady-state temperature of the array (for sunlight and shadow periods) is within allowable tolerance limits, this will not impose any difficulties.

#### 4) Micrometeoroid bombardment

Bombardment from micrometeoroid showers can cause erosion (similar to that caused by sand blasting) of the solar cell coverglass, and the substrate thermal coating. The erosion of the substrate thermal coating will result in a decrease of the thermal emissivity, causing the steady-state operating temperature to rise. Erosion of the coverglass will result in greater reflectivity and lower the transmittance of light to the actual cell. All of the above effects will thus tend to lower the overall efficiency of the array. Heavier than normal particles could possibly even crack the coverglass, however, the probability of this occurrence is very small. A fused silica coverglass of .006" thickness will provide adequate protection of the solar cell.

#### 3.3.3 Satellite-Produced Effects

There are basically two other effects that are not produced by the space environment. The following two effects are inherent in the satellite system itself and must be considered in the solar array design. Those effects are: (1) magnetic fields (2) angle of incidence variation.

##### 1) Magnetic fields

The solar cell array will produce magnetic fields that (through interaction with the geomagnetic field) will cause a torque on the vehicle. This will produce an undesirable effect on the attitude control system of the satellite. Also, if our vehicle happens to be supplying power to an experiment which employs sensitive measuring devices, the magnetic field can present problems in this area.

The magnetic field produced by the array is caused by current loops within the wing and is potentially large due to the large size of our array system. To minimize this field problem the solar cell circuits in the array will be designed in such a fashion that the fields produced by neighboring circuit loops will cancel each other out.

##### 2) Angle of incidence

The solar array panels employ the use of sun sensors to keep the panels oriented toward the sun. The array pointing control system keeps the variation from normal sunlight incidence to less than  $1^\circ$  therefore a significant reduction in power will not occur.

#### 3.4 PHYSICAL CHARACTERISTICS OF SOLAR CELLS

The following table presents a detailed summary of the physical characteristics of the solar cells:

Table 3.2 Solar Cell Characteristics

<u>Cell type</u>	single crystal N/P silicon
Size (cm x cm)	2 x 4
Active Area (cm <sup>2</sup> )	7.8
Thickness (inches)	.008
*Power (mW/cell)	135.84 at 90°C
Base Resistivity (ohm-cm)	2.0 (nominal)
*Efficiency	13.5% at 28°C; 10% at 90°C
Contacts (wraparound)	TiAg
<u>Coverglass</u>	fused silica
Size (cm x cm)	2 x 4 (same size)
Thickness (inches)	.006
Anti-reflective Coating	SiO (silicon monoxide)
UV reflective Filter	blue-red (cut-on wavelength = $400 \times 10^{-9}$ )
Cover Adhesive	DC 93500 (Dow Corning)

\* "Voltage-current characteristics vs cell temperature" graph can be found in Appendix A.3.

### 3.5 SOLAR CELL ARRAY DESIGN

#### 3.5.1 Wing Design

The solar cell array design consists of 2 deployable/retractable wings that measure 23.89' (7.28 m) by 236.7' (72.15m) in their normal operating position (i. e. when docked to the Orbiter). Each wing of the solar array consists of 2 blankets symmetrically located about the deployment boom (see Figure 3.4), and contains a total of 312,000 solar cells for a total of 624,000 cells for the entire array.

Each solar array blanket consists of 13 sub-blankets measuring 10.3' (3.14 m) by 18.21' (5.55m) with a thickness of 1.12 inches (2.85 cm). Each sub-blanket consists of 12 submodules and 2 reflector modules (which measure 5.714' (1.74 m) by 10.3' (3.14 m) in a flat-out position). Figure 3.5 gives a description of the sub-blanket.

The sub-blanket will always be in a tilt position (as opposed to the flat-out shown in Figure 3.5) as shown in Figure 3.6. The reflector modules (concentrators) will be inclined at an angle of 126.38° from the horizontal whereas the cell area (2 cellular modules) will remain in a flat position. This,



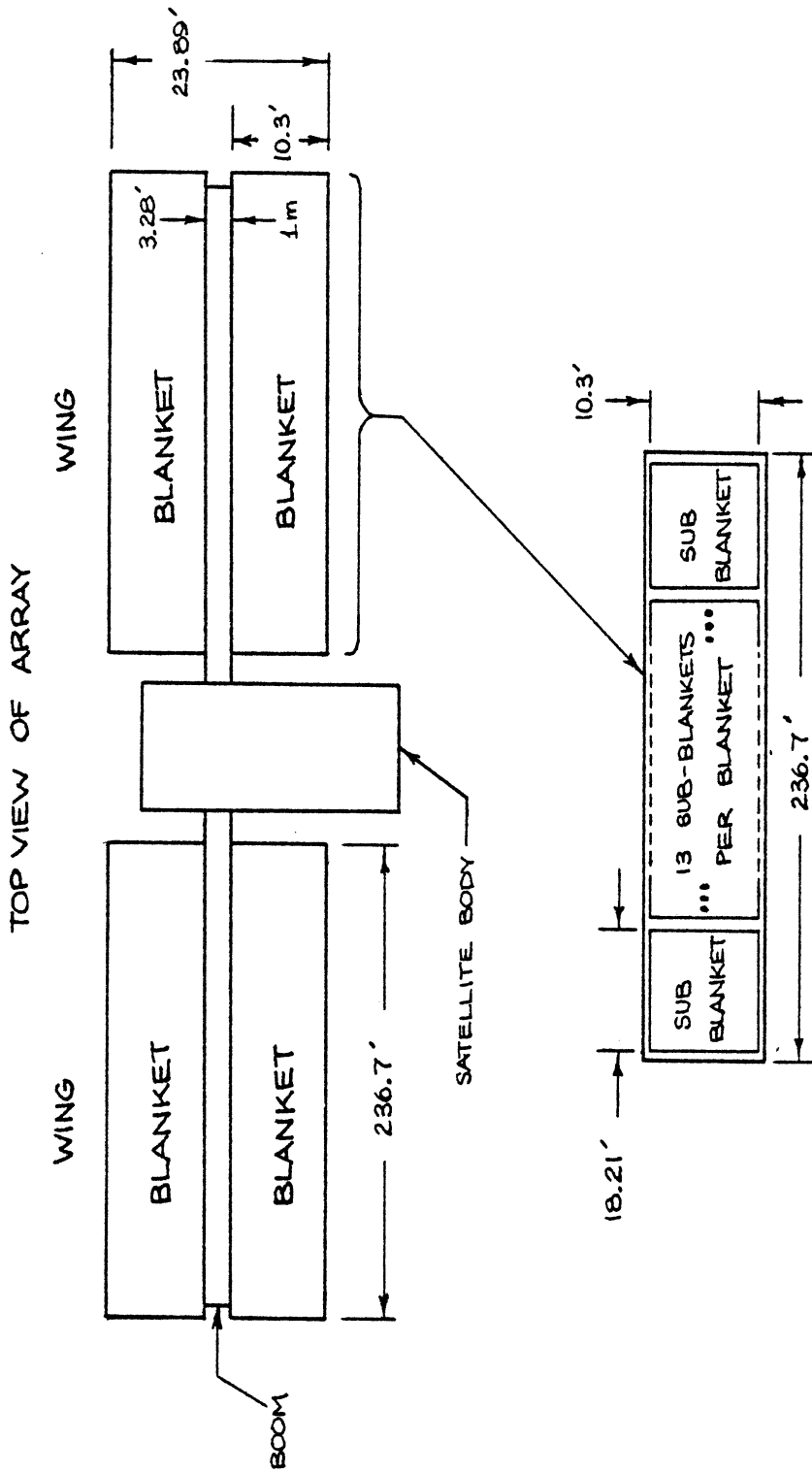
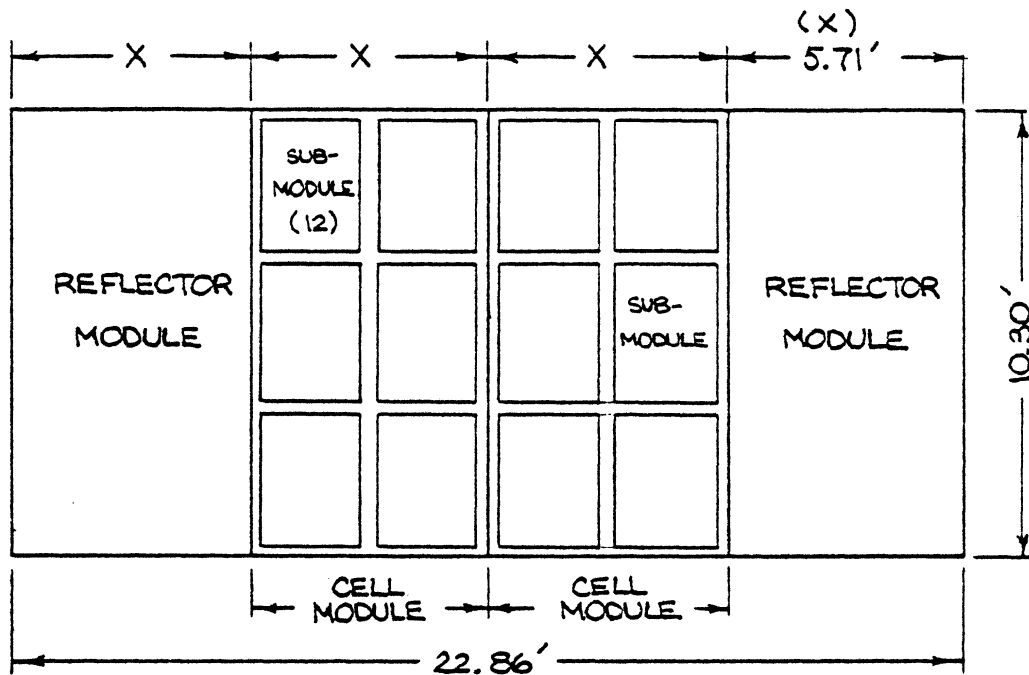
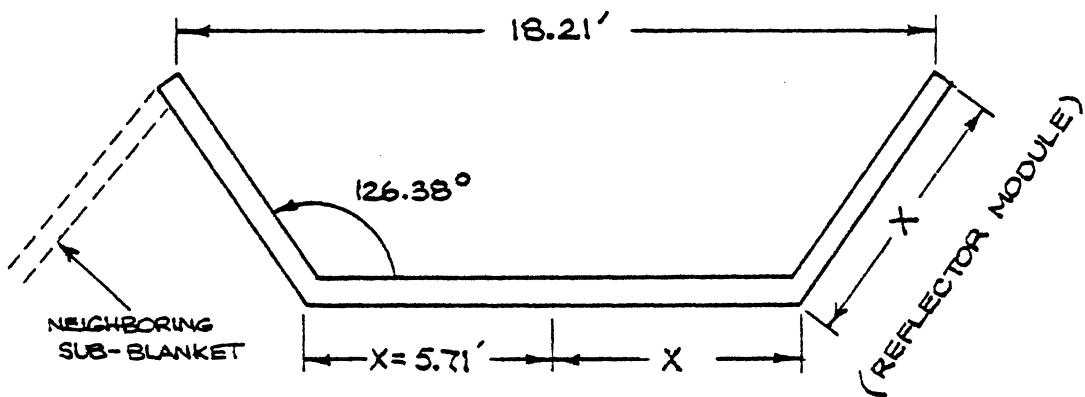


FIGURE 3.4



TOP VIEW OF  
SUB-BLANKET  
(FLAT-OUT POSITION)  
FIGURE 3.5



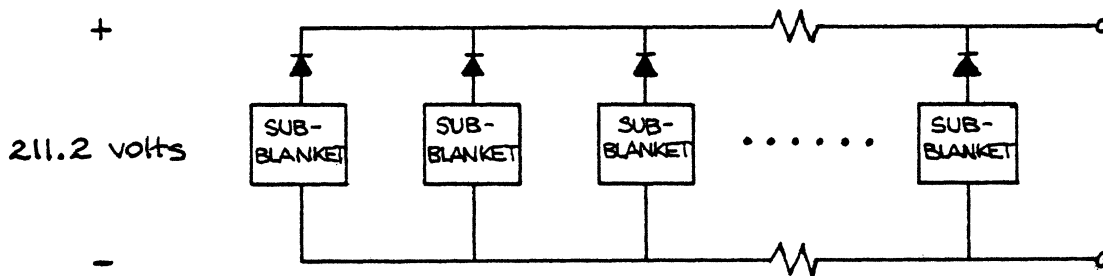
SIDE VIEW OF  
SUB-BLANKET  
(NORMAL TILT POSITION)

FIGURE 3.6

therefore, makes the overall length of each sub-blanket 18.21' (5.55 m) and the wing length (13 sub-blankets x 18.21') of the array 236.7'.

### 3.5.2 Electrical Aspects of Array

Each submodule has an open circuit voltage of approximately 17.6 volts (refer to Section 3.5.4). The submodules of a sub-blanket (recall Figure 3.4) are all connected together in series to bring the total open circuit voltage of 1 sub-blanket to 211.2 volts. Each sub-blanket of the blanket is then connected in parallel (see Figure 3.7). Blocking diodes are inserted in each parallel sub-blanket to prevent reverse current flow (during shade period).



ELECTRICAL CONNECTIONS  
OF BLANKET

FIGURE 3.7

The array therefore may be deployed sub-blanket by sub-blanket as required by the amount of power needed by the user system (satellite subsystems or Orbiter). Note that each sub-blanket may be considered electrically "independent" of the others thereby producing a higher reliability for the array system. It also removes the need for electrical connections across the deployment boom.

OASIS will employ slip-rings, as opposed to wraparound cabling, to electrically connect the wings to the main body of the satellite. Slip-rings are used because OASIS may be utilized in a number of orbital planes that will require the wings to rotate around in a complete circle. Although slip rings are not as reliable as wraparound cabling, their ability to rotate freely without restriction gives them the crucial advantage. Future advances in slip-ring design should improve reliability.

It should be noted that wraparound cables with their high degree of reliability may be considered as an alternative. They would however restrict rotation of the wings to a certain range (greater than  $360^{\circ}$ ) and an unwinding period would be required. This unwinding could be done during the dark period of orbit. For a sun synchronous mission sufficient batteries could be carried to "cover" for the solar array during unwinding.

### 3.5.3 Concentrators

The use of concentrators to increase the amount of incident sunlight on the solar cells is used for the array design. These concentrators consist of a 0.5 mil Kaplon plastic that is coated by 0.5 mil Aluminum, making the weight addition very small (see weight breakdown in Table 3.3).

There are a total of 26 concentrators located along the array inclined at an angle of  $126.4^{\circ}$  from the horizontal (see Figure 3.6). This angle is calculated in Appendix A.2.

As stated previously, the addition of concentrators increase the output power of each cell but decrease the cell's efficiency. This decrease in efficiency is due to the increased temperature that occurs by the addition of concentrators. The tradeoff is desirable, however, because an increase in power of 24.6% occurs at 15.5% loss in cell efficiency.

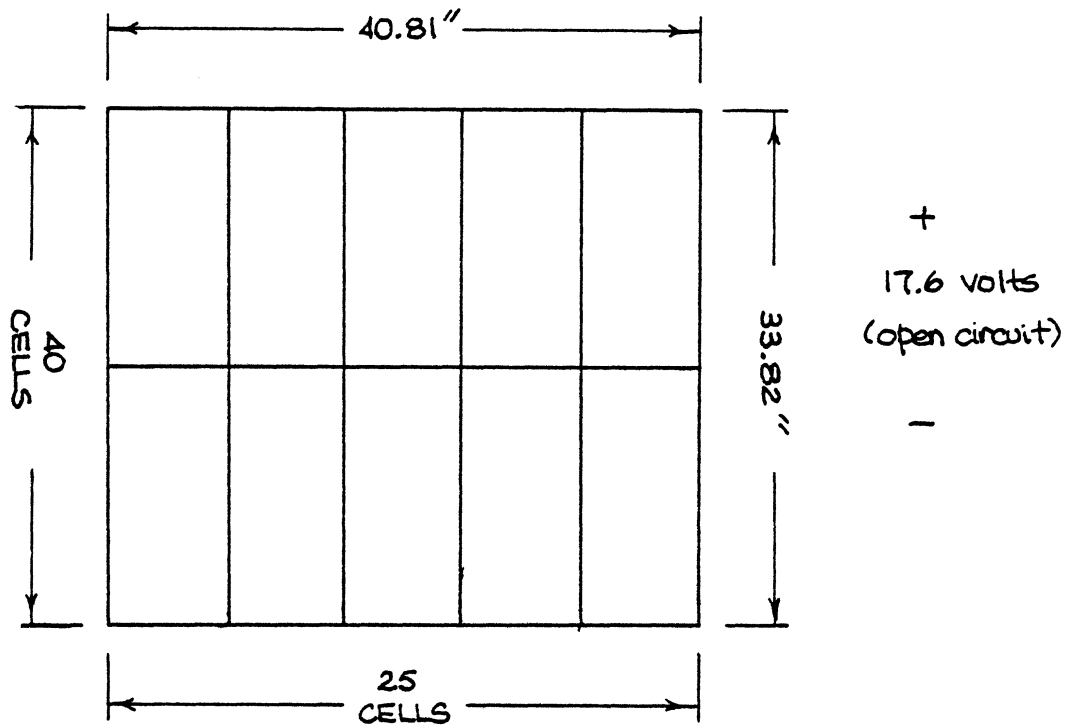
Another advantage to the use of concentrators is a savings in the number of solar cells required for the array. It is expected that a savings of 240,000 ce is gained, making the number of cells required 624,000.

Also, aluminum concentrators will not be appreciably affected by particle radiation as are the solar cells. Therefore, the replacement in cell area by concentrator material will reduce the amount of cell failure thereby increasing the array system reliability.

### 3.5.4 Submodule Size and Construction

As stated earlier, a single wing consists of 2 blankets, where each blanket contains 13 sub-blankets. Each one of the sub-blankets holds 12 submodu (recall Figure 3.4) for a grand total of 312 submodules per wing.

The submodule contains a total of 1000 cells wired into a configuration of 5 cells parallel and 20 cells series (see Figure 3.8). This arrangement of cells greatly increases the array reliability by minimizing the effect of individual cell failure.



5 CELLS PARALLEL , 20 CELLS SERIES  
INTERCELL SPACING = 60 mils

CELL SUBMODULE DESIGN  
FIGURE 3.8

An open circuit voltage of 440 mV/cell was estimated. Therefore the voltage across one submodule will be approximately 17.6 volts.

### 3.5.5 Array Mass

A weight breakdown for the solar array system is shown in Table 3.3. This includes the weight of both solar array wings, however, the booms used for deployment of the wings are not included.

Table 3.3 Solar Array Weight Breakdown\*

Component	Component Weight	Total Weight (lbs)
Solar Cell	.382 g/cell	525.51
Coverglass	.269 g/cell	370.06
Contacts	$3.695 \times 10^{-6}$ g/cell	$5.083 \times 10^{-3}$
Adhesives (clear)	$5.488 \times 10^{-2}$ g/cell	75.49
Thermal Paint (over total backside of array)	1.55 g/cm <sup>3</sup>	387.12
Substrate (aluminum honeycomb)	1.12 kg/m <sup>2</sup>	2797.25
Concentrators (0.5 mil Kapton Plastic coated by 0.5 mil aluminum)	.002 g/cm <sup>2</sup>	12.49
Diodes, cables, buses, misc.		25.0
Total Array Weight		4192.9 lbs

\* does not include weight of the deployment booms.

### 3.6 BATTERY SYSTEM

#### 3.6.1 Requirements

The battery system is a very important component of the OASIS mission. From the estimated power breakdown, Table 3.1, a total supplied power of 39 kW is required by the OASIS subsystems, Orbiter, and payloads. For dark-side operations, then, the battery system must provide this power. A worst

case orbit of 150 nm in the ecliptic plane yields a shade time of 37.4 min of a 90 min orbit. Thus calculations will be based on an orbit of 58% battery charging time, 42% discharge time. For a power conditioning and distribution efficiency of 88% (see Figure 3.2) a useable battery capacity of 27.5 kW-h is required.

Nickel-cadmium (Ni-Cd) batteries have long been used for space applications, but there is a concentrated effort by NASA and the Air Force to improve battery performance. Several new types of batteries are under development, all of which give significantly higher energy densities (Reference 6). Nickel-hydrogen cells, while being easier to recondition and thus extend lifetime, have much greater volume than Ni-Cd cells. They have not been fully tested, but are the closest of the new systems to becoming operational. Silver-hydrogen cells, while yielding 60 to 75% depth-of-discharge (DOD), currently have too short a lifetime for a 5 year low earth orbit mission. Metal sulfide-lithium cells offer much higher energy densities but will not be available until the late 1980's. Present technology Ni-Cd cells are a logical choice for this system, offering a long cycle lifetime and good reliability.

Ni-Cd batteries in low earth orbit usually use a DOD of 10 to 20% (Reference 1), so that a total rated capacity of between 138 and 275 kW-h is required. Battery design identical to the NASA 25 kW Power Module (Reference 10), is used, including cells to be flown on SEASAT. Cell characteristics are described in detail in AFAPL TR-76-47. Each battery has a rated capacity of 6.96 kW-h. A system of 20 batteries gives 139.2 kW-h and satisfies the requirements at 19.7% DOD.

### 3.6.2 Battery Characteristics

Each battery is comprised of 4 modules, each module containing 29 cells and one reconditioning circuit. These cells are described in Air Force Report AFAPL TR-76-47. Battery configuration is the same as that used in the NASA 25 kW Power Module design.

Battery capacity can be severely degraded by excessive temperature (see Appendix A.4). A nominal battery temperature of  $10^{\circ} + 5^{\circ}\text{C}$  will be maintained by cold plates on which the batteries are mounted. Cell capacity, under normal operation, will degrade significantly after many charge/discharge cycles. Reconditioning, which involves totally discharging each cell periodically, can restore both cell voltage and capacity (Reference 7). More research must be done, but preliminary test results are shown in Appendix A.4.

Lifetime estimates are given in Appendix A. 5. Based on 20% DOD at a maximum temperature of 15°C, battery lifetime is estimated at 2.3 years without reconditioning. Since the OASIS spacecraft will be in standby mode (not attached to an Orbiter or payload) for a large part of its 5 year lifetime, battery DOD will often be 1.4%. This condition, together with reconditioning, is expected to extend the battery lifetime to 5 years. A summary of battery characteristics is given in Table 3.4.

Table 3.4 Battery Characteristics

Cell capacity	50 to 60 A-h
Cells per module	29 series
Modules per battery	4 series
Battery dimensions	7.9 x 25.6 x 3.9 in (20 x 65 x 10
Battery weight	680 lbs (308 kg)
Battery voltage	140 volts
Battery recharge fraction	1.25
Battery rating	6.96 kW-h
Operating temperature	10° ± 5°C
Lifetime (with reconditioning)	5 years

### 3.6.3 Battery Charging and Control

Battery lifetime is critical to overall mission success and endurance. To maximize this lifetime, battery conditions must be monitored carefully during charging and discharging. Battery charging is performed by 20 chargers each connected to one battery. Each of these systems can be cut out by the solar array distributor should a failure occur.

To adequately control the battery charge level, each charger must monitor battery voltage, current and temperature, as well as the input voltage from the solar array distributor. Battery conditions will also be monitored by ground facilities. Table 3.5 lists charger characteristics.

Table 3.5 Charger Characteristics

Dimensions	9.8 x 13.0 x 6.7 in (25 x 33 x 17
Weight	40 lb (18 kg)
Input voltage	140 to 211 volts



### 3.7 POWER CONDITIONING AND DISTRIBUTION

Power conditioning and distribution on OASIS is performed by 24 regulators and 2 distributors. Technology for these high-voltage components is under development. Table 3.6 provides a summary of conditioning and distribution component characteristics.

Table 3.6 Power Conditioning and Distribution  
Component Characteristics

#### Solar Array Distributor

Dimensions	30 x 35 x 40 in (76 x 89 x 102 cm)
Weight	200 lb (91 kg)
Voltage	211 volts

#### Regulators

Dimensions	9.8 x 13.0 x 7.9 in (25 x 33 x 20 cm)
Weight	62 lb (28 kg)
Input voltage	140 to 211 volts
Output voltage	
fixed regulator	28 to 32 volts
variable regulator	0 to 211 volts
Rating (avg/peak)	1.8/3.0 kW

#### Power Interface Distributor

Dimensions	30 x 35 x 10 in (76 x 89 x 25 cm)
Weight	200 lb (91 kg)
Voltage	0 to 211 volts

#### 3.7.1 Solar Array Distributor

The voltage and current at the base of each array will depend on the power demand from all other systems. Open circuit voltage for the solar array is approximately 211 volts (see Section 3.4). Power from the array enters the solar array distributor and is divided between the regulators and the battery chargers. Power to the chargers will be carried by 20 buses, one for each independent charger/battery pair. The solar array distributor will be tied to the OASIS control system which will select the system's operational modes. The distributor will have switching (on/off) capability for each of the charger buses. Solar array power to the regulators can be shut off at this point also.

### 3.7.2 Regulators

Voltage from the solar array and batteries is much higher than that required by the OASIS subsystems and Orbiter. Regulators are employed to change this possibly varying high voltage to a constant, useable output.

From Figure 3.9, 10 regulators will normally supply power to the Orbiter buses and OASIS subsystems, at an output voltage of 28 to 32 VDC. The remaining 14 regulators, supplying power to the payloads, will have a variable voltage output, controllable from the Orbiter or ground. These variable regulators provide a unique capability to OASIS. Should a payload require a voltage out of the 28 to 32 volt range, these regulators can supply voltages up to the steady state input voltage of the regulators. During sunlit periods this is the solar array base voltage (170 - 211 volts depending on power drain), and battery voltage (140 volts) during dark periods. Since high-voltage, high-power payloads will be common for manufacturing and industrial experiments, this feature allows flexibility and upward compatibility with future payloads and applications.

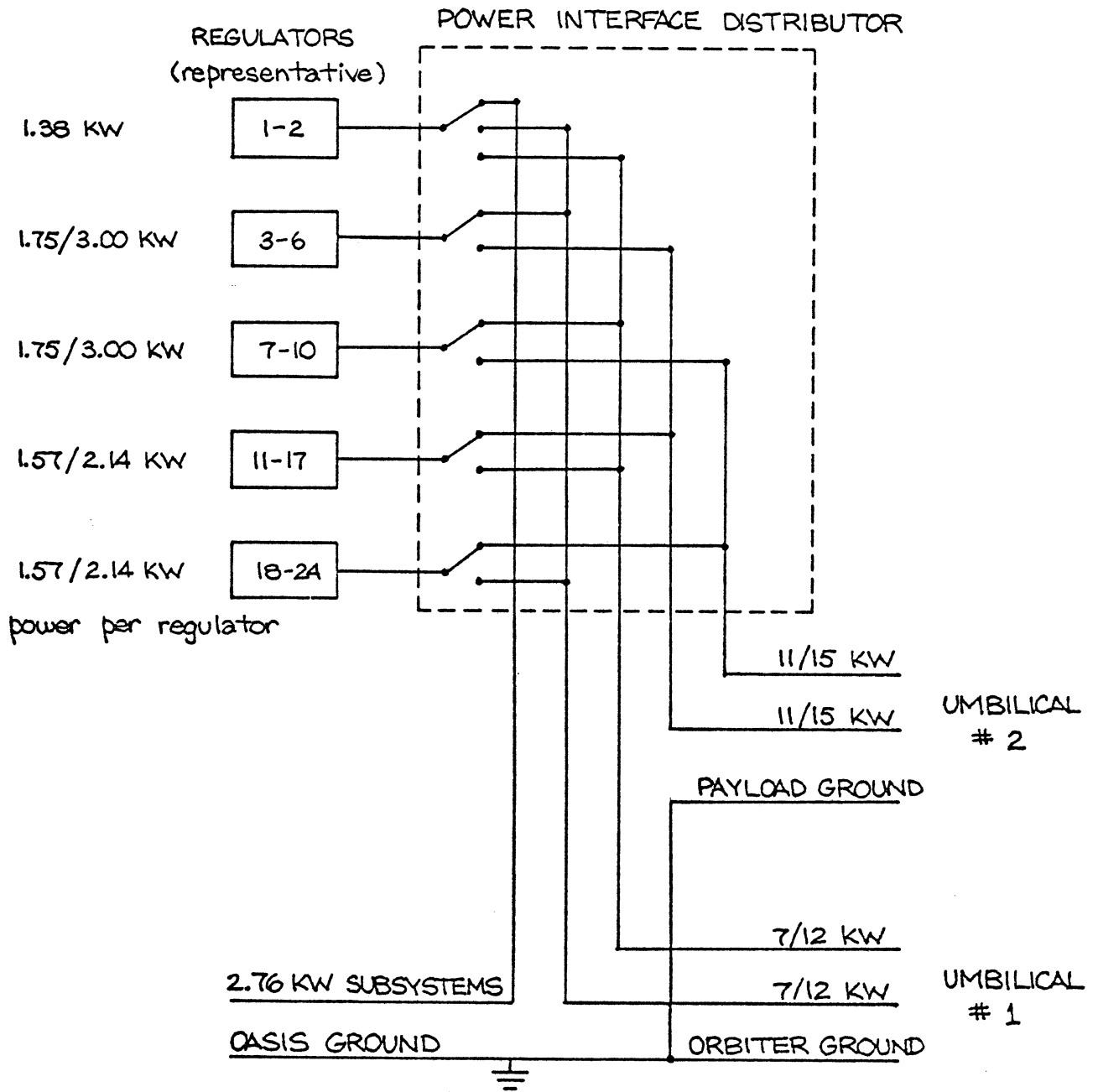
### 3.7.3 Power Interface Distributor

The power interface distributor controls switching between the regulators and the payload, Orbiter, and OASIS subsystem buses (Figure 3.9). Since power requirements of the Orbiter and payloads may vary, the distributor will aid in equalizing the power load through each regulator. Also, if a regulator should fail it can be removed from the system here. Regulator switching will be controlled automatically by the onboard control system, but may be changed by the Orbiter or ground. An interlock system will insure that if variable regulators are connected to the Orbiter buses they will put out the required 28 to 32 volts, and fixed output regulators will be connected to payload buses only if the bus voltage is acceptable.

### 3.7.4 Interfacing

During normal operational periods, OASIS will be tied electrically to the Orbiter through two umbilicals, each having appropriate safety/emergency disconnects (see Figure 3.1 and 3.9).

Umbilical #1 will provide electrical power to the Orbiter through two buses, connected within the Orbiter to Orbiter buses B and C respectively. These buses are rated to supply 7 kW average and 12 kW peak each at the 28 to 32 VDC required by the Orbiter. Orbiter monitoring and control will be tied to the OASIS communications and data handling and control systems through this umbilical. OASIS and Orbiter grounds will also be connected here.



AVERAGE / PEAK POWER GIVEN  
 REGULATORS 1-10 FIXED VOLTAGE  
 REGULATORS 11-24 VARIABLE VOLTAGE

REGULATORS AND POWER  
 INTERFACE DISTRIBUTOR  
 FIGURE 3.9

The second umbilical supplies power to the Spacelab and/or other Orbiter payloads. This power is carried through two buses, each rated at 11 kW average, 15 kW peak. A ground return is also supplied. Umbilical #2 is assumed to be connected directly to a mission dependent Spacelab/payloads distributor in the Orbiter bay.

As described in Section 3.7.2, umbilical #2 can supply steady-state voltage up to the battery voltage of 140 volts, and no lower than 170 volts during sunlit periods. Also, since this umbilical is separate from the Orbiter umbilical, it can be connected to a "free-flying" (separate from the Orbiter) payload.

The Orbiter will dock with OASIS by means of the Airlock Docking Modules (Section 8.7.2) which will be permanently attached to the Orbiter. The electrical line between OASIS and the Orbiter will be made via this interfacing system.

Two sets of electrical cabling will exist in the interior of the docking module to connect the OASIS umbilicals to the systems requiring power. One set of these permanent cables will extend to the Orbiter systems and the other will extend to the payload of the Orbiter. After docking has occurred the OASIS umbilicals need only be connected to the cabling in the docking module in order to supply power. Since an Orbiter crew member can reach the OASIS umbilicals through the airlock docking module an EVA will not be necessary to make this electrical connection.

Although the above mentioned electrical connecting system will satisfy most mission requirements it may be desirable in some cases to deploy the payload away from the Orbiter and still supply power to it. It is to satisfy this contingency that umbilicals are "given" to OASIS at all. Exclusive use of the cabling in the docking module would require only that OASIS have a "power outlet" which the cabling could plug into.

Umbilical cables are anticipated to be about 2 inches (5.1 cm) in diameter and should be flexible. However, at this point, it should be noted that umbilical length, composition, and storage configuration are all areas of further study.

## 3.8 SYSTEM PERFORMANCE

### 3.8.1 Operational Modes

During the OASIS mission, there are several distinct phases of operation. These phases are characterized by widely differing modes of operation for the electrical power system.

The launch and deployment phase covers the period from mounting the satellite in the Orbiter bay until the solar array wings have been sufficiently deployed for the next mission phase, standby mode. Batteries will be fully charged prior to launch and will supply initial power upon OASIS system activation when the desired orbit is reached. When enough separation is achieved between the satellite and the delivering Orbiter, solar array deployment will begin. It is estimated that each wing will be deployed at a rate of 1.5 inches per second (3.8 cm/sec), dictated by the two array deployment motors. Thus it will take 2.4 minutes to reach standby mode configuration.

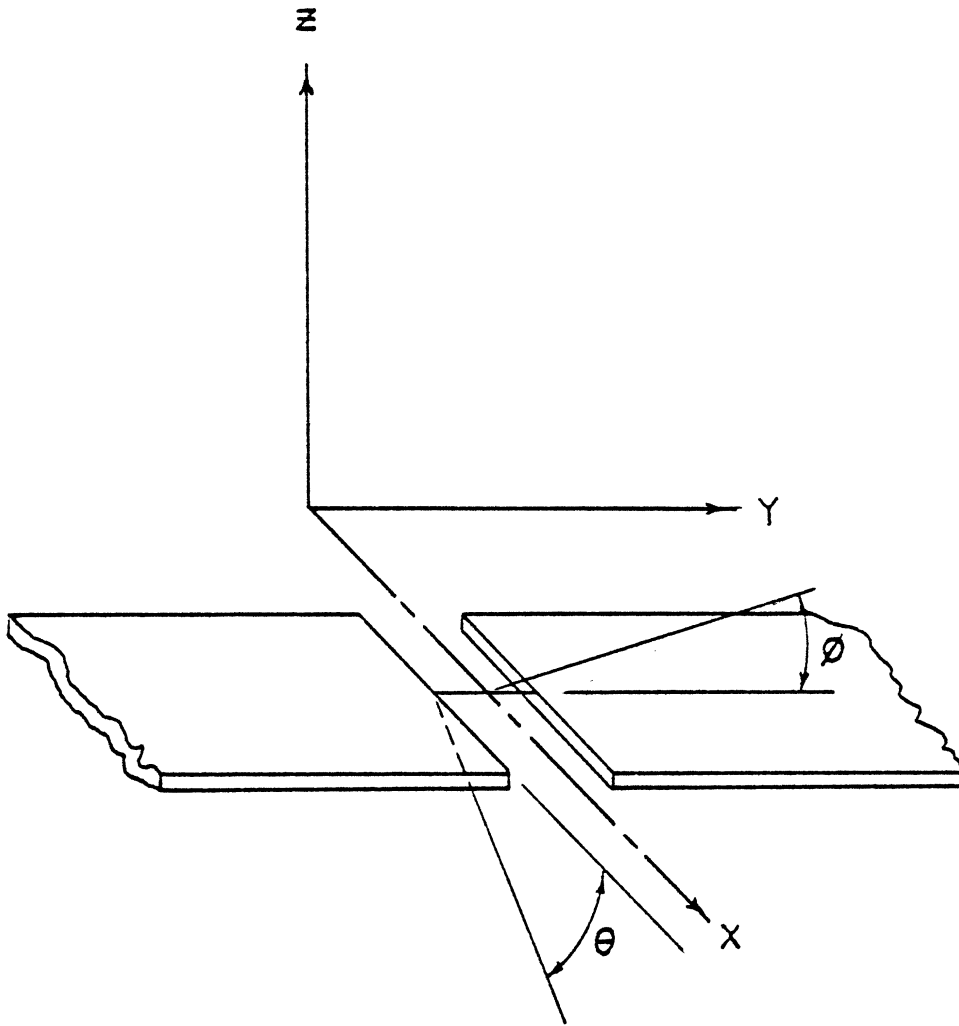
When the OASIS satellite is not docked to an Orbiter, it is in standby mode. Here power from the solar array or batteries is supplied to OASIS subsystems only. During sunlit periods, deployment of two sub-blankets (18.21 ft or 5.55 m) of each wing supplies ample power for subsystems and battery charging. (These sub-blankets, however, will suffer an 8% per year degradation due to radiation (see Section 3.3.2), requiring four sub-blankets per wing for standby mode after about 1 year of operation. This 15.4% deployment is used in orbital drag calculations, Chapter 5.) The remainder of the solar array will remain stowed to avoid this radiation degradation. No distinction is made at this point between subsystem power requirements for standby versus operational mode.

OASIS is in full operational mode when supplying power to an Orbiter and/or payloads. Deployment of the solar array from standby mode to maximum extension for operational mode will take approximately 30 minutes. In this mode, BOM (beginning-of-mission) power available to the Orbiter and payloads is 36.0 kW, and EOM (end-of-mission) power is 32.9 kW (see Table 3.1). This assumes average solar cell exposure of 1 year out of the mission lifetime of 5 years.

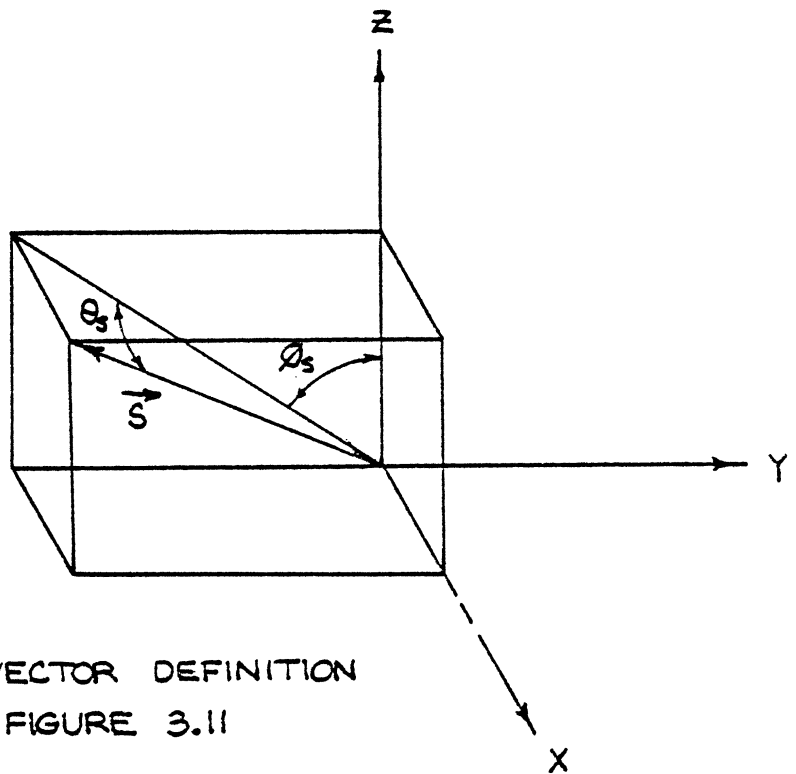
### 3.8.2 Solar Array Pointing Considerations

For the solar array pointing system, certain aspects of operation must be considered. Limits of travel of the array and maximum angular rates provided by the pointing motors may put restrictions on both orientations for normal operational mode (pitch, roll, and yaw at approximately orbital rate) and maneuvering programs before or after main propulsion burns.

The OASIS solar array is pointed by means of two pointing motors, one providing rotation about the satellite x-axis, the other, rotation about a longitudinal axis along the array wings. Angles of rotation, measured about these axes from the stowed orientation are  $\phi$  and  $\theta$  respectively (see Figure 3.10). This provides two degrees of freedom in pointing the array and ensures the ability to point at the sun, no matter where it is with respect to the satellite. The sun vector  $\vec{s}$  will be defined as a unit vector pointing towards the sun.



SOLAR ARRAY ROTATION ANGLES  
FIGURE 3.10



SUN VECTOR DEFINITION  
FIGURE 3.11

Its direction is defined by angles  $\phi_s$  and  $\theta_s$  (Figure 3.11). The solar array is then correctly aimed for  $\phi$  and  $\theta$  equal to  $\phi_s$  and  $\theta_s$ , respectively. Slip-rings are used to transfer power from the solar array to the solar array distributor, allowing continuous rotation in either degree of freedom. This system is described in Section 3.5.2.

Maximum angular rates for the array will depend both on the array pointing motors and on structural analysis of the array wings. Certain problem areas, however, can be identified. When the sun vector coincides with the positive or negative x-axis,  $\phi$  can be any angle. If the sun vector now changes, the solar array may not be able to follow it without an instantaneous change in  $\phi$ . During normal operational periods with no changes in pitch, roll, or yaw, the solar array would be tracking the sun as it passed through this point and no discontinuity in  $\phi$  would be encountered. However, while the satellite is maneuvering, this situation can occur. The amount of maneuvering that can be done with the wings extended has to be determined, but the batteries may have to be used and/or the array retracted. Maximum  $\dot{\phi}$  for normal operation will occur when the sun vector passes close to the x-axis. For a closest approach of  $1^\circ$ ,  $\dot{\phi}$  must be greater than  $3.8^\circ/\text{sec}$ . This effect may restrict the orbital orientation of the OASIS/Orbiter combination.

### 3.8.3 Sun Synchronous Orbit

It has been proposed that the OASIS satellite be used in a sun synchronous orbit. Several alterations to the electrical power system and its operation must be made in this case.

Orbiter payload weight is severely restricted for launch into sun synchronous orbit. In order to meet this requirement, OASIS satellite weight must be reduced. Since there are no orbital shade times, the battery system must supply power only for the launch and deployment phase and Orbiter docking times. Two batteries, with a useable energy of 2.7 kW-h are adequate. Thus 18 charger/battery pairs can be removed. Each pair weighs 720 lb (326.6 kg), reducing satellite weight be 12960 lb (5879 kg).

For the major part of the mission, this battery charging is not needed and the solar array only needs to generate 44 kW for full operational mode power. Two options are available for solar array deployment, either to generate more power than originally planned, or to reduce the solar array size. Generation of more power is not considered feasible for this design first because of added heat rejection requirements by the thermal control system and second the need to upgrade the internal wiring, regulators and umbilical buses to carry

the added power. Preliminary sizing indicates that full power could be supplied by 7 sub-blankets per blanket instead of 13, reducing the solar array wing length to 127.4 ft (38.83 m). This further reduces the satellite weight by 6/13 of the total array weight (Table 3.3), or 1935 lb (877.7 kg). In this orbit, standby mode power can be supplied by two sub-blankets on each side, even after 5 years of exposure degradation.

### 3.9 REFERENCES

1. R. S. Bogner and A. A. Uchiyama, "Coordinated NASA Nickel-Cadmium Battery Technology Program," AIAA Paper 77-516, presented at the AIAA Future of Aerospace Power Systems Conference, St. Louis, Mo., March 1-3, 1977.
2. "Design Data for Space Power Systems," Bendix Corporation, 1973.
3. "A Forecast of Space Technology, 1980-2000," NASA SP-387, January 1976.
4. P. Goldsmith and G. M. Reppucci, "Advanced Photovoltaic Power Systems," AIAA Paper 77-506, presented at the AIAA Future of Aerospace Power Systems Conference, St. Louis, Mo., March 1-3, 1977.
5. Mr. Jack Keller, personal communication, NASA Lewis Research Center, Cleveland, Ohio.
6. R. L. Kerr and D. F. Pickett, "Present Trends in Space Batteries for the 1980's," AIAA Paper 77-482, presented at the AIAA Future of Aerospace Power Systems Conference, St. Louis, Mo., March 1-3, 1977.
7. R. Lanier, "A Nickel-Cadmium Battery Reconditioning Circuit," NASA TN D-8508, Marshall Space Flight Center, Alabama, June 1977.
8. Millman and Halkias, Integrated Electronics, McGraw Hill, 1972.
9. NASA Workshop on Small Self-Contained Payloads, Washington, D. C., November 11, 1977 (J. Hudgins, Goddard Space Flight Center).
10. "25 kW Power Module Preliminary Definition," Marshall Space Flight Center, Alabama, September 1977.
11. E. L. Ralph and F. Benning, "The Role of Solar Cell Technology in the Satellite Solar Power Station," Spectrolab.



12. "Satellite Solar Power Station," Student Project, Department of Aeronautics and Astronautics, Massachusetts Institute of Technology, 1973.
13. Solar Cell Array Design Handbook, Volumes 1 and 2, NASA Jet Propulsion Laboratory, Pasadena, California, October 1976.
14. "Solar Power Satellite Concept Evaluation," NASA JSC-12973, Johnson Space Center, Houston, Texas, July 1977.
15. "Space Shuttle System Summary," Space Division, Rockwell International, May 1975.

4  
THERMAL CONTROL

4.1 INTRODUCTION

In order to increase the Orbiter mission capabilities in space a supplementary heat rejection system must be provided. The OASIS satellite incorporates a freon-radiator cooling system to reject waste heat produced by the payloads in the Orbiter and by the satellite itself.

4.2 SUMMARY AND CONCLUSIONS

4.2.1 System Overview

The Thermal Control System for the OASIS satellite is similar to the engine cooling system on a modern automobile. Freon (or water) carries the waste heat from the Orbiter to the interface heat exchanger in the satellite. Here the heat is transferred to the satellite's coolant (Freon 21), which in turn is pumped to the radiators where the heat is rejected to space. For internal cooling of the satellite, the freon is pumped past cold plates, on which various electronic components are mounted, then to the radiators.

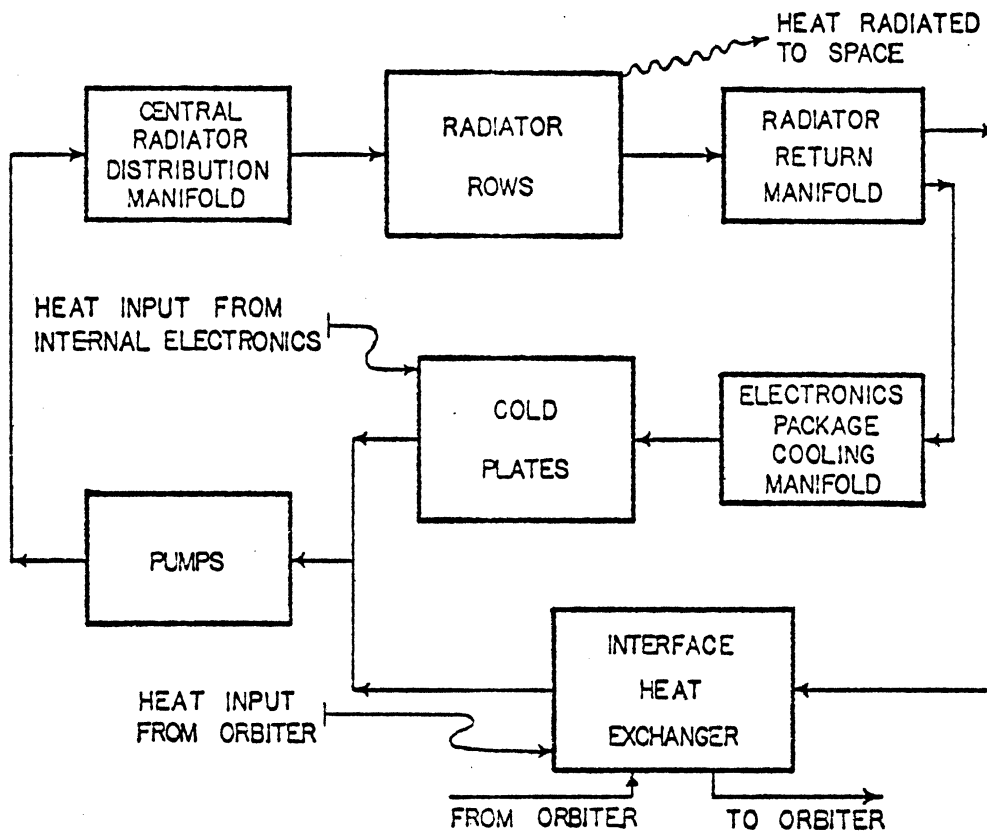


FIG 4.1 THERMAL CONTROL SYSTEM DIAGRAM

#### 4.2.2 Conclusions

a) Through this system optimum temperatures can be maintained on board the Orbiter, not only for extended missions, but also for missions which require greater amounts of heat rejection. This will increase the variety of missions which the shuttle Orbiter will be able to perform.

b) By maintaining optimum operating temperatures of the electronic equipment on board OASIS, better efficiencies will be achieved, and the OASIS components will have a longer lifetime, enabling the satellite to remain in space for longer periods of time without equipment failure.

#### 4.3 DISCUSSION

##### 4.3.1 Radiators

a) The three large rectangular shaped objects protruding from the aft end of the OASIS satellite are the heat rejection radiators. The mounting configuration is based on two major design requirements: 1) to keep the primary radiating surfaces from overlapping any other heat producing surfaces, i. e.

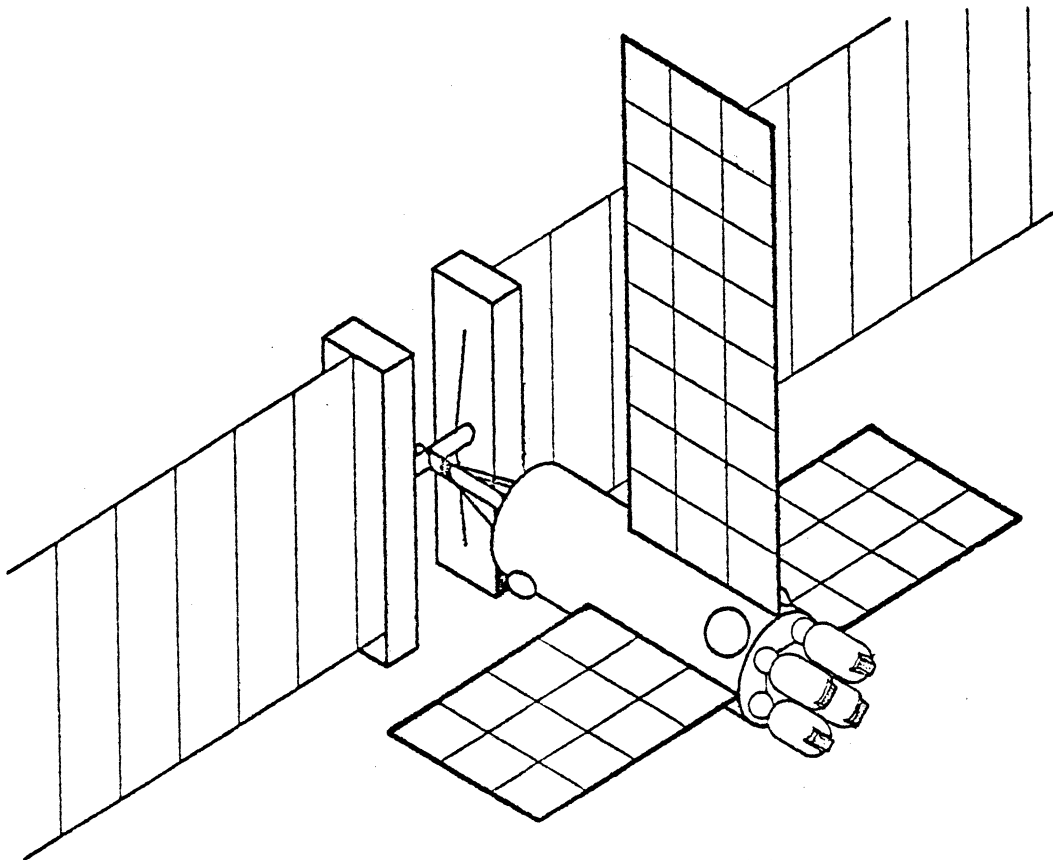


FIG 4.2 RADIATOR CONFIGURATION

the solar panels. This improves the efficiencies of both systems by reducing the input radiant energy to the respective systems; and 2) to facilitate shuttle docking by leaving one side of the satellite free of large obstructions.

b) The radiators are modular in construction to facilitate assembly in space and future expansion. The 2400 ft<sup>2</sup> (216 m<sup>2</sup>) of radiator surface necessary to reject 50 KW (to accommodate 39 KW produced plus 11 KW transferred from the Orbiter) of heat to space is configured in the following manner: Each of the two side radiators have 600 ft<sup>2</sup> (54 m<sup>2</sup>) of surface area (double sided radiators) and are made up of 12 radiator panels.

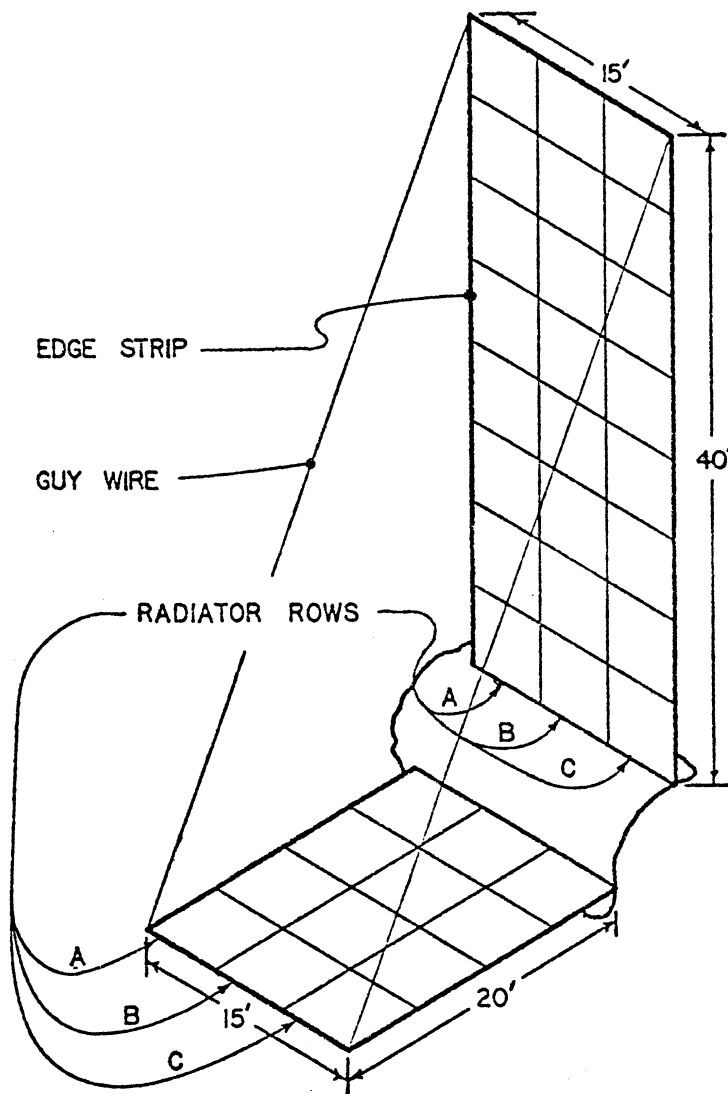


FIG 4.3 PANEL CONFIGURATION

The top radiator protrudes twice as far from the satellite as the side radiators yielding 1200 ft<sup>2</sup> (108 m<sup>2</sup>) (double sided radiator) of radiating surface consisting of 24 radiator panels.

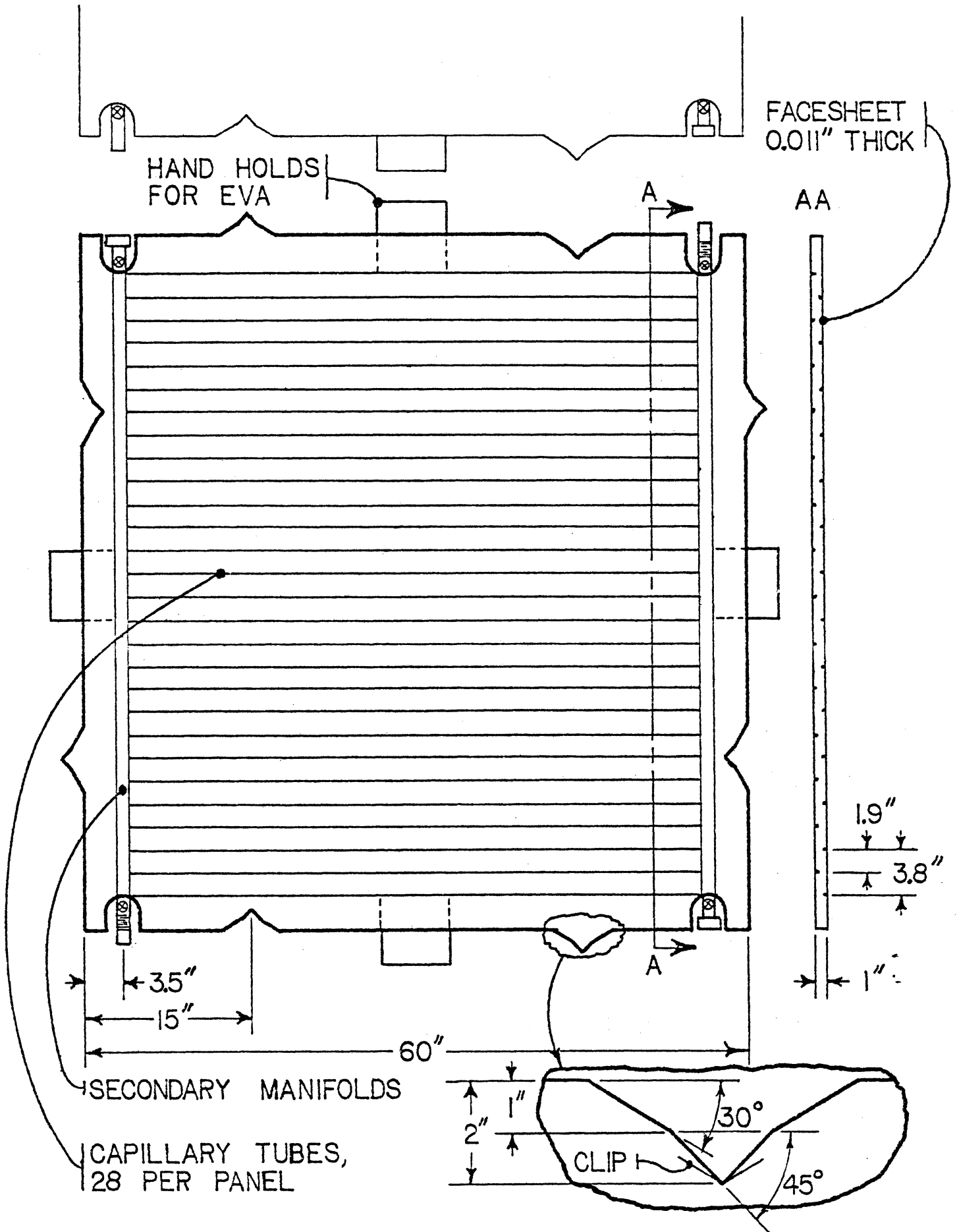


FIG 4.4 RADIATOR PANEL DETAIL

c) The building blocks of the Thermal Control System are the radiator panels. The 48 panels used in the system are identical in design to provide economy in construction, ease of assembly in space and the possibility of system expansion. The panels are made of honeycomb aluminum, as used in the shuttle Orbiter radiator. The face sheet is coated with highly reflective silver backed Teflon, already developed for NASA (Reference 6), to maximize heat rejection and minimize heat absorption from the Sun and Earth. It has been found that the radiators work best when they are not facing the Sun; however, the radiator is still capable of rejecting heat when it is directly facing the Sun. Each row of panels contains a coolant loop; the loops of adjacent rows do not connect in the radiators, but rather at a manifold inside the OASIS satellite. In the radiator rows the freon to be cooled flows through secondary supply manifolds to very small (0.19 inch diameter (4.75 mm)) capillary tubes bonded to the inner surface of the radiator. These tubes transfer the heat from the fluid to the radiator surface. The "cold" freon flows from the capillary tubes to secondary return manifolds and leaves the radiator row. Parallel flow through the radiator panel was deemed the best alignment as opposed to a snake configuration because there is a smaller pressure drop across the capillary tubes. Also, the parallel arrangement weighs less and costs less than other arrangements.

d) By the use of "snap-lock" panel connectors and positive isolation disconnects for fluid connections, the three radiators can be easily assembled and disassembled by astronaut EVA, while providing structural integrity to the system. Further structural support is provided by radiator edge strips and guy wires. The entire extra-vehicular assembly of the radiators is rather simple. For launch the 48 radiator panels, precharged with freon, will be stacked in the Orbiter cargo bay. All that is required of the astronaut is to transport the panels from the cargo bay to the radiator under construction, make the necessary connections and open the appropriate valves to complete the freon loops. The entire construction operation is expected to take between 4 and 8 hours of EVA.

#### 4.3.2 Coolant Loop

a) As previously described there are two primary sources of waste heat which the Thermal Control System must handle (the Orbiter and the internal electronics of the satellite). Included in the docking mechanism is a pipe to connect the shuttle Orbiter's cooling system to the heat exchanger on board the OASIS Satellite. The Orbiter's pumps provide the necessary flow rate within this loop. A quick disconnect coupling is used at the docking port as a fail-safe measure. Once the heat is transferred through the heat exchanger to the satellite's coolant, the pumping responsibility rests with the OASIS pumps. The heat exchanger is similar to that developed by NASA for the NASA Power Module (Reference 4).

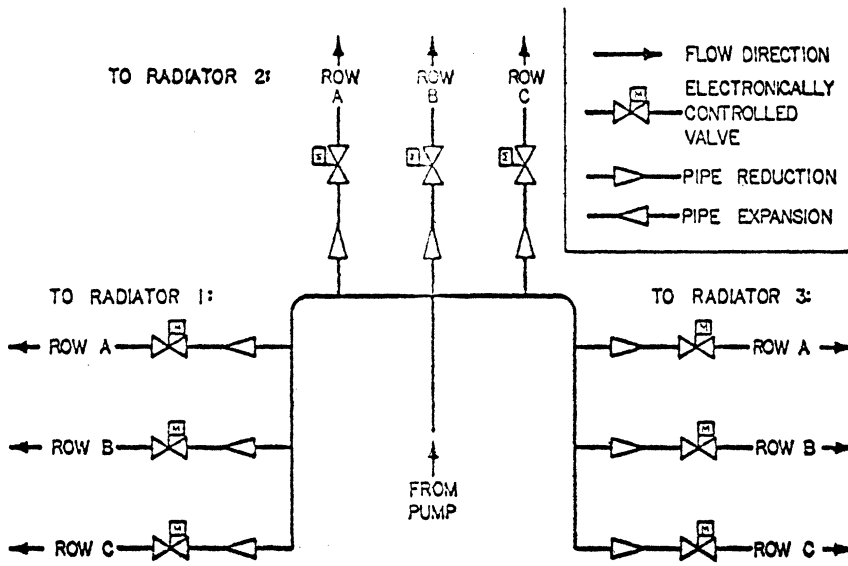


FIG 4.5 RADIATOR DISTRIBUTION MANIFOLD

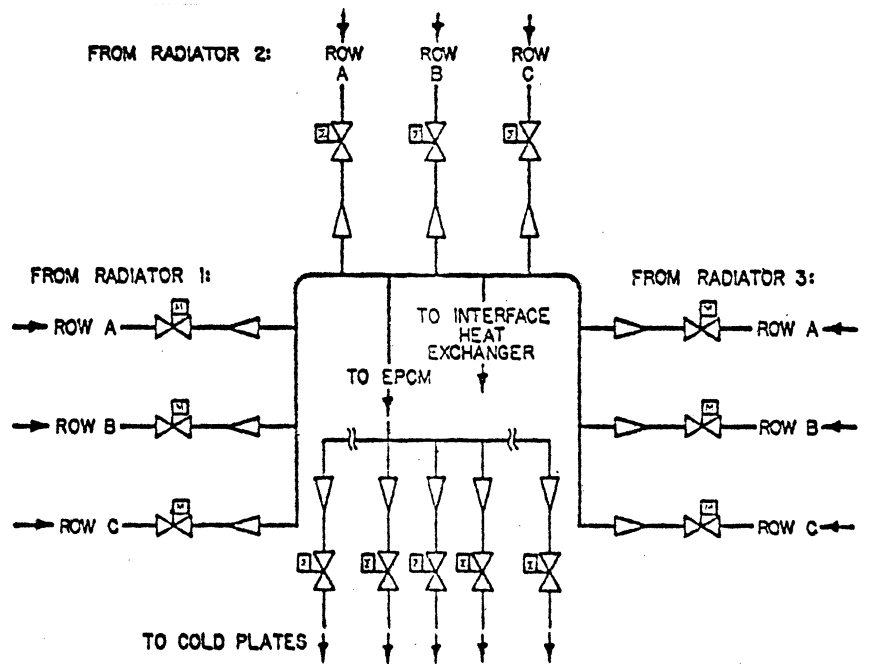


FIG 4.6 RADIATOR RETURN MANIFOLD AND ELECTRONICS PACKAGE COOLING MANIFOLD

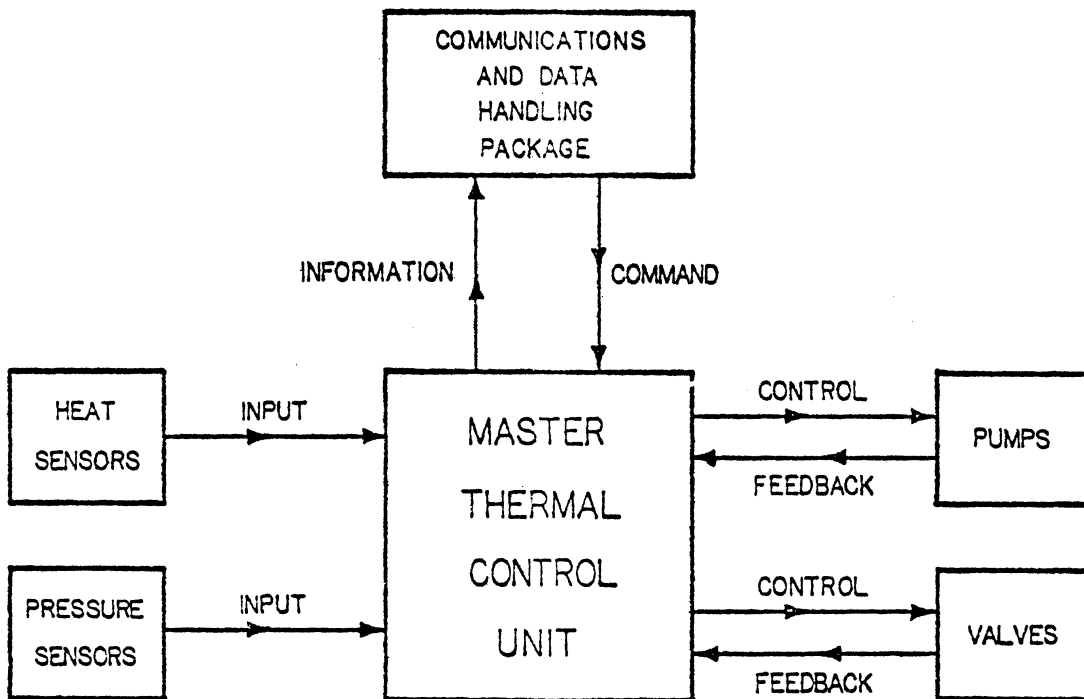


FIG 4.7 THERMAL CONTROL AUTOMATIC CONTROL SYSTEM

b) The pumps used are variable speed electric pumps, capable of providing a flow rate of 2500 to 3000lb/hr (1136 to 1363 kg/hr) for 20,000 hours (Reference 4). To extend the system lifetime, it is designed to use two pumps in parallel. This allows the pumps to run at lower speeds, extending the overall lifetime, and provides a back-up should either pump fail. The electrical power required for each pump is 0.4 KW. The pumps will maintain a pressure throughout the system high enough that the freon will remain in the liquid state.

c) From the pumps, the freon coolant flows through a 3 in (7.62 cm) diameter pipe made of 5083-H32 aluminum, a material chosen because of its ability to provide high strength weld joints. This pipe carries the coolant to the Central Radiator Distribution Manifold (CRDM). By use of electronically controlled valves the CRDM directs the coolant to the appropriate radiators determined by the heat load being carried and radiator conditions. In the event of a radiator failure (micro-meteorite penetration of tube, etc.) this manifold, in conjunction with the Radiator Return Manifold (RRM), isolates the effected radiator row.

d) After being cooled in the radiators, the freon flows to the Radiator Return Manifold (RRM). Some of the "cold" freon flows from the RRM back to the heat exchanger to repeat the cycle. The remainder of the "cold" freon flows from the RRM through the Electronic Package Cooling Manifold (EPCM) and then past cold plates. These are aluminum plates, similar in concept to the radiators, where heat is transferred from the plate to the freon being piped through it. The satellite's electronic components (radios, batteries, pumps, etc.) are mounted on these plates and the components transfer the heat produced to the plates through metal to metal conduction. Thus, the components are maintained at their optimum operating temperatures. The Electronics Package Cooling Manifold (EPCM) directs the "cold" freon to the desired cold plates.

#### 4.3.3 Control

a) Because the OASIS satellite is unmanned, the entire Thermal Control System must be automatically regulated. Input for the automatic control comes from heat sensors and pressure sensors strategically placed throughout the cooling system. These sensors are used to detect temperature and pressure changes in the system and relay this information to the Master Thermal Control Unit (MTCU). The MTCU analyzes this information, compares it to programme specifications and other data, and then gives output in the form of changes in pump speed and valve line-up. Valve positions and pump status information is returned to the MTCU as updating feedback. The MTCU accepts command



inputs through the Communications & Data Handling package and provides information output (temperatures, pressures, valve status, pump status, flow rate, etc. ) to the Communications & Data Handling package.

#### 4.3.4 Other Areas

a) An inexpensive yet effective method of maintaining optimum temperatures in a satellite is through insulation (Reference 2). The inner surface of the OASIS satellite's main body is covered with aluminized Mylar 0.5 inches (1.27 cm) in thickness. The outer surface is coated with S13-G white paint to minimize the heat absorbed from solar and Earth radiation.

b) It was determined that the solar array is capable of rejecting its own excess heat to space without exceeding its optimum operating temperature range. Therefore, no heat rejection is supplied by the Thermal Control System.

c) The OASIS satellite propulsion system is also self sufficient with respect to thermal control.

d) Freon was chosen as the coolant fluid because of its availability, its wide working temperature range, its efficiency as a coolant, and the fact that it contracts when it freezes.

e) In the past, the primary method of thermal control for University of Michigan satellites has been through passive systems, such as heat pipes. Such systems were rejected for Project OASIS because of their inability to handle the high heat loads associated with the satellite's mission. It is noted that with research this system might be able to meet the high heat load requirements.

f) Also considered for use was a thermionic generator (direct conversion of heat to electricity). This was rejected because of its low thermal efficiency and the high cost involved. If advances in this type of system can be made, its use may become profitable.

g) No thermal control services are provided by OASIS during the satellite launch phase, because during this time period all the systems within OASIS are dormant.

#### 4.4 REFERENCES

1. Project STRATUM, Department of Aerospace Engineering, The University of Michigan, Appendix J.

2. Lucas, J. W., Fundamentals of Spacecraft Thermal Design, "Progress in Astronautics and Aeronautics" Volume 29, MIT Press, Cambridge, Ma, 1972.
3. Mason, J. L., 'Vehicle Energy Balance,' UCLA, Los Angeles, Ca, September 1961.
4. '25 KW Power Module Preliminary Definition,' NASA Marshall Space Flight Center, Al, September 1977.
5. Space Planners Guide, USAF Air Force Systems Command, July 1965.
6. Williams, J. L. and French, R. J., 'Space Shuttle Orbiter Radiator System,' ASME, New York, April 1977.

## PROPULSION

## 5.1 INTRODUCTION

The baseline design of OASIS took on a new dimension of versatility by adding a propulsion unit. The propulsion unit for OASIS has enabled it to utilize a greater range of orbital altitudes. As a result, OASIS will have the same capability as the Orbiter of attaining altitude heights of up to 600 nm (1111 km). In addition, the system will relieve the shuttle from rendezvous launch window constraints. The shuttle will no longer have to rely on one ideal launch time since OASIS has the ability to phase its orbit to that of the shuttle.

It is the purpose of this chapter to describe in detail the final design of the propulsion unit used in OASIS. The chapter is organized such that the constraints, the components and the performance of the system are the main areas covered.

## 5.2 SUMMARY

The propulsion unit for OASIS is based on a modular design utilizing four propulsion kits which are existing components from the Martin Marietta Aerospace Teleoperator presently under design as well as a Viking Orbiter subsystem. Each kit includes the pressurant tank, propellant tank, rocket thrusters and all necessary plumbing and structure. All kits are complete and independent units requiring only electrical power from OASIS for operation.

A major advantage of the system is that EVA can be used to maintain the propulsion system in space. All kits are designed to be removed separately when the tanks are empty, and replaced with a refurbished one. Another advantage of the propulsion unit is the use of monopropellant fuel. Besides simplifying the system, hydrazine monopropellant is also a very stable fuel which will allow it to be transported safely by the Orbiter.

## 5.3 MISSION CONSTRAINTS AND CONSIDERATIONS

OASIS is equipped with a propulsion unit that gives it the capability to make altitude changes. The Orbiter altitude range of operation is up to 600 nm (1111 km). Therefore any propulsion unit that is chosen has to have the  $\Delta V$  capability to operate in this range. Another consideration is the magnitude of the majority of altitude changes in which OASIS will be involved. An altitude change of 400 nm (741 km) for instance, requires a large  $\Delta V$  and therefore large amounts of propellant. The propulsion system has the capability to handle this type of mission. The majority of missions, however, require far less  $\Delta V$  because of the smaller altitude changes needed.

### 5.3.1 Altitude Range and Orbit Selection

One of the users of OASIS is the Orbiter Spacelab. Over a period of 5 years, this payload will need OASIS for approximately 42 missions. In Table 5.1, the altitude range of OASIS needed during these missions is given at the inclination angle of  $50^{\circ}$  (Reference 1).

<u>Inclination (Deg)</u>	<u>Altitude Range (N. M. )</u>	<u>No.</u>	<u>%</u>
28.5	189-216	14	16
50	135-240	59 (42)	67
57	194	1	1
90	189-230	14	16

#### Missions Utilizing Power Module

It can be seen from the table that OASIS missions for Spacelab are primarily in the altitude range of 135 nm (250 km) to 240 nm (445 km).

Another location where OASIS may be needed is in a sun synchronous orbit. The orbit inclination is in the range of  $96^{\circ}$ - $101^{\circ}$  and an altitude range of 100 nm (185 km) to 500 nm (927 km). Since OASIS is not capable of large plane changes, another OASIS satellite will have to be launched into such an orbit.

## 5.4 DESIGN CONSTRAINTS AND CONSIDERATIONS

### 5.4.1 Maximum Acceleration

Maximum allowable acceleration of the in-orbit OASIS configuration is limited by the resulting structural deflections and stresses induced in the deployed solar array and thermal radiators. Although it is possible to retract somewhat the solar array during orbital maneuvers, the thermal radiators are fixed. Thus the propulsion thrust output must be designed so as not to exceed the above acceleration limits.

The thrust for the standard 4-kit configuration propulsion system along with its respective maximum accelerations can be seen in Table 5. 2.

<u>Orbit Inclination</u>	<u>Thrust</u>	<u>OASIS Initial Weight</u>	<u>Maximum Acceleration</u>	
			<u>First burn</u>	<u>Final burn</u>
50°	1248 lbf (5551 N)	37844 lbs (17210 hg)	.033 g	.039 g
96°-101° (Sun Synchronous)	1248 lbf (5551 N)	23100 lbs (10478 hg)	.054 g	.071 g

Table 5. 2

#### 5. 4. 2 Safety Factors

OASIS has two design constraints in regard to safety factors for propulsion. The first consideration involves the safety factors of the propellant while OASIS, or later separate refueled propellant units, are being transported into space. The second involves a fail-safe system for the rocket engine modules (REM). Such a system is needed in case a REM should fail to shut down after a burn.

In regard to the first consideration, the safest propellant for transport is hydrazine monopropellant. By being a monopropellant, there is no need for an oxidizer, thereby reducing the complexity of the system and the possibility of leaks within it. Hydrazine will not react until it is brought into contact with the catalyst in each REM. Therefore, if there is a leak in one of the propellant tanks, the possibility of an explosion is greatly minimized. Hydrazine will not react without the catalyst until the temperature reaches 491F (255 C) (Reference 2). The use of hydrazine meets the first design constraint regarding transport safety.

The second design constraint requires the use of a fail-safe system for the REM. First of all, there is a mechanical safe-fail system built into each REM. In order for the monopropellant to come in contact with the catalyst for each burn, a solenoid valve has to open to allow the fuel to flow into the thrust chamber. If at any time the power is shut off to the propulsion system, all the valves will return automatically to the closed position. In the event that one or several of the REM's should remain open, there is a fail-safe system that shuts off the propellant flow from the tank. In each unit, there are two isolation valves which can act independently of each other, but are both capable of shutting off the fuel flow from the tank. The isolation

valves are closed by commands from the communication systems. There is also a back-up system should the isolation valves fail to close. This system utilizes a dump valve that is located on each propellant tank. In the event that all systems fail to operate, the dump valve can be activated to open and empty the remaining amount of propellant in the tank. In summary, for each hydrazine tank, there are two fail-safe systems in addition to the safe-fail system built into the REM.

#### 5.4.3 Convenience of EVA

One of the prime considerations in the selection of the propulsion unit for OASIS is that it can be refurbished and checked by EVA quite easily. Based on a current design used for a teleoperator, each propellant tank, pressurant tank, and REM's are placed on a structure as one unit. When empty, each unit is exchanged with a refurbished one. In addition to making EVA easier and reducing the chance of an astronaut coming in contact with the caustic hydrazine fuel since no fuel connections need be made or broken, each component of the used system can be overhauled on earth while another one is used in space. The convenience of using an existing system based on an integrated design can be seen.

#### 5.4.4 Weight Considerations

A design weight for OASIS was initially set at 40,000 lbs (18182 kg). Of that 40,000 lbs, a limit of 10,000 lbs (4546 kg) was allowed for a propulsion system. By using existing systems, the propulsion unit in its 4-unit configuration has a weight of 7600 lbs (3455 kg) which is well within the limit. A complete breakdown of weights is given in Appendix C.

#### 5.4.5 Positioning of the Propulsion Unit on OASIS

The propulsion unit is positioned at the end such that no damage can be done to the solar array panels. In addition, by having the propulsion unit entirely at the end, the center of thrust acts along the longitudinal c. g. line of OASIS. This minimizes the possibility of unwanted moments on OASIS during a burn.

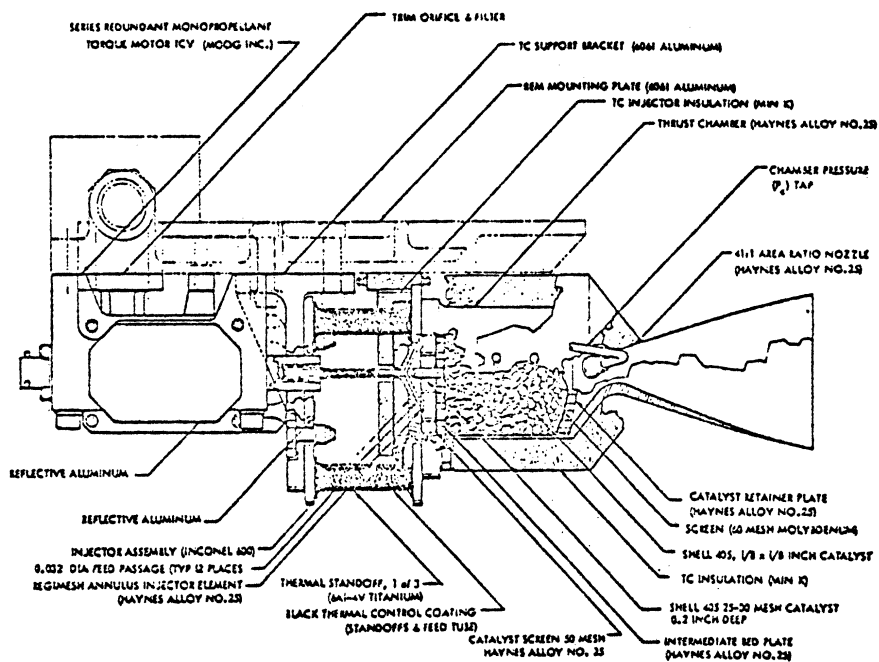
### 5.5 COMPONENT DESCRIPTION OF THE PROPULSION UNIT

#### 5.5.1 Rocket Engine Modules (REM)

The rocket engine modules are based on a design used for the USAF Transtage Vehicle for the Titan III missile. For the OASIS propulsion unit, there are twelve REM's per each integrated unit, therefore, for the 4-unit configuration there are a total of 48 REMs.

Each REM is a monopropellant hydrazine thruster assembly capable of 26 LBF (116 N) of thrust with a specific impulse of 220 seconds at 360 PSIA (250 N/cm<sup>2</sup>) inlet pressure. The weight of each REM is 15.2 lbs (7 kg) maximum. The minimum on-time of each REM is 40 milliseconds, and the operating life as a function of total burning time is 1000 sec minimum, 2000 sec maximum with 12,500 pulses during this lifetime.

Thrust is developed when a solenoid valve is opened allowing the monopropellant to come in contact with the catalyst pellets in the thrust chamber. Once the hydrazine makes contact with the catalyst, there is a hypergolic reaction which causes combustion and finally thrust. The total thrust developed by the 4-unit configuration is 1248 LBF (5551 N). See Figure 5.1 for the diagram of the REM.



THE ROCKET ENGINE MODULE THRUSTER  
FIGURE 5.1

Each engine is capable of many starts and restarts. Since the only mechanism that is needed in starting the REM is the opening of a solenoid valve, problems of igniters failing and uncontrolled combustion are virtually non-existent.

### 5.5.2 Propellant and Pressurant Tanks

The propellant tank used for the OASIS propulsion system is based on those used on the Martin Marietta Aerospace Teleoperator and the Viking 75 Orbiter propulsion subsystem. The spherical tank used in the P95 program is the same helium pressurant tank utilized in OASIS.

The propellant tank is made of 6Al4V titanium. It has a volume of 43,800 in<sup>3</sup> (.7178 m<sup>3</sup>) and a mass of 93.6 lbs (42.5 kg). The tank operates at an internal pressure of 330 PSIG (230 N/cm<sup>2</sup>), and has the dimensions of 57 in (1.45 m) in length and 36.5 in (.93 m) diameter.

The pressurant tank is also made of 6Al4V titanium. It has a volume of 5300 in<sup>3</sup> (.0869 m<sup>3</sup>) and a mass of 54.8 lbs (23.9 kg). This tank operates at an internal pressure of 3000 PSIA (210 N/cm<sup>2</sup>), and is a sphere of 22.25 in (.57 m) in diameter.

### 5.5.3 Propellant and Pressurant

The propellant used in the OASIS propulsion unit is hydrazine mono-propellant (N<sub>2</sub>H<sub>4</sub>). It is chosen for this system since it can deliver the highest specific impulse of any monopropellant and is also a safe fuel especially for transport in the Orbiter.

Hydrazine has an indefinite shelf life in space. At room temperature and sealed in a glass container, it showed no appreciable decomposition for a period of one year. Longer periods of time showed the decomposition of hydrazine only resulted in a small release of ammonia. It is found that no decomposition takes place when the vapor pressure of hydrazine above the liquid is kept below 12.8 PSI (8.8 N/cm<sup>2</sup>) (Reference 2). This makes hydrazine an ideal propellant since this type of pressure is not realized within the propellant tank.

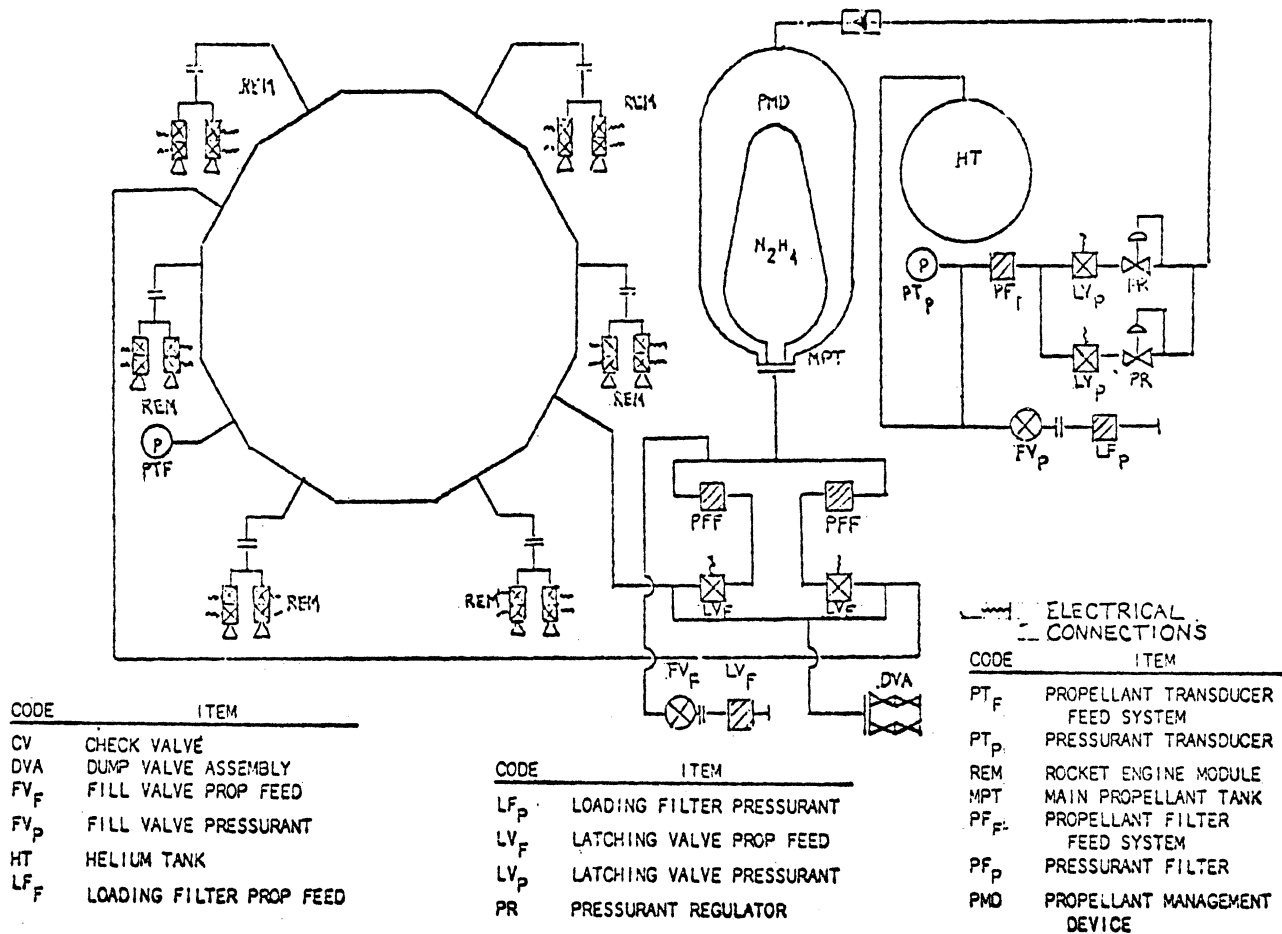
The pressurant used is helium, since it has a low molecular weight thereby resulting in a low overall weight.

### 5.5.4 Plumbing and Electrical Connections

Having the propulsion unit based on a monopropellant system greatly reduces the need for plumbing and electrical connections. A plumbing and electrical diagram is given in Figure 5.2 for each unit assembly. The electrical connections are brought together into a multiple pronged plug which is inserted into the OASIS power circuit. There are 4 such plugs located at various points in the propulsion unit main supporting structure.

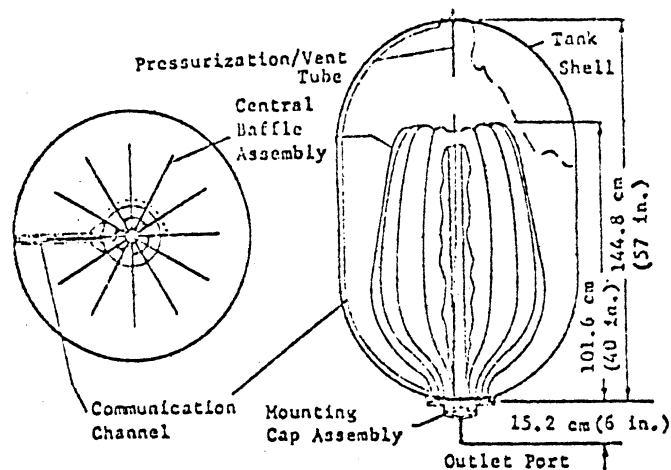
One internal system in each hydrazine tank is a propellant management device. This device allows an ullage maneuver to be unnecessary before each burn. A diagram in Figure 5.3 shows the device to be a system of vanes that makes up a baffle assembly. By virtue of the shape of the baffles in relation to the tank wall, an off axis helium ullage bubble is distorted to produce higher





PLUMBING & ELECTRICAL DIAGRAM  
FIGURE 5.2

liquid pressure at the leading end of the ullage bubble. As a result, the bubble will move toward a centered position on top of the baffles. Surface tension of the liquid creates a difference between the gas pressure and the liquid pressure at any curved liquid-gas interface. Basically, the propellant management device keeps the helium bubble at the top of the tank so that the pressurization vent tube is somewhere within that bubble. By using the pressure regulators in the helium pressurant tank system, a constant ullage bubble pressure can be maintained. As a result of keeping the helium ullage bubble at the top of the tank, and using the surface tension of the liquid, it is possible to keep the propellant at the outlet port at all times. This propellant management device insures the flow of hydrazine will occur each time a burn is initiated. (Reference 5).



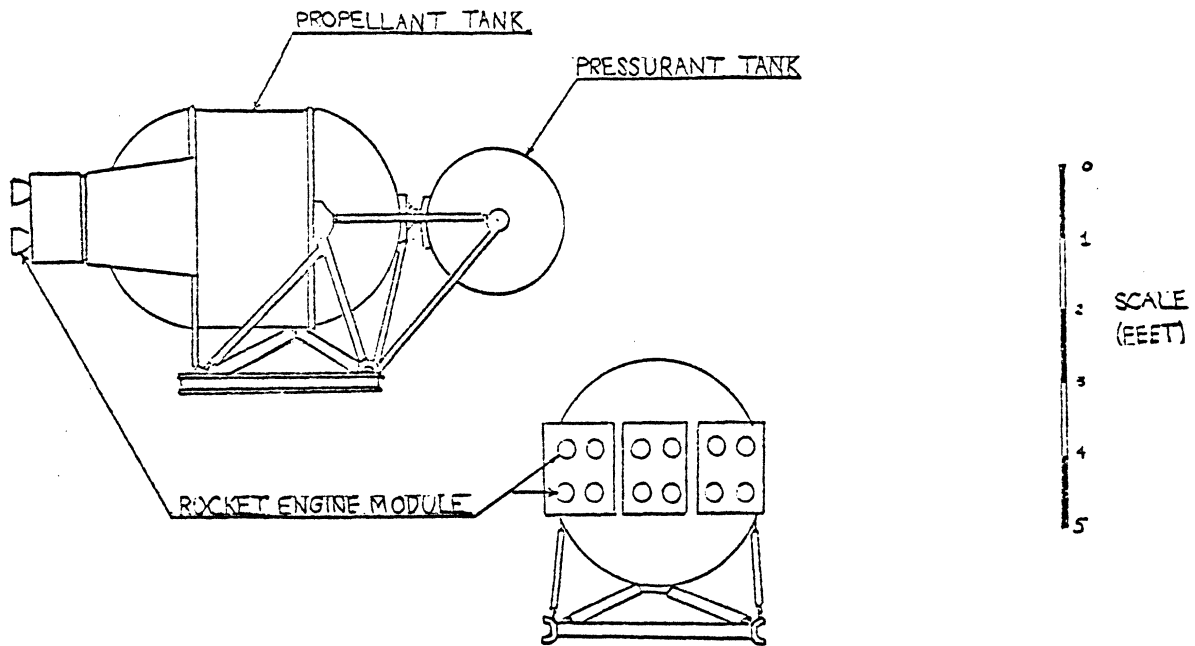
## PROPULSION MANAGEMENT DEVICE

FIGURE 5.3

### 5.5.5 Overall System

All the components as one unit or kit are seen in Figure 5.4. The overall length is 8 ft (2.44 m) and is 36.5 in (.93 m) at its widest point. Each unit assembly slides into the propulsion main frame and locks into place. The appropriate electrical connection is plugged into the OASIS power circuit, and the unit is ready for operation. The complete 4-unit configuration is seen in Figure 5.5.

The total weight of each assembly empty is 382 lbs (173 kg). With full propellant and pressurant tanks, the total weight of each unit assembly is 1900 lbs (862 kg). The complete 4-unit configuration has a total weight of 7600 lbs (3447 kg), and a propellant capacity of 6000 lbs (2722 kg).



PROPUSION UNIT  
FIGURE 5.4

## 5.6 PERFORMANCE

### 5.6.1 $\Delta V$ Capability

The  $\Delta V$  required to complete an orbit altitude change can be found in the following chapter on Orbital Operations. Any  $\Delta V$  chosen for a certain altitude change will have a corresponding burning time with a proportional amount of propellant consumption. This can be seen in Figures 5.6 and 5.7.

The  $\Delta V$  requirement is based on the following relation:

$$\Delta V = (I_{sp}) (g_o) \text{LN} \frac{W_t}{W_t - W_p}$$

$I_{sp}$  = specific impulse

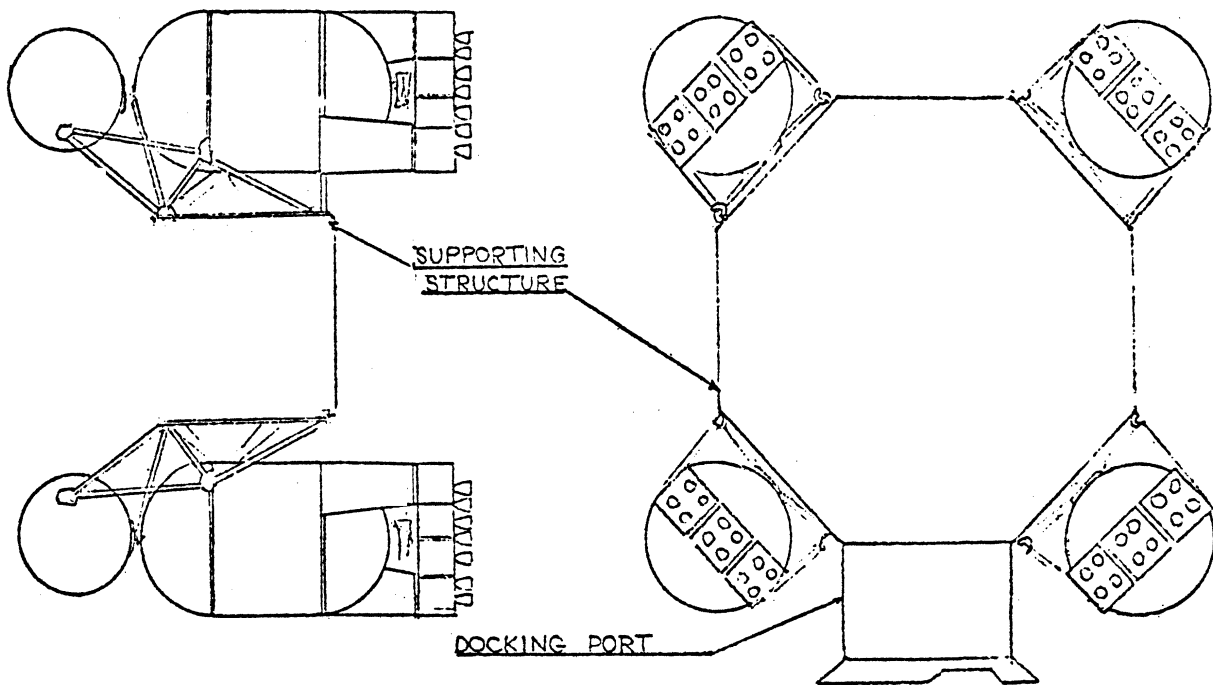
$g_o^{sp}$  = acceleration due to gravity at sea level

$W_t$  = total weight of OASIS previous to maneuver

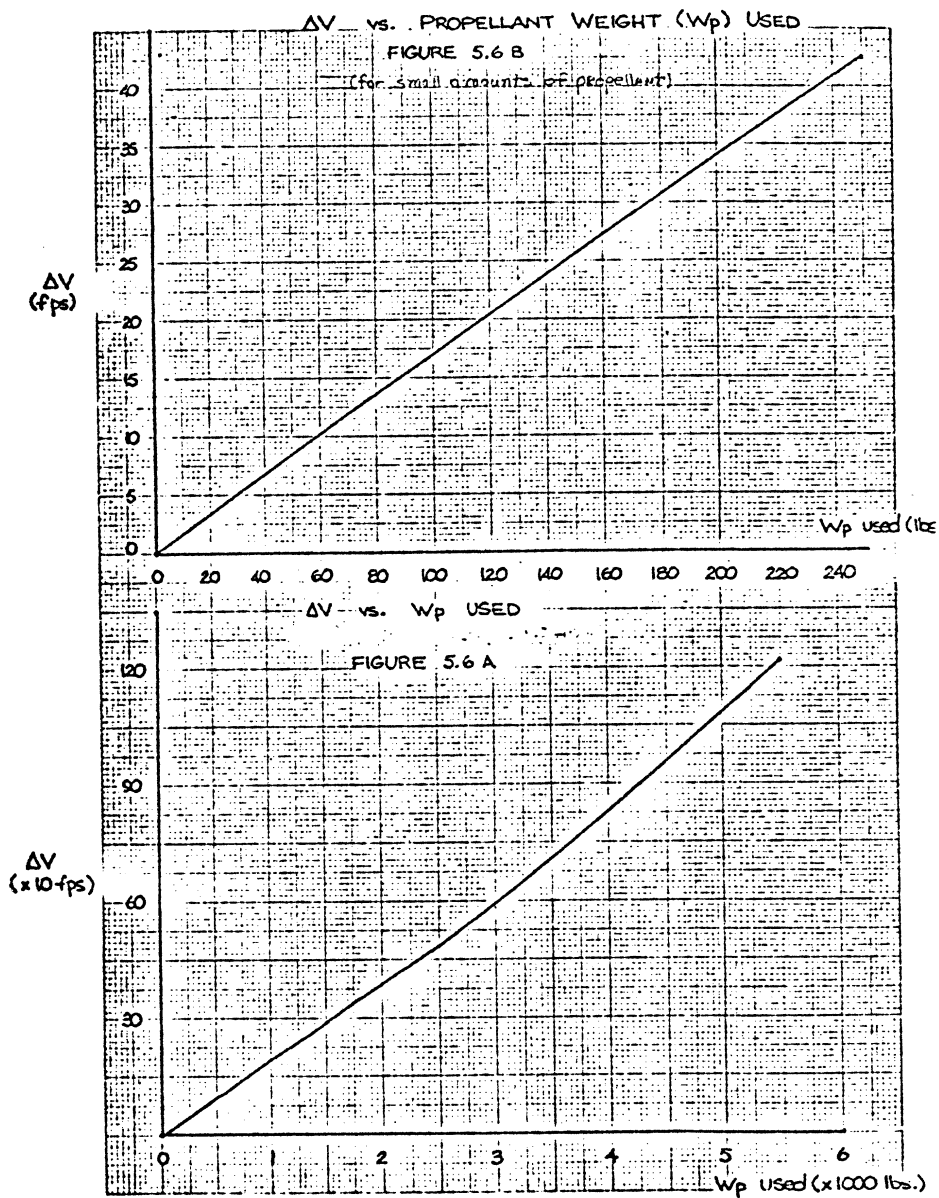
$W_p$  = weight of propellant needed for  $\Delta V$

#### Maximum $\Delta V$ Capability at 50° Inclination

<u><math>W_t</math></u>	<u><math>W_p</math></u>	<u><math>\Delta V</math> Max.</u>
37,844 lbs	6000 lbs	1222 ft/sec
17,210 kg	2728 kg	373 m/sec

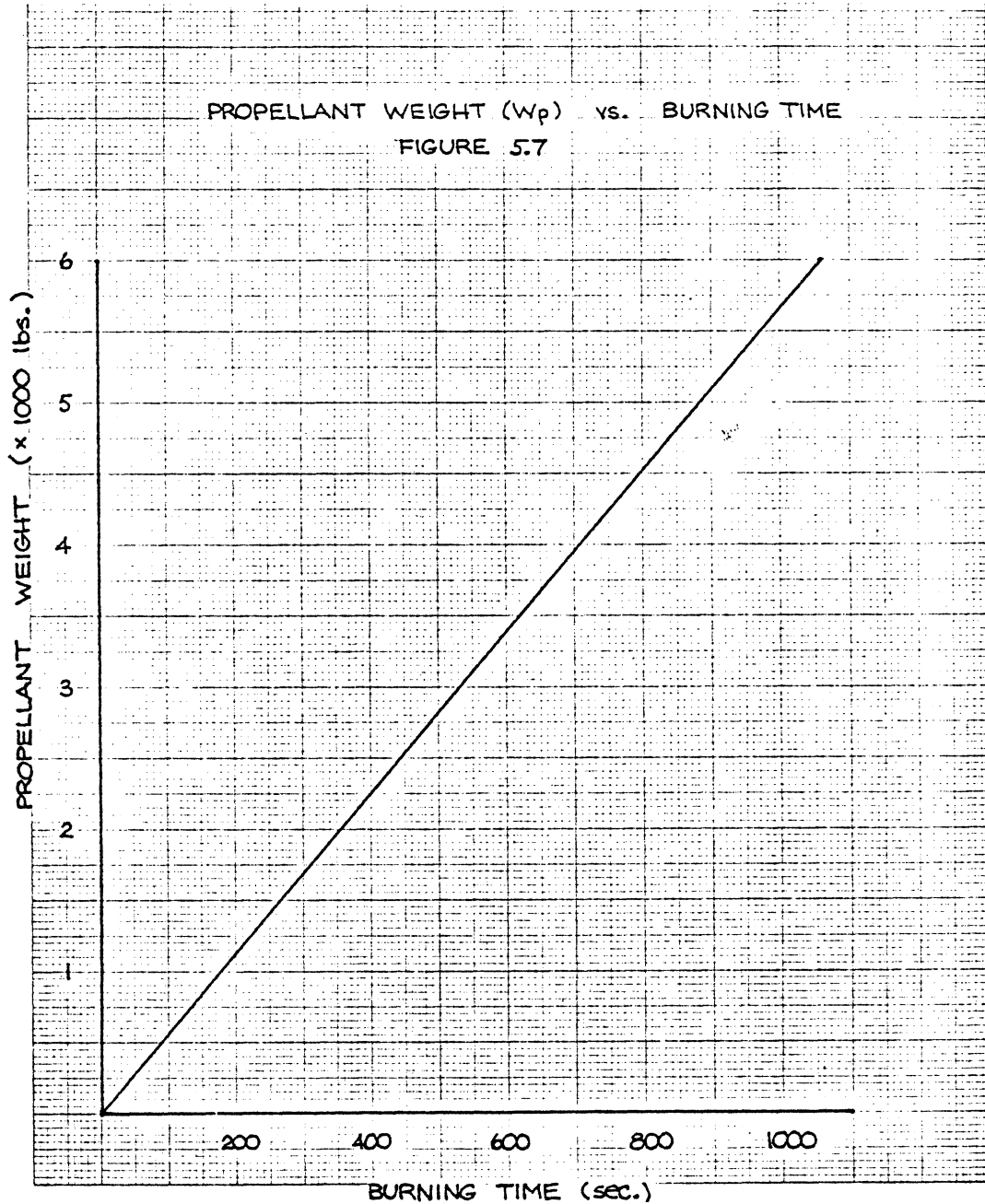


FOUR PROPUSION UNIT CONFIGURATION  
FIGURE 5.5



## Maximum $\Delta V$ Capability at Sun-Synchronous

<u>Wt</u>	<u>Wp</u>	<u><math>\Delta V</math> Max.</u>
23,100 lbs	6000 lbs	2129 ft/sec
10,478 kg	2728 kg	649 m/sec



### 5.6.2 Maximum Thrust and Burning Time

The maximum thrust is 312 lbf (1388 N) per unit. The 4-unit configuration then has a maximum thrust of 1248 lbf (5551 N).

The burning time is based on amount of propellant and thrust. It can be found from the following relation:

$$T_b = \frac{(I_{sp})(W_p)}{F}$$

$I_{sp}$  = specific impulse  
 $W_p^{sp}$  = weight of propellant  
 $F$  = thrust

The total burning time is 1058 sec (17.6 min) and represents the time of actual REM burns between refueling.

### 5.6.3 Time Between Refueling

Having to project the frequency of refurbishment of the propulsion system for OASIS requires making educated assumptions from known data. This project is based on the first assumption that nearly all of the missions using OASIS will also involve the Spacelab.

Referring to Table 5.1, it is seen that at a 50° inclination, 42 missions will need OASIS over a five year period. This averages out to be roughly eight missions each year, 70% or 6 of which will be located below 200 nm (371 km). It is assumed that those missions will require a 39 nm (52.6 km) altitude change and those above 200 nm (371 km) a negligible orbit change. For each altitude change of 39 nm (52.6 km), a  $\Delta V$  of 140 ft/sec (42.7 m/sec) is necessary. From the relation:

$$\Delta V = (I_{sp})(g_o) LN \frac{W_t}{W_t - W_p}$$

It is found that 741 lbs (346 kg) of propellant is used in this maneuver. This means that the propellant is consumed at a rate of 4447 lbs (2021 kg) every year. Since the entire system contains 6000 lbs (2728 kg) of propellant, refurbishment is necessary only once every 16 months.

## 5.7 OTHER SYSTEMS CONSIDERED

A number of other previously developed systems and variations of such were considered as a propulsion system for OASIS. Initially, it was proposed to use the entire teleoperator as developed by Martin Marietta (Reference 4). However, this meant including unnecessary navigation and communication equipment along with a cold gas propulsion system. The reboost-deorbit kits, which are in effect for the propulsion unit previously described, were deemed sufficient as the means of propulsion finally selected.

Other systems considered were the Interim Upper Stage (IUS) and the Spin Stabilized Upper Stage (SSUS) which are being designed to supplement the delivery of shuttle payloads to higher orbits and to planetary trajectories. The IUS provided too high a thrust and had a limited lifetime before replacement. The SSUS used a solid propellant engine making restarts impossible.

## 5.8 REFERENCES

1. "25 kW Power Module Preliminary Definition," NASA Marshall Space Flight Center, Alabama, September 1977, Chapter 4, p. 29.
2. Kit, Boris, Evered, Douglas: Rocket Propellant Handbook, MacMillan 1960, Chapter 7, p. 101-116.
3. "The Viking Mission to Mars," Martin Marietta Aerospace, Denver, Co., 1975
4. Covault, Craig, "Early Shuttle Mission to Skylab Planned," Aviation Week and Space Technology, November 7, 1977.
5. "Development and Qualifications of the Propellant Management System for Viking 75 Orbiter," AIAA Journal of Spacecraft, March 1977, Vol. 14, No. 3.

## ORBITAL OPERATIONS

## 6.1 INTRODUCTION

The onboard propulsion system enables OASIS to execute various orbital maneuvers. This ability makes OASIS a very versatile service satellite.

The purpose of this chapter is to discuss the aspects of orbital mechanics as they apply to OASIS.

## 6.2 SUMMARY AND CONCLUSIONS

OASIS is to be delivered to a low inclination orbit of  $50^\circ$  and 225 nm (417 km) altitude. A modified OASIS is to be delivered to  $97^\circ$  inclination also at 225 nm (417 km) altitude which will be a sun synchronous orbit. The  $50^\circ$  inclination orbit was chosen to maximize the satellites availability to the Orbiter on Spacelab missions. The altitude was selected on the basis of providing easy access to the Orbiter while still being high enough to avoid serious orbit decay problems.

The primary orbital maneuver is to execute the phasing during rendezvous with the Orbiter. This is accomplished through use of the Hohmann transfer. This feature enables the Orbiter to remain on location and still receive supporting services. Due to the large  $\Delta V$  requirements needed for orbital plane changes, the only maneuvers discussed are coplanar.

While the satellite is in the  $50^\circ$  inclination orbit the shade percentages of the orbital period range from 0% to 39% throughout the course of a year.

## 6.3 ORBITAL OPERATIONS

6.3.1 NASA Shuttle

The Space Shuttle can be launched from two locations. The Kennedy Space Center (KSC) at Cape Canaveral Florida and Vandenberg Air Force Base (VAFB) in Southern California. The range of altitudes the Shuttle Orbiter can attain is dependent upon orbital plane inclination and payload weight. Allowable inclinations from KSC are  $28.5^\circ$  to  $57^\circ$  corresponding to launch azimuths of  $35^\circ$  to  $120^\circ$ . The maximum payload that can be launched from KSC is 65,000 lb (29,484 kg). From VAFB the inclinations are  $56^\circ$  to  $104^\circ$  corresponding to launch azimuths of  $140^\circ$  to  $201^\circ$ . When launching from VAFB, the maximum payload weight is reduced to 62,500 lb (28,350 kg) at  $56^\circ$  inclination and 32,000 lb (14,515 kg) at  $104^\circ$  inclination.



### 6.3.2 Parking Orbit Selection

OASIS will be delivered to its parking orbit as an Orbiter payload. The parking orbit is selected to minimize the amount of orbital maneuvering necessary to service various shuttle missions.

#### a. Orbit Inclination

Since the primary purpose of OASIS will be to service Spacelab missions, the orbital inclination selection is based on the NASA 25 kW Power Module Preliminary Definition, MSFC which indicates that the optimum inclination angle in which to place a service satellite is  $50^\circ$ . As explained below, OASIS will not change the inclination of its orbital plane. Thus the first OASIS will be delivered to an orbit with an inclination of  $50^\circ$ . Placing an OASIS in a sun synchronous orbit would require the removal of batteries and the reduction of solar panels. This would reduce the total weight sufficiently to enable the shuttle to deliver the satellite to such a high inclination orbit. The minimum weight attainable is 23,100 lb (10,478 kg). The shuttle can deliver a payload of this weight to an inclination of  $97^\circ$  at an altitude of 225 nm (417 km), which satisfies the sun synchronous requirements.

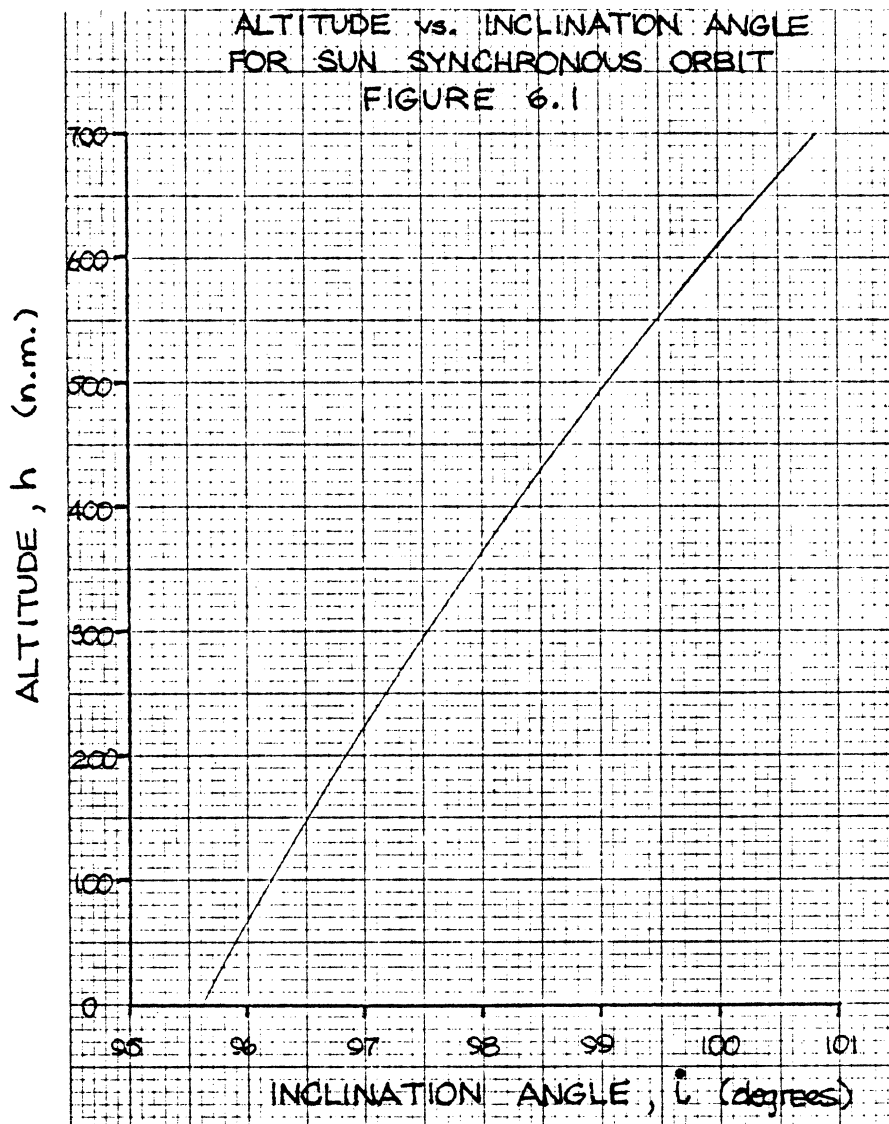
#### b. Altitude

The orbit of any satellite will tend to decay to a lower altitude due to the drag force of the atmosphere, solar wind and other effects. The higher the altitude of a given satellite, the slower the rate of its orbital decay. Thus a higher orbit is more desirable from the standpoint of orbital lifetime. The primary concern is with decay problems while OASIS is in a parking orbit rather than while it is docked with an Orbiter. The NASA Spacelab model projects that 70% of all missions at an inclination of  $50^\circ$  will be at an altitude of 200 nm (370 km) or less, and that none will be above 240 nm (444 km). So from the standpoint of accessibility, it is advantageous to keep the parking orbit below 200 nm (370 km). The drag weight parameter,  $C_D A/W$ , determines the effect of drag on a particular satellite. In order to calculate this parameter conservatively, the largest possible area was assumed. The OASIS that will be in an orbit with an inclination of  $50^\circ$  will have a  $C_D A/W = .07$ . The OASIS that will be put into a sun synchronous orbit will be reduced in weight and area, which will result in a  $C_D A/W = .08$ . On the basis of these calculations the altitude of the circular parking orbit has been selected as 225 nm (417 km). At this altitude the satellite will take more than two months for its orbit to decay to an altitude of 200 nm (370 km), yet it will still be reasonably accessible for Spacelab missions. This is acceptable, based on the assumption of one service

mission per month. It is unlikely that OASIS will be parked for more than two months, but should this be the case OASIS has the capability of re-boosting to the desired altitude.

c. Sun Synchronous Orbit

The advantage of the sun synchronous orbit is that it provides constant sunlight to the satellite. This is accomplished when the orbital plane precesses at one revolution per year, .986 deg/day. Orbital plane precession is due to the oblateness of the earth. The precessional rate is a function of altitude and orbital plane inclination. Attainment of the proper direction of precession requires orbital plane inclinations greater than  $90^{\circ}$ , i.e. retrograde precession.



### 6.3.3 Orbital Maneuvers

#### a. Available $\Delta V$

The propulsion system onboard OASIS enables the satellite to execute three types of maneuvers: altitude changes, the phasing maneuver used in rendezvous and if necessary, small orbital plane changes. The propulsion system has an available  $\Delta V$  of 1222 ft/sec (373 m/sec). Due to the comparatively high  $\Delta V$  requirements needed to execute a plane change, such maneuvers have been excluded from the nominal OASIS missions.

#### b. Altitude Changes

Altitude changes are accomplished through use of the Hohmann transfer maneuver. The geometry for a typical Hohmann transfer for rising from altitude  $h_1$  to  $h_2$  is shown in Figure 6.2. Figure 6.3 shows the  $\Delta V$  expenditure needed for transferring from a circular orbit with radius  $h_1$  to a circular orbit with radius  $h_2$ .

HOHMANN TRANSFER

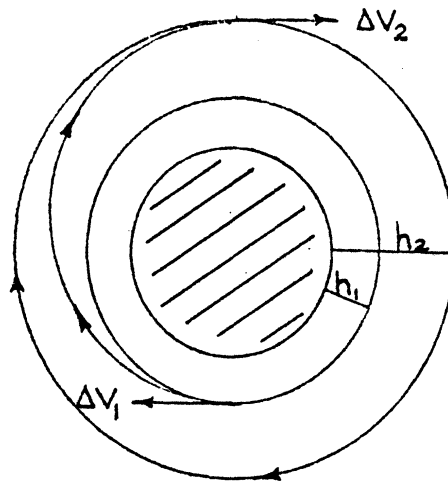


FIGURE 6.2

$$\Delta V_1 = \sqrt{\frac{\mu}{R_e + h_1}} \left\{ \left[ 1 + \frac{h_2 - h_1}{2R_e + h_1 + h_2} \right]^{1/2} - 1 \right\}$$

$$\Delta V_2 = \sqrt{\frac{\mu}{R_e + h_2}} \left\{ 1 - \left[ 1 - \frac{h_2 - h_1}{2R_e + h_1 + h_2} \right]^{1/2} \right\}$$

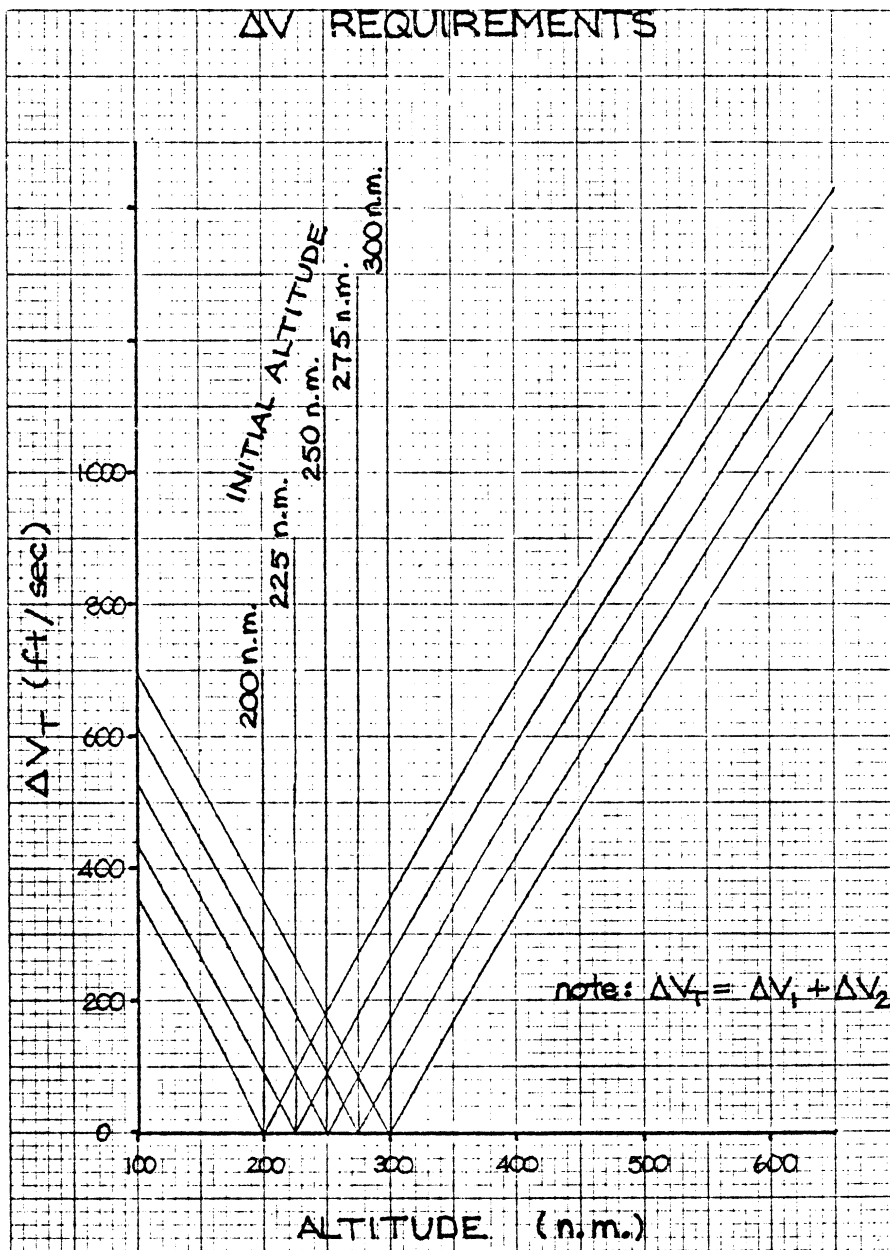


FIGURE 6.3

c. In-Plane Rendezvous

There are three parts to the in-plane rendezvous maneuver

- . Phasing
- . Terminal Phase Maneuver
- . Docking

## 1. Phasing

This maneuver is handled by OASIS. It consists of making the appropriate altitude change so that the two spacecraft are brought close enough together to begin the terminal phase maneuver. Initially, the spacecraft would be in coplanar circular orbits at different altitudes and generally separated by an angle  $\beta$ . The satellite executes a Hohmann transfer to position itself approximately 10 nm (19 km) higher than the Orbiter, and far enough ahead of it to allow the Orbiter to coast underneath prior to beginning the terminal phase maneuver. The satellite may either be above or below the Orbiter at the start of the phasing maneuver. Once the transfer is completed, it is desirable to have a known time interval,  $t$ , before the two spacecraft are in the proper alignment for the terminal phase maneuver. This time interval, together with the initial altitudes of the two spacecraft and the desired separation distance,  $\delta$ , determine the angular separation,  $\beta$ , needed between the two spacecraft at the start of the transfer. The expressions for the angle  $\beta$  are given in Figure 6.4 for the case when the satellite transfers up to the Orbiter and when it transfers down. During the transfer the satellite travels from A to B, while the orbiter travels from C to D.

### PHASING

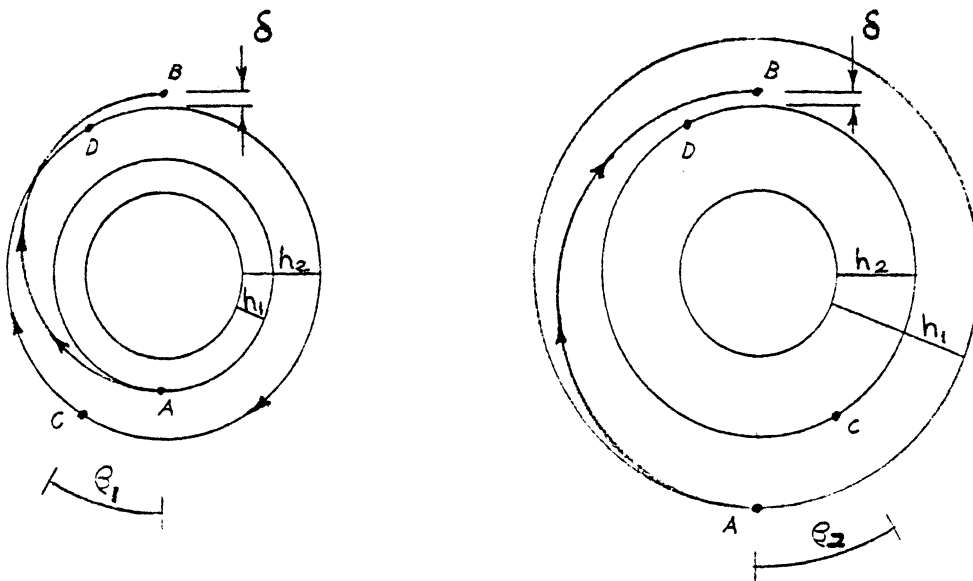


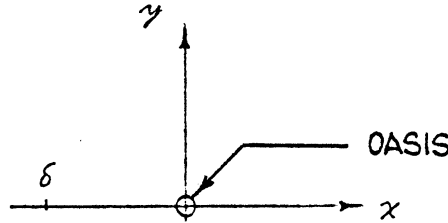
FIGURE 6.4

$$\beta_1 = \pi - \frac{(V_{lc_L}) \tau_t}{(R_e + h_2)} + t \left[ \frac{V_{lc_H}}{(R_e + h_2 + \delta)} - \frac{V_{lc_L}}{(R_e + h_2)} \right] - \frac{\delta}{(R_e + h_2)} \text{ radians}$$

$$\beta_2 = \frac{(V_{lc_L}) \tau_t}{(R_e + h_2)} + t \left[ \frac{V_{lc_L}}{(R_e + h_2)} - \frac{V_{lc_H}}{(R_e + h_2 + \delta)} \right] + \frac{\delta}{(R_e + h_2)} - \pi \text{ radians}$$

## 2. Terminal Phase Maneuver

The terminal phase maneuver is used to bring the two spacecraft together once the phasing maneuver has brought them to a small predetermined separation. The Orbiter is responsible for the terminal phase maneuver since it is better equipped and designed to handle terminal phasing routinely. In the given case OASIS is  $\delta$  nm above and  $\delta$  nm ahead of the Orbiter, as shown in Figure 6.5.



### TERMINAL PHASE COORDINATES

FIGURE 6.5

Two velocity changes are needed in the terminal phase maneuver. The first is to redirect the Orbiter, sending it on an intercept course with OASIS. The second is to provide braking, cancelling the relative motion and preventing a collision. These velocity changes are  $\Delta \vec{V}_1$  and  $\Delta \vec{V}_2$  respectively.

$$\Delta \vec{V}_1 = (\dot{x}_d(0) - V_{1cL} + V_{1cH}) \vec{e}_x + (\dot{y}_d(0)) \vec{e}_y$$

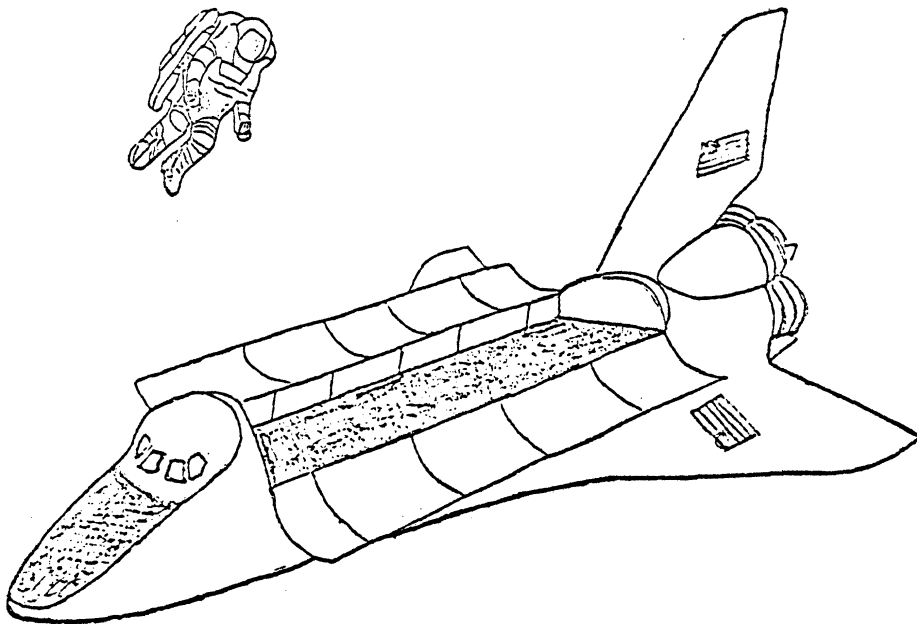
$$\Delta \vec{V}_2 = (3\dot{x}_d(0) - 6\omega\delta + 2\dot{y}_d(0) \sin \omega T - [4\dot{x}_d(0) - 6\omega\delta] \cos \omega T) \vec{e}_x \\ + ((3\omega\delta - 2\dot{x}_d(0)) \sin \omega T - \dot{y}_d(0) \cos \omega T) \vec{e}_y$$

## 3. Docking

Once the Orbiter has completed the braking maneuver, the two spacecraft will drift along with very little relative motion. The manipulator arm of the Orbiter can then be used to bring OASIS in, while making the necessary attitude adjustments to permit engagement of the docking mechanism.

#### 6.3.4 Extravehicular Activity

Extravehicular activity (EVA) will initially be needed for the assembly of the thermal control panels. EVA will also be necessary during the lifetime of OASIS for tasks such as the exchange of propulsion units, general maintenance and inspection. Each orbiter mission has provisions for two, two-man EVA of six hours each, plus one for contingency. An oxygen pre-breathing period of three hours is necessary prior to each EVA. A manned maneuvering unit (MMU) is available to an astronaut during an EVA. The MMU is a propulsive backpack device which allows the astronaut to "fly" untethered in the vicinity of the Orbiter. It has six degree of freedom control and electrical outlets to provide power for tools, lights and other equipment. It uses low-thrust, cold gas nitrogen propellant, which causes minimal disturbance with no adverse contamination. The manipulator arm of the Orbiter can also aid the astronaut during an EVA such as the exchange of propulsion units. The manipulator arm is a 50 ft (15 m) long electromechanical device with shoulder, elbow and wrist joints and an end effector. The arm is controlled from within the Orbiter.



EVA

FIGURE 6.6

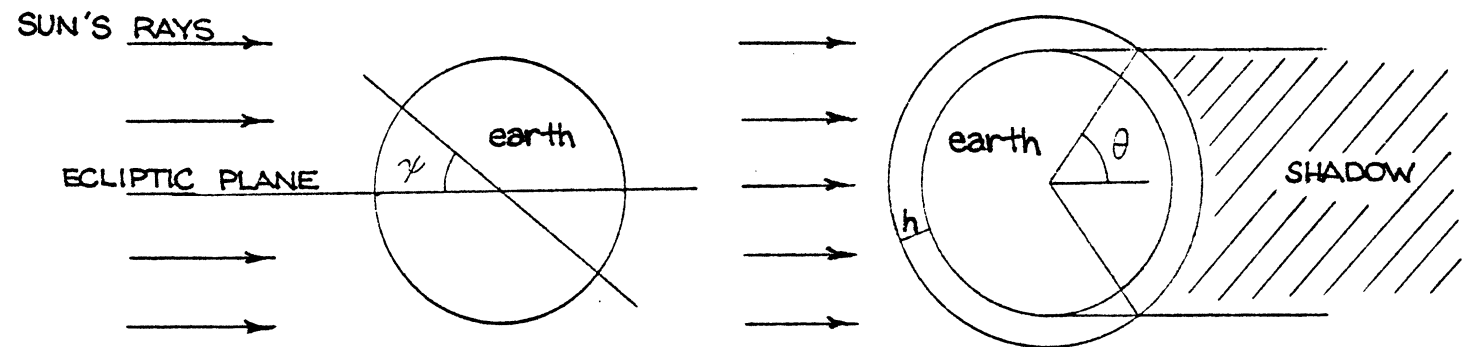
#### 6.3.5 Sun-Shade Relationships

An important consideration is the relationship between the sun and shade times of the orbit of OASIS.

a. Geometry

SUN-SHADE RELATIONS

FIGURE 6.7



b. Analysis

The sun-shade relationship is a function of both the altitude of the circular orbit,  $h$ , and the angle between the ecliptic and the orbital plane,  $\psi$ . Due to the precession of a satellite in its orbit about the Earth, and the Earth's revolution about the Sun, the angle  $\psi$  is not constant. Thus the Sun-shade relationship also varies, even though the satellite's altitude and inclination angle remain constant.

The angle  $\theta$  is defined as the half angle of orbital darkness. Since the circular orbit of OASIS has a constant velocity,  $\theta$  is used to determine the portion of each orbit during which OASIS is shaded from the Sun. The two extremes of maximum and minimum shade time are of interest for OASIS. In the case of maximum darkness,  $\theta$  is given by the equation

$$\theta = \sin^{-1} \left( \frac{R_e}{R_e + h} \right)$$

For the parking orbit of OASIS at  $50^\circ$  inclination and 225 nm (417 km) altitude  $\theta = 69.8^\circ$ . This indicates that the satellite is in darkness 39% of the time, or approximately 36 minutes of the 92.5 minute orbital period.

For the case of minimum darkness

$$\theta = \sin^{-1} \left( \frac{\sqrt{R_e^2 - [(R_e + h)^2 - R_e^2] \tan^2 \psi}}{R_e + h} \right)$$



and  $\psi = 73^\circ$ . In this case, the equation indicates that there exists an interval when the entire orbit of OASIS is in sunlight. Thus the shade percentage of the nominal parking orbit varies from 0% to 39% during the course of a year.

#### 6.4 REFERENCES

1. Wolverton, Raymond W. , Flight Performance Handbook for Orbital Operations, John Wiley & Sons, N. Y. 1963.
2. "25 kW Power Module Preliminary Definition," NASA Marshall Space Flight Center, Alabama, September 1977.
3. Space Shuttle System Summary, Rockwell International, May 1975.
4. Space Shuttle, NASA Johnson Space Center, Texas, February 1975.
5. "Space Shuttle EVA Opportunities," JSC-11391, NASA Johnson Space Center, Texas.

## ATTITUDE CONTROL

## 7.1 INTRODUCTION

The Attitude Control System is an important part of a satellite. The mission objectives of OASIS require that the satellite must be capable of maintaining or changing its attitude. Since a satellite is subject to disturbing torques, a system is needed that will counter these torques, and maintain the attitude. Also when a change of attitude is desired, the system must be able to supply the torques necessary.

## 7.2 SUMMARY AND CONCLUSIONS

The Attitude Control System on OASIS uses momentum wheels, optical sensors, and a gravity gradient method of desaturation. Emphasis was put on finding a system which utilized existing hardware, and minimized fuel use.

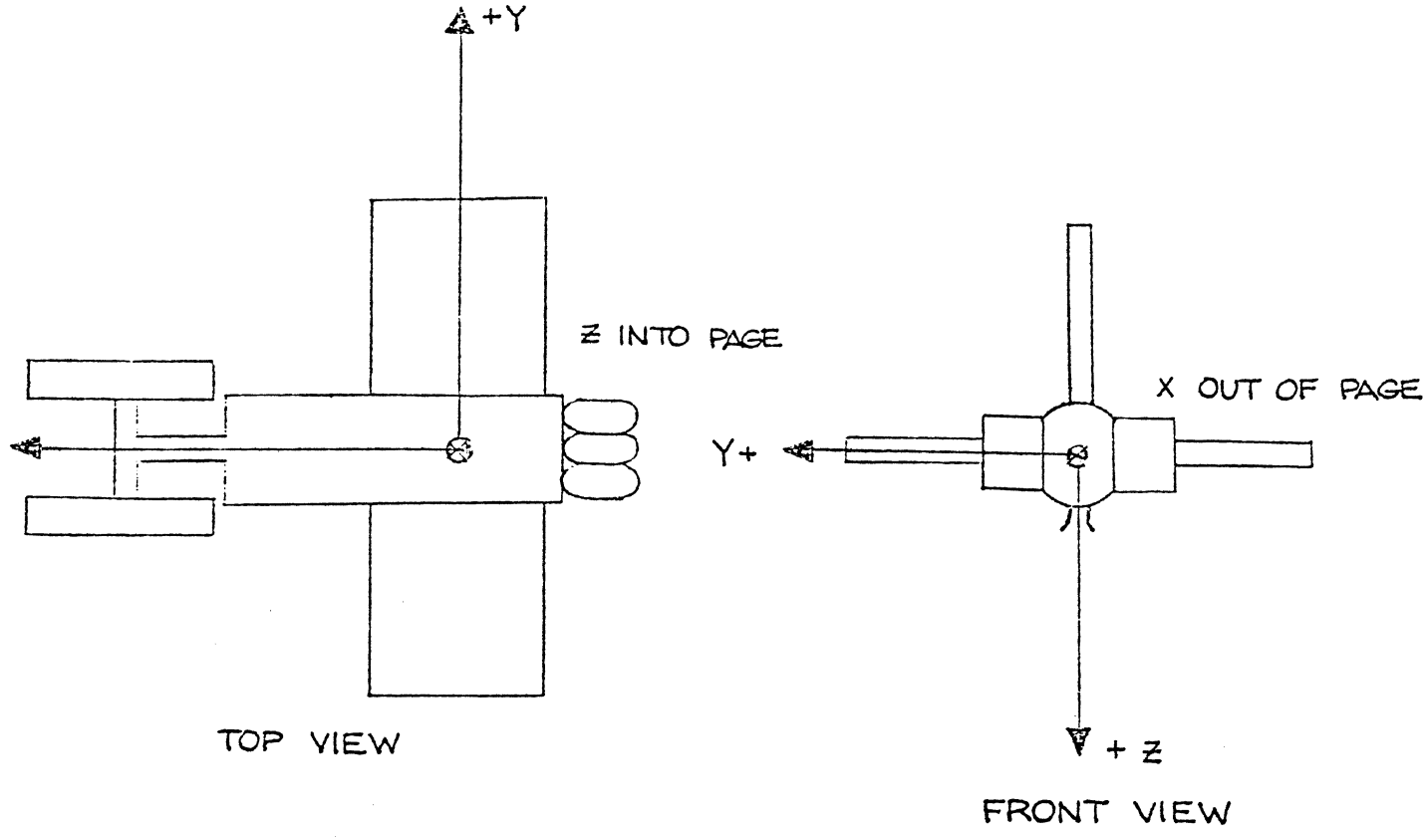
All components used for attitude control on OASIS have been used on the Apollo Telescope Mount (ATM). The system is 100% electric powered and needs no fuel. Also the system meet the accuracy requirement, having a pointing accuracy of 2 arc-min.

## 7.3 DEFINITION OF AXIS

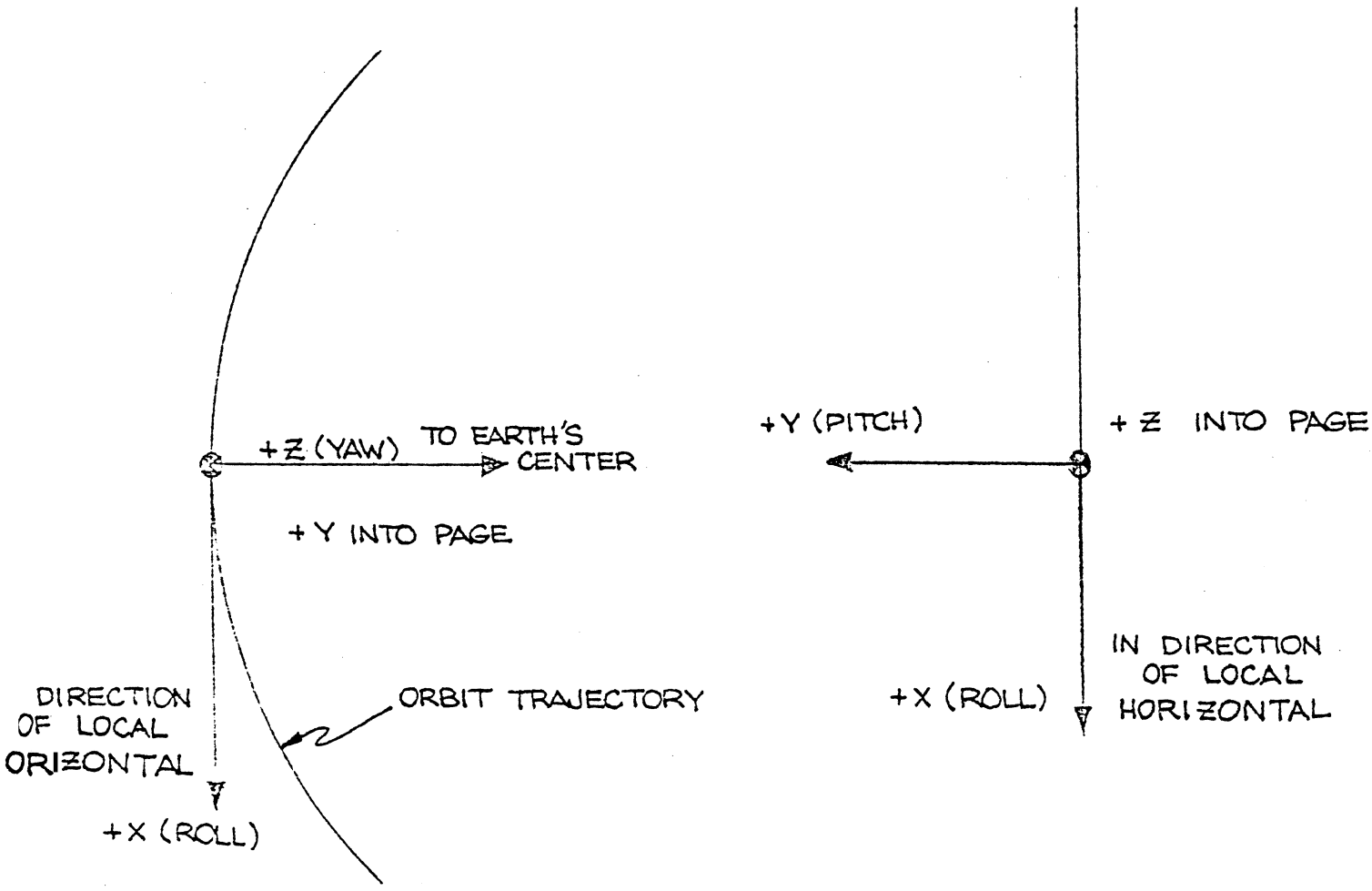
In order to discuss the attitude of a satellite, two sets of reference axes must be defined: the body-fixed system for defining the moments of inertia, and the earth-fixed system for comparison with the body fixed system in determining attitude.

The body fixed system is a right handed coordinate system with its origin at the satellites center of mass. The x-axis is along the centerline of the cylindrical section. The y-axis is perpendicular to the x-axis and lies in the plane formed by the two heat radiators. The z-axis completes the right hand system (Figure 7.1).

The orbital reference axis system also has its origin at the satellites center of gravity. The x-axis is the local horizontal. The z-axis is the local vertical, and the y-axis is perpendicular to the orbital plane and completes the right hand system (Figure 7.2).



BODY FIXED REFERENCE AXIS SYSTEM  
FIGURE 7.1



ORBITAL REFERENCE AXIS SYSTEM  
FIGURE 7.2

## 7.4 PRIMARY ATTITUDE CONTROL UNIT

### 7.4.1 Purpose

The purpose of the primary attitude control unit is to supply the torque necessary for changing the attitude of the satellite, and to counter any disturbing torques that the satellite might encounter. The disturbing torques are caused by:

- . Gravity forces
- . Moving parts in satellite
- . Earth's magnetic, electrical fields
- . Aerodynamic forces
- . Sun radiation pressure
- . Meteorite impacts

### 7.4.2 Options

There are several types of attitude control systems available. Each type of system has advantages and disadvantages, and the choice of system is dependent on the design constraints of the satellite. For OASIS, the design constraints are the following:

- . Emphasize existing hardware
- . Minimize fuel use
- . Achieve desired accuracy
- . Insure reliability
- . Minimize weight and size of the system

With the above design constraints in mind, the following types of systems were investigated. The results of this investigation are as follows:

#### a) Mass Expulsion System (thrusters)

##### - Advantages

- . Insensitive to disturbance torques
- . Provides widest variety of control orientations
- . Precision limited to that of attitude sensor

##### - Disadvantages

- . Becomes quite heavy for long missions when used alone due to fuel use

## b) Momentum Storage Devices

### - Advantages

- . Relieves gas system fuel expenditures for long missions
- . Very precise nulling control
- . Precision limited by attitude or sighting sensors.

### - Disadvantages

- . Requires auxiliary system to unload momentum saturation
- . Increased system complexity and power consumption

## c) Gravity Gradient System

### - Advantages

- . Involves no active control elements
- . Requires no attitude sensors
- . High reliability

### - Disadvantages

- . Sensitive to environmental torques and payload motion
- . Limited to near circular orbits
- . Limited accuracy

## d) Magnetic Systems

### - Advantages

- . Negligible weight
- . Requires no attitude sensors
- . High reliability

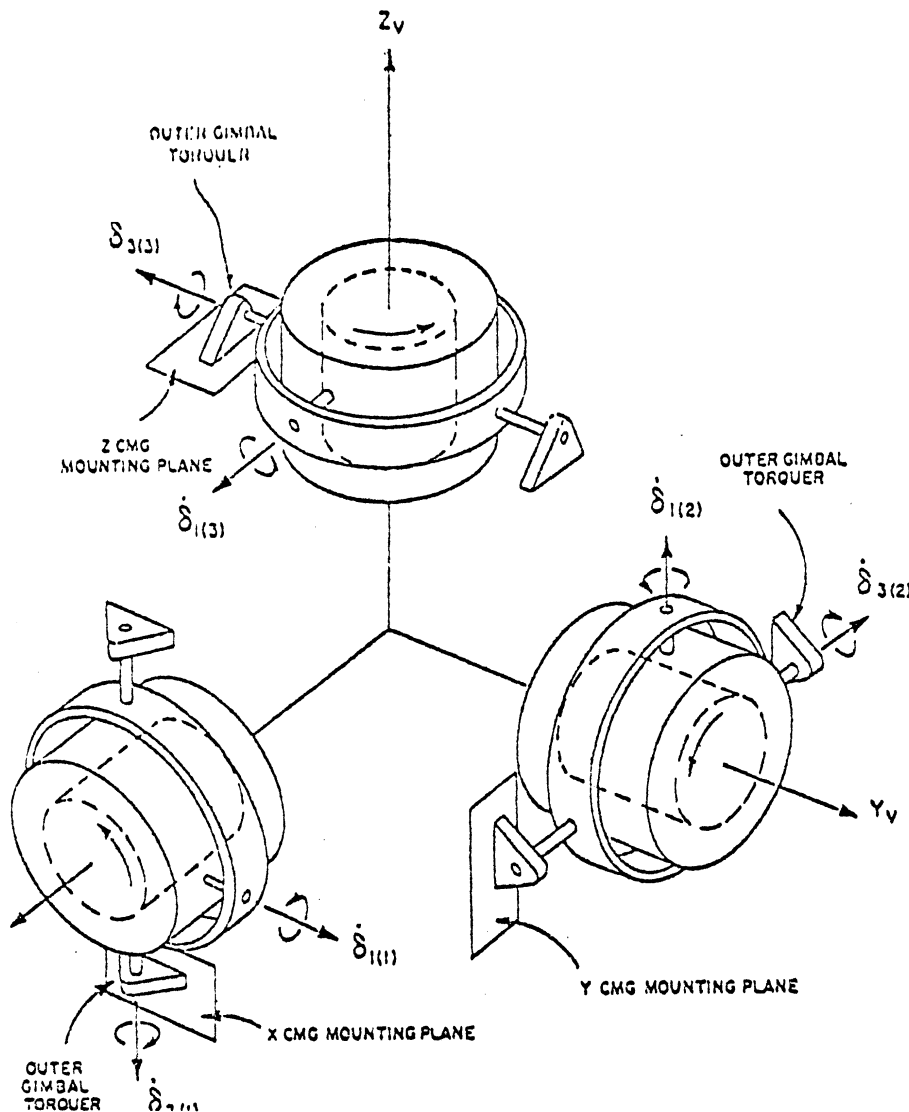
### - Disadvantages

- . Very limited applications
- . Limited accuracy

### 7.4.3 Momentum Wheels

Momentum storage (i. e. momentum wheels) was chosen for use on OASIS. Emphasis was put on the fact that momentum wheels require no fuel use, and existing hardware from the Apollo Telescope Mount (ATM) could be used.

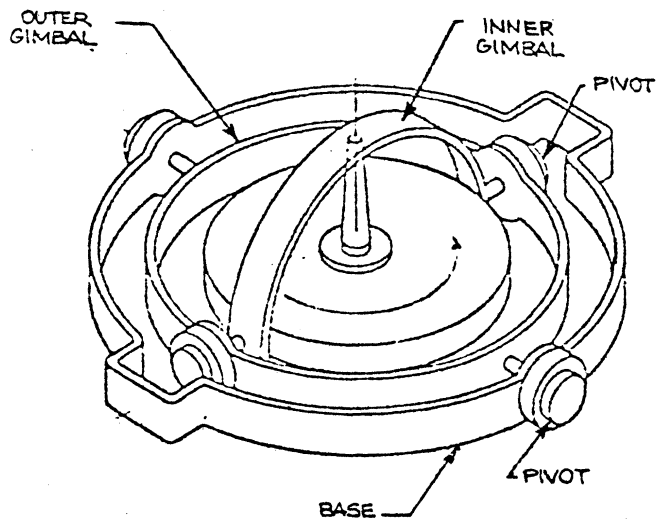
A momentum wheel is a device which can store and exchange angular momentum. The angular momentum of a wheel is the product of the angular velocity of the wheel times the moment of inertia. This angular momentum can be expressed in vector form as shown in Figure 7.3.



MOMENTUM WHEEL CONFIGURATION  
 FIGURE 7.3

Since the wheel is at a constant angular velocity, the change in angular momentum is in direction but not in magnitude.

The momentum wheel is double gimballed so that a momentum change is possible about any of the three coordinate axes. To achieve the change in angular momentum, a torque is applied to the desired gimbal. On OASIS there are six wheels which work simultaneously to achieve a distribution of the required momentum change. This provides a good degree of redundancy in case a wheel were to fail.



GIMBAL SCHEME FOR  
MOMENTUM WHEELS  
FIGURE 7.4

#### 7.4.4 Maintaining Attitude

If a disturbing torque were to act on the satellite, an appropriate counter torque would be applied to the wheels. The counter torque required is determined by the attitude control computer such that the total momentum remains constant. The result is that the satellite remains in its original attitude.

#### 7.4.5 Changing Attitude

In the standby mode if an attitude change is desired, the total momentum of the satellite must change. In the standby mode a torque is applied to the momentum wheels to start the satellite rotating slowly in the desired direction. An equal but opposite torque is applied to the wheels when the desired attitude has been achieved. This will stop the rotation rate of the satellite and hold it steady at its new attitude. In operational mode the gimbals will be unlocked and the Orbiter RCS system will supply the necessary torque.

#### 7.4.6 Momentum Wheel Saturation

Momentum wheels do not have an infinite capacity for changing angular momentum. They reach a point where they no longer have the capacity to increase angular momentum in a given direction. This is called momentum wheel saturation.

## 7.5 DESATURATIONS OF MOMENTUM WHEELS

### 7.5.1 Purpose

Non-cyclic disturbance torques acting on the satellite cause a net momentum buildup on the momentum wheels. Saturation of the momentum wheels occur due to the finite momentum storage capacity of the wheels in a give direction. A scheme for the desaturation of the momentum wheels is thus necessary. This can be achieved through the use of mass expulsors, gravity gradient, or magnetic torquers.

### 7.5.2 Options

Different methods were investigated for desaturation of the momentum wheels. These fall into the three categories mentioned above and are briefly described below.

#### a) Mass Expulsors

The thrust needed to desaturate the wheels within minutes would be on the order of 10 pounds. On this basis alone devices such as pulsed electric microthrusters and cold gas thrusters were abandoned.

Chemical thrusters capable of producing thrust on the order of 10 pounds would be able to desaturate the wheels in a reasonable time.

Advantages of the chemical thrusters are:

- . There are no restrictions arising from the geometric properties of OASIS
- . They can be used at any time for desaturation

The disadvantages are:

- . The finite fuel storage capacity of the thrusters puts a lifetime constraint on the satellite and requires refueling
- . Safety considerations necessitate quick release mechanisms for the fuel tanks to avoid contamination of the solar panels, heat radiators, or Orbiter bay is possible.

#### b) Gravity Gradient

Gravity gradient works on the principle that the gravitational restoring torques acting on a satellite will rotate it toward a position in which the axis of minimum moment of inertia is aligned with the local vertical.



The advantages are:

- . There are no operating costs involved
- . The system has no weight and is passive
- . The system can work continuously
- . The system needs no equipment.

The disadvantages are:

- . It could become inconvenient to use in a sun synchronous orbit
- . The geometry of the satellite must be such that the moment of inertia about two axes are large enough.

### c) Magnetic Torquers

Torquer bars react with the Earth's magnetic field to produce the required torque on the satellite to desaturate the momentum wheels. The weight and cost of such a system is prohibitive.

### 7.5.3 Gravity Gradient

Cost, weight, and ease of operation led us to choose gravity gradient as a means of desaturation. If OASIS is in a sun synchronous orbit, the solar panels may not always point directly at the sun. However, this poses no problem since overdesign of the solar panels will allow up to 30% of the orbital period for desaturation maneuvers. The two degree of freedom solar panels will be locked into position while the momentum wheels are being desaturated. There are two schemes for desaturation, depending on whether OASIS is in the standby mode or is docked to the Orbiter.

The achievement of desaturation in standby mode is done by maneuvering the vehicle about the two axes of largest moments of inertias such that the net accumulated momentum vector is equal and opposite to the gravity gradient momentum vector. The desaturation method can be separated into two parts. One part consists of sampling the angular momentum accumulation at the momentum wheels. The other part consists of computing the desaturation angles  $\epsilon$ , given the accumulation angular momentum. The last part also involves the calculation of the vehicle's principal moments of inertia. This calculation is necessary since movement of the solar panels will change the moments of inertia. For a more detailed analysis of the desaturation commands refer to Appendix E.

When OASIS is docked to the Orbiter, desaturation will be handled by the Orbiter RCS system. The RCS system is used instead of gravity gradient because payload pointing constraints make movements in the gravity field undesirable. The RCS thrusters will be fired producing a torque in a given direction such that the momentum wheels desaturate when they react.

#### 7.5.4 Capabilities and Constraints

The major constraint in using gravity gradient for desaturation, is that pointing accuracy is sacrificed during the maneuvers. This sacrifice is reflected mainly as a power loss from the solar array. Since 30% of the orbit is in the shade, this time could be used for desaturation with no sacrifices made.

In a sun synchronous orbit, there is no shade time, and hence no ideal time for desaturation. This should present no problem however, because the solar array is designed to produce more power than needed, and is always in the sun. Because of this, the maneuvers can be made at any time without experiencing power shortage.

### 7.6 ATTITUDE SENSING

#### 7.6.1 Purpose

In order to correctly enact velocity and trajectory changes and corrections it is necessary that the satellite's attitude be known to a high degree of accuracy. Such attitude knowledge is obtained from attitude sensors located onboard the spacecraft. The types of sensors used are determined by the satellite and its mission.

#### 7.6.2 Requirements

The OASIS attitude sensor system must be able to obtain the pointing accuracy required by the Orbiter. Improvement upon the 10 arc minute pointing accuracy that can be achieved using the Orbiter RCS is desired. Demands upon the attitude sensing and control system normally made by solar panel pointing requirements on conventional satellites are eased on the OASIS satellite due to its 2 degree of freedom solar panels. The sensor system should also be inexpensive and reliable enough to meet the proposed 5 year lifetime.

Required modes of operation of the attitude sensors are the acquisition and maintenance modes. Acquisition involves the establishment of attitude after a gross change in satellite position (i. e. initial deployment). Maintenance requires sustenance of a desired satellite attitude or controlled change from one attitude to another.

#### 7.6.3 Options

Two main types of sensors, inertial and optical, were evaluated for use on OASIS. Inertial sensors operate on the principle of detection of satellite accelerations. Analysis of such changes in acceleration over time yields indications of linear or angular displacements. Optical sensors, on the other hand, rely on detecting an existing attitude with respect to reference directions. For satellite control celestial bodies are sighted and the satellites orientation in space is deduced.

Other types of attitude sensors considered involved detection of the variation of magnetic and electric fields in space and radar type devices. These types of sensors were deemed inapplicable to OASIS due to accuracy and weight considerations.

Inertial sensors can give continuous attitude monitoring. However, current inertial sensors for attitude control (i. e. rate gyros) have the disadvantage of inaccuracy due to drifts in rotation rates. Optical sensors, although highly accurate, are difficult to use in a continuous monitoring mode. Such an operation would require continuous viewing of celestial bodies, thus limiting possible satellite orientations.

The decision on the type of attitude sensor used emphasized three main points:

- . Performance and meeting of requirements
- . Reliability
- . Availability of equipment and cost.

With these points in mind we chose a combination inertial-optical system employing much of the present equipment available on the ATM. The system uses rate gyros, optical sensors (Sun, Star and Earth sensors), and electronics. Some modifications of the ATM system will be needed to meet OASIS requirements.

#### 7.6.4 Sensors

Angular motions are constantly monitored by rate gyros placed redundantly about three orthogonal axes. The changes in the rates of rotation of the gyros are integrated over time by the attitude control computer to yield angular displacements. The decision to use 9 gyros instead of only 3 was based upon reliability and performance considerations.

While the rate gyros are the basic sensing elements of the attitude control sensor systems, reference directions from which displacements are measured are provided by optical means. Rate gyro drifts are also accounted for by optical attitude establishment. Three types of optical sensors will be used: Sun, Star, and Earth sensors. All are from the ATM. The Sun sensor has both course (acquisition) and fine (pointing) optics. The Star seeker is intended to aim at Canopus although other stars can be sought. The Earth sensor is provided for use at any time that optical establishment is needed when the Sun and Star trackers are blocked (perhaps by docking configuration).

#### 7.6.5 Operation

Upon deployment the satellite will acquire the Sun by angular rotations. Upon Sun acquisition a roll about the Sun line will be performed until Canopus is referenced, thus establishing initial attitude. Subsequent operations will concern either maintenance of a desired orientation or aiming of the craft for thrusting or pointing.

The sensor system presented will yield 2 arc minute visual pointing accuracy over a linear range of  $\pm 5$  degrees in 2 axes. The sensor system should be extremely reliable due to redundancies throughout (9 rate gyros instead of the minimum 3, 3 optical sensors instead of 1 or 2).

## 7.7 DATA HANDLING (Figure 7.5)

Attitude is continuously monitored by the rate gyros. Output from the gyros represent changes of the satellite's rotation rate. Thus, these signals must be integrated over time to yield angular displacements so that appropriate corrective measures, if desired, can be implemented. Optical sensor outputs are in the form of voltages representing angular displacements of sighted objects from the optic null-line. The momentum wheels require an input to the torquer motors and deliver information concerning the degree of wheel saturation.

The attitude control computer unit must monitor and command the aforementioned elements. Basic operation is as follows. The vehicle attitude is deduced by the time history of the rate gyros. This attitude is compared to the desired attitude. If a correction of attitude is required, commands are sent to the momentum wheel torquer motors which will cause the correct change in the wheel's angular momentum. This will initiate a corresponding change in the satellite's angular momentum (i. e. roll). The momentum wheels are commanded similarly to cease the roll.

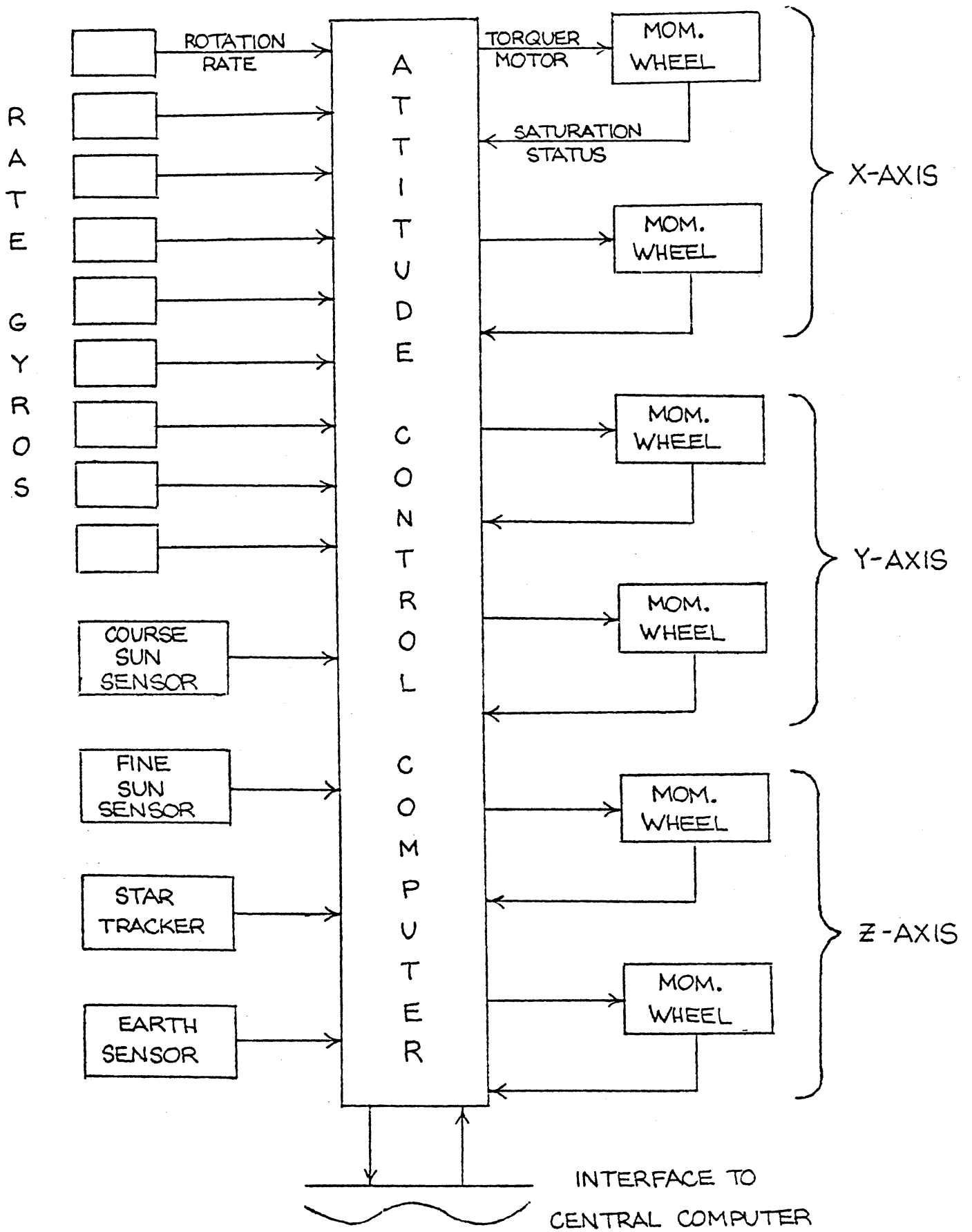
The satellite's attitude is periodically checked by the optical sensors. This allows correction of the gyro drift errors, thus allowing accurate long term attitude information.

The momentum wheels are monitored to prevent saturation. When a saturation situation is approached, desaturation measures are enacted (see Modes of Operation).

## 7.8 MODES OF OPERATION

### 7.8.1 Mode Descriptions

There are three basic satellite operating configurations: operational (docked to Orbiter), standby (satellite only), and satellite with payload. In the operational mode OASIS will provide attitude maintenance for both OASIS and the Orbiter. However, any appreciable changes in the satellite-Orbiter system's attitude will be made using Orbiter RCS. Also, momentum wheel desaturation will be achieved using the Orbiter RCS instead of gravity gradient techniques.



ATTITUDE CONTROL BLOCK DIAGRAM

FIGURE 7.5

In the standby and satellite with payload modes, OASIS will be the sole provider of attitude control. Desaturation of the momentum wheels will be achieved only by the use of gravity gradient.

### 7.8.2 Operational Mode

Information concerning the degree of momentum wheel saturation will be transmitted to the Orbiter. The Orbiter will then use its RCS to desaturate the OASIS momentum wheels when needed.

If any large attitude changes are required, the OASIS momentum wheels will be allowed to move freely (gimbal release) while the Orbiter uses its propulsion system to achieve the change. Upon completion of the attitude change the OASIS momentum wheel gimbals will engage and OASIS will again provide attitude control for both itself and the Orbiter.

The attitude control system chosen for OASIS will be able to provide adequate attitude control in all three modes of operation. If more stringent pointing accuracies are required they would have to be provided by the individual experiment package.

## 7.9 REFERENCES

1. "Surveyor VII Mission Report; Part 1" Jet Propulsion Laboratory, Pasadena, California, 1969.
2. "Project SPIDAR", Department of Aerospace Engineering, University of Michigan.
3. "Project RODAN", Department of Aerospace Engineering, University of Michigan.
4. "Project MISSAC", Department of Aerospace Engineering, University of Michigan
5. Clark, K. E. , "Survey of Electric Propulsion Capability," Journal of Spacecraft and Rockets, Vol. 12, Number 11, November 1975.
6. Kennel, Hans F. , "Angular Momentum Desaturation for Skylab Using Gravity Gradient Torques," NASA TMX-64628, December 1971.
7. Chubb, William B. and Epstein, Michael, "Application of the Control Moment Gyros in the Attitude Control of the Apollo Telescope Mount," AIAA Paper No. 68-866.

8. "25 KW Power Module Preliminary Def. " NASA, Marshall Space Flight Center, Alabama, September 1977.
9. "Solar Sensor Capabilities," Ball Brothers Research Corporation, October 1968.
10. Seaman, L. T. , "Active Space Pointing Systems," General Electric Company, 1964.
11. Kleinman, Louis A. , "Project Icarus," M. I. T. Press, Cambridge, Mass. 1968.
12. Pitman, George R. , Inertial Guidance, John Wiley & Sons, New York, 1962.
13. Quasis, Glen and McCanless, Floyd, Star Trackers and Systems Design, Spartan Books, Washington, D. C. 1966.
14. "Mariner-Venus 1967 Final Project Report," NASA, Scientific and Technical Information Office, Washington, D. C. , 1971.
15. Corliss, William R. , Scientific Satellites, NASA SP-133, 1967.
16. Kaplan, Marshall H. , Modern Spacecraft Dynamics and Control, Wiley & Sons, 1976.

## 8 STRUCTURES

### 8.1 INTRODUCTION

The primary structural design requirements of OASIS are its compatibility with the Orbiter, while providing the necessary services. Among the constraints are that all mounting hardware and brackets are based on a safety factor of 1.4. In addition, while the satellite is mounted in the payload bay, its center of gravity (C. G. ) must fall within a certain envelope, represented in Figure 8.1.

The major structural characteristic of OASIS is its modular design. OASIS is divided into five structural components. Each of these substructures supports a self-contained system. This design allows easy replacement or repair of the satellite components, if necessary. The substructures are: 1) support tube, 2) solar array, 3) heat rejection thermal radiators, 4) docking mechanism, and 5) propulsion system.

The satellite arrangement in the bay is designed to remain stable during all phases of flight. The Orbiter bay includes payload retention fittings to distribute the load from the satellite to the Orbiter to meet this goal. The load is distributed along the side and keel longerons inside the payload bay. The satellite/Orbiter interfaces are shown in Figure 8.2.

### 8.2 SUMMARY AND CONCLUSIONS

The design and analysis behind the structure of Project OASIS conforms to the services required. All structural systems were designed with the necessary safety factors. Total weight of the satellite is 37844 lbs (17166 kg). Overall dimensions include 57 ft (17.4 m) in length, 14.1 ft (4.3 m) maximum width, and an 11 ft (3.35 m) maximum depth. (See Figure 8.3.) Modular concepts became beneficial in regard to the ease of EVA repair of specific structures.

#### 8.2.1 Support Tube

With a total volume of 1963 ft<sup>3</sup> (55.6 m<sup>3</sup>), this 25 ft (7.6 m) long, 10 ft (3.1 m) diameter, cylinder carries most of the required equipment for operation. Its 3/16 in (.48 cm) thick skin, along with its internal longerons provide strength for large loads. A hatch is available for entry inside the support tube by EVA.



OASIS CENTER OF GRAVITY

PAYLOAD WT.  $\times 1000$  LBS.

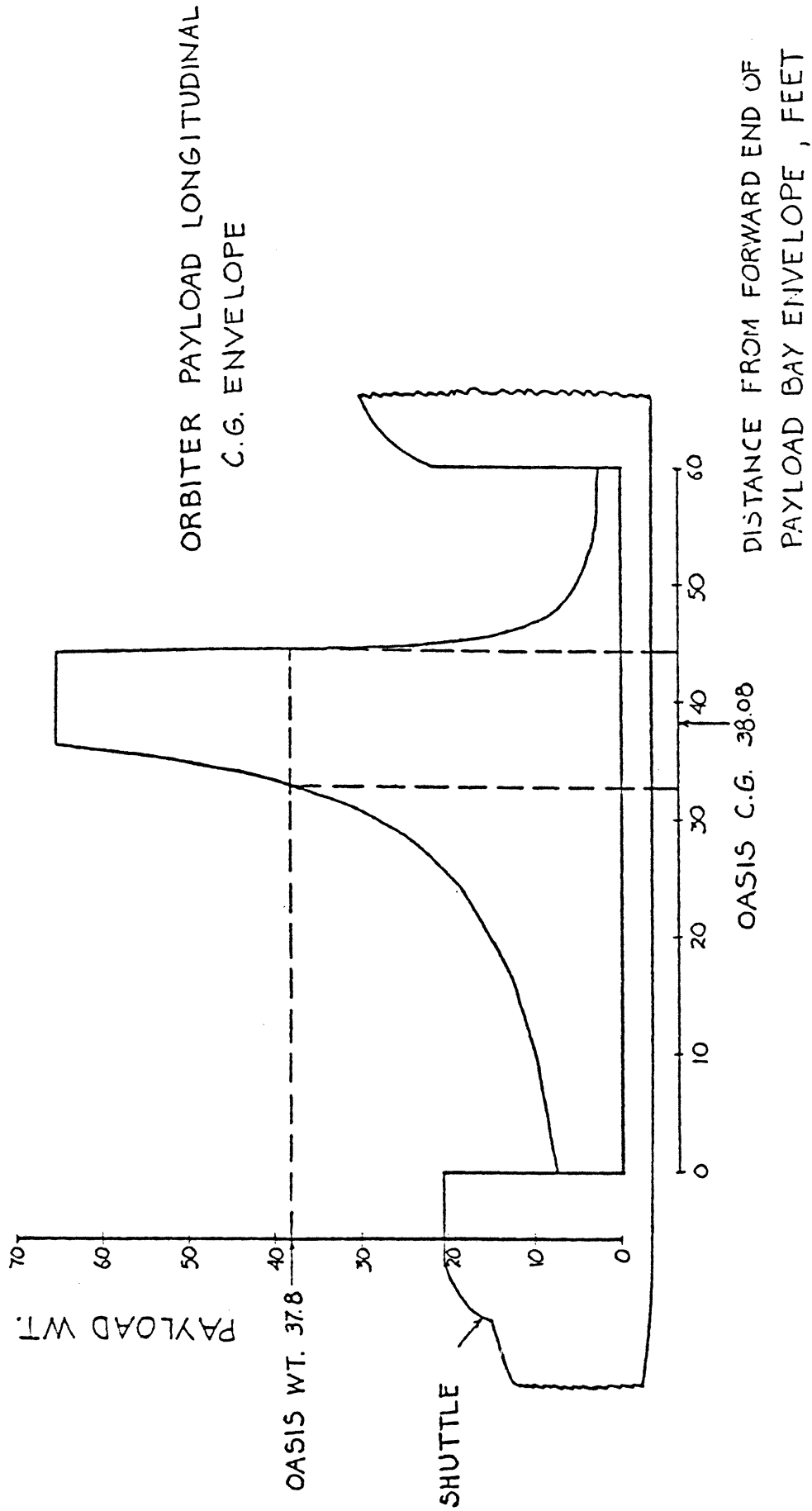


FIGURE 8.1

# OASIS LAUNCH CONFIGURATION

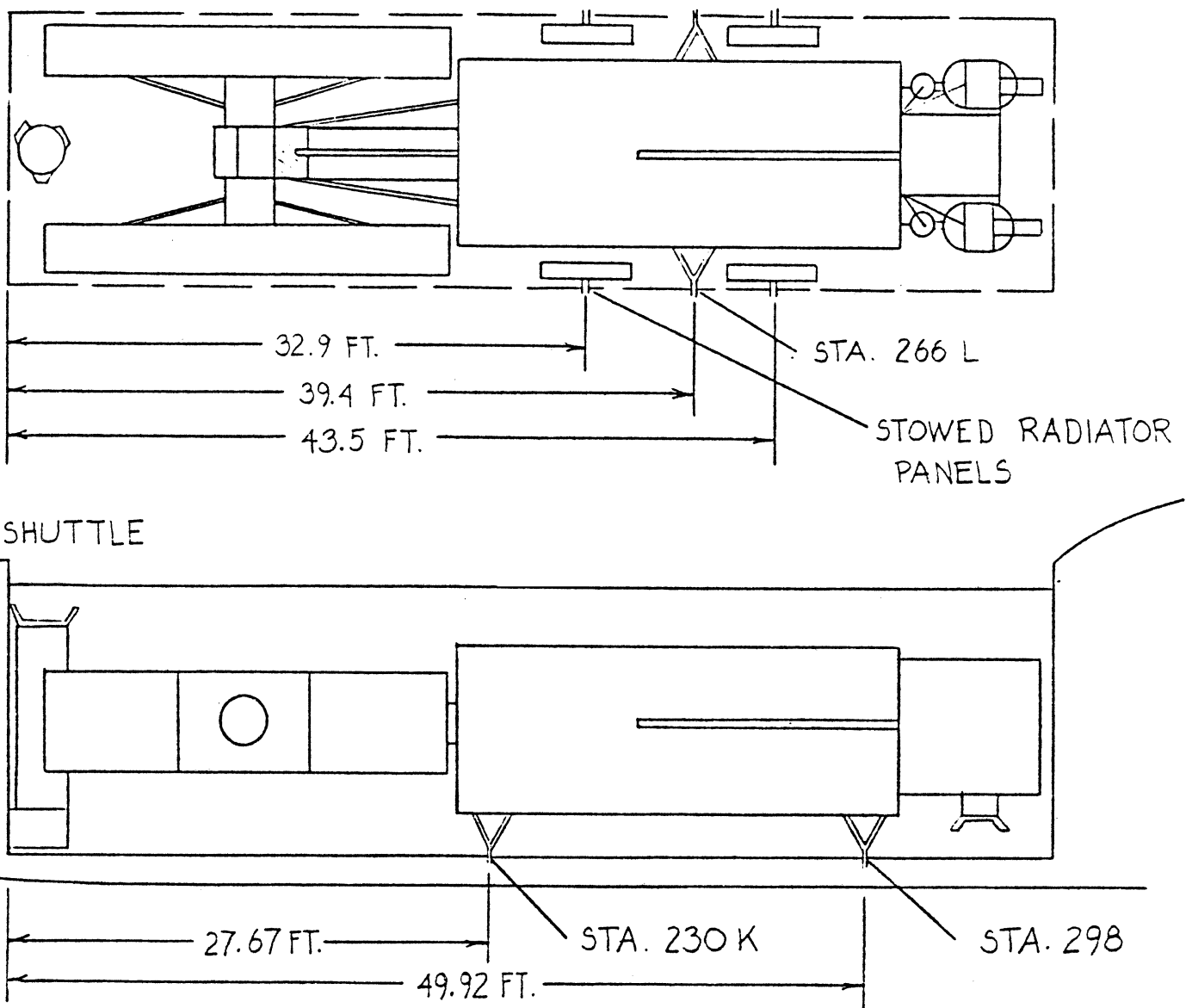


FIGURE 8.2

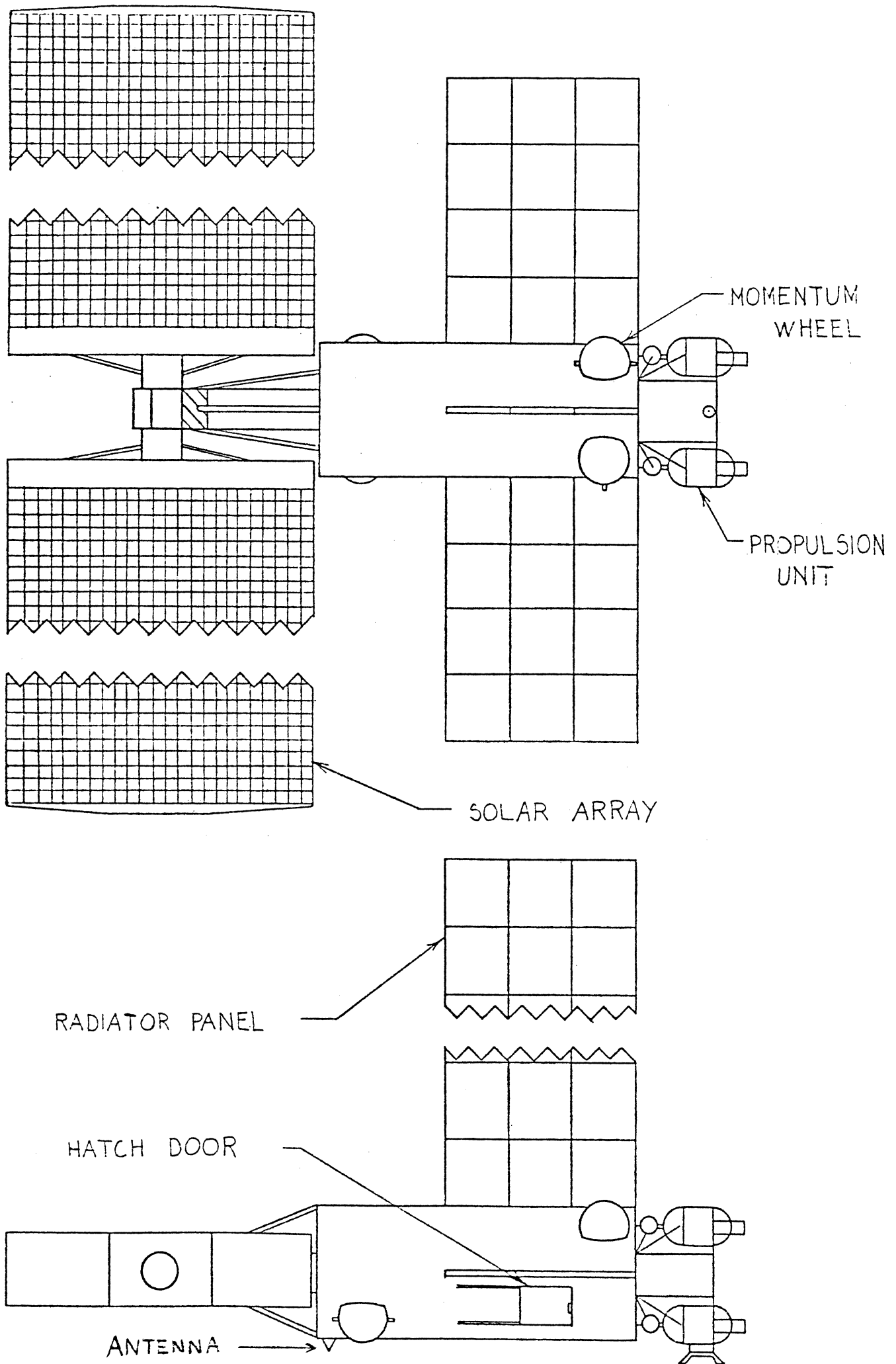


FIGURE 8.3 OASIS DESIGN

### 8.2.2 Internal Structure

Eight annular plates comprise the basis for the interior. The 48 in (1.2 m) hole permits passage through the internal structure for easy access to all components. The plates carry the avionic systems and other equipment, while also aiding in stiffening the support tube.

### 8.2.3 Solar Array Substructure

The solar array substructure consists of a deployment mechanism which opens the solar array at a rate of 1 1/2 inches per second (3.8 cm/s). Two degrees of freedom provide for maximum solar absorption for the panels. Motors in the canisters rotate for one degree of freedom. The second degree of freedom comes from a rotation of the main shaft by another motor.

### 8.2.4 Heat Rejection System

A safe distance is necessary between this system and the solar arrays and 10 feet (3.05 m) was considered sufficient. The radiating panels are systematically constructed by EVA. Structural stability is accomplished by setting the panels into a recessed groove in the support tube. Required thermal tubing is also attached to the satellite through these grooves.

For launch, the individual panels are packaged and pinned to the side of the Orbiter bay, away from any obstacles.

### 8.2.5 Access and Docking

EVA access is possible through the hatch for all electrical power systems and heat units. Most mechanical apparatus, can be reached by external EVA.

The docking port enables the power and heat transfer between the satellite and Orbiter. No internal EVA access is provided here.

### 8.2.6 Propulsion

A strong octagonal rack supports the four propulsion units. The docking port is designed to accommodate this system. Simplicity in replacing the propulsion units is due to the 'slide on and lock' arrangements.

### 8.3 SUPPORT TUBE

The function of the support tube is to absorb forces from the component substructure. During launch the tube transfers forces to the attach pins of the Orbiter. It is designed to withstand all launch accelerations and has a safety factor of 1.68.

The support tube is a cylinder with skin  $3/16$  inch (.48 cm) thick, supported by 8 longerons traversing the entire length (see Figure 8.2). Both skin and longerons are made of 7178-T6 aluminum, a strong alloy suitable for long duration missions. The tube is 25 ft (7.6 m) long and 10 ft (3.0 m) in diameter. Located inside the tube are 8 annular mounting plates adding to the structural integrity of the cylinder. The external surface of the support is continuous except for the areas grooved for the heat rejection units. Also, an EVA access hatch is located on the surface of the tube.

A four point structural attachment system will interface with the Orbiter cargo bay. Payload retention fittings will be attached to the supporting longerons and mounting plates to achieve the structural stability to withstand launch loadings.

### 8.4 INTERNAL STRUCTURE

The internal structure of OASIS consists of mounting plates and equipment. The eight mounting plates support batteries, chargers, regulators, fluid pumps, computers, communications and data systems, and all other equipment for OASIS operation. The plates are attached to the support tube with angle bars on both the top and bottom surfaces (see Figure 8.4).

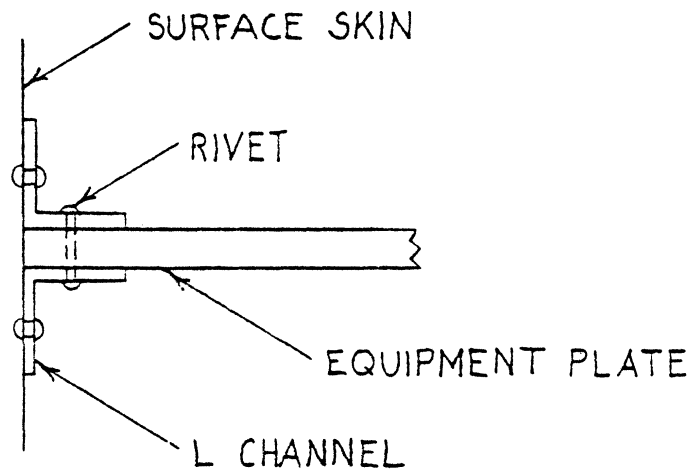


FIGURE 8.4 PLATE ATTACHMENT

This attachment method is analyzed as a clamped boundary condition. A center hole, 48 in (1.22 m) in diameter, provides passage between storage sections to ease in repair or replacement of equipment. Detailed diagrams showing locations of mounting plates and equipment are shown in Figure 8.5. Analysis is shown in Appendix F.

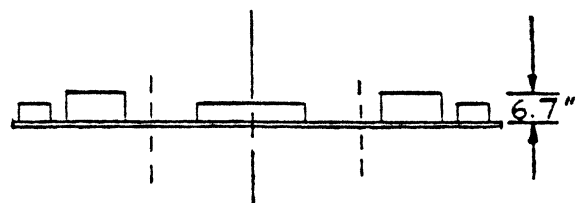
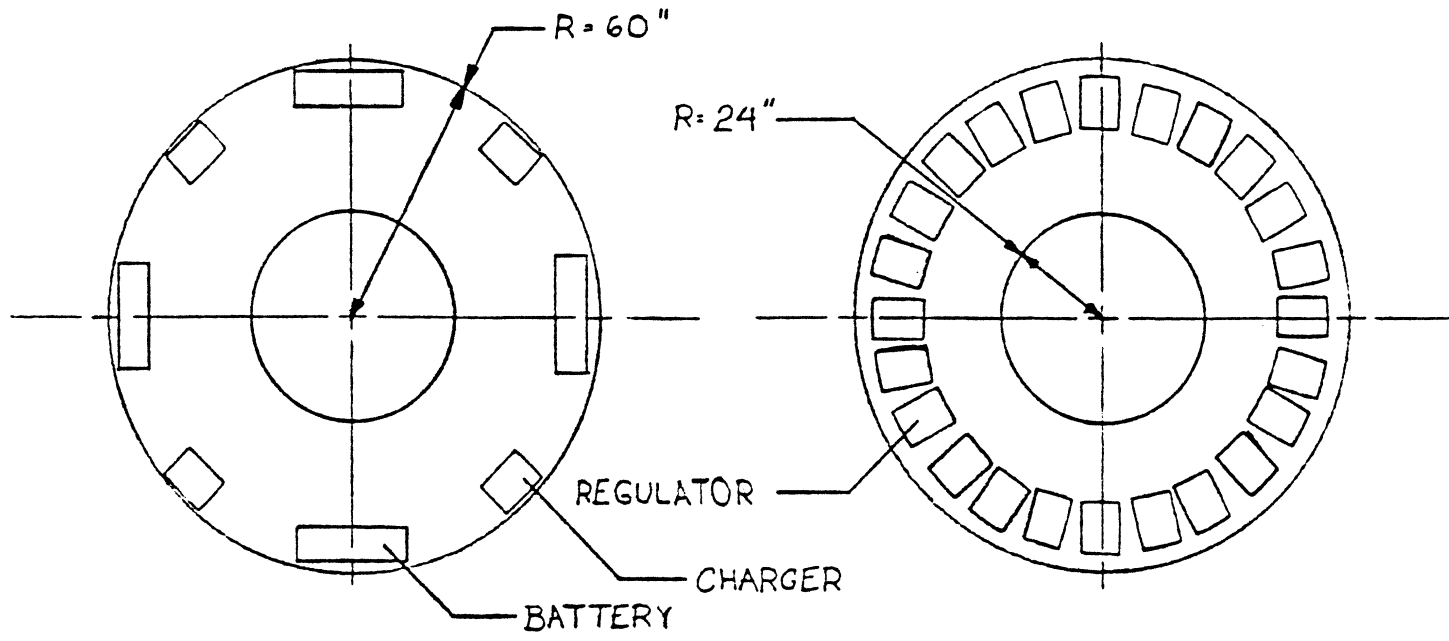
The batteries and chargers are shown in Figure 8.5A. They are mounted symmetrically about the y and z axis on five plates. The 24 regulators are mounted on one plate symmetrically as shown in Figure 8.5B. Figure 8.5D shows the plate, locating digital computers, heat exchanger, memory load unit, and interface unit. Located in Figure 8.5C is the communication and data handling, the coolant pumps, and rate gyros.

## 8.5 SOLAR ARRAY

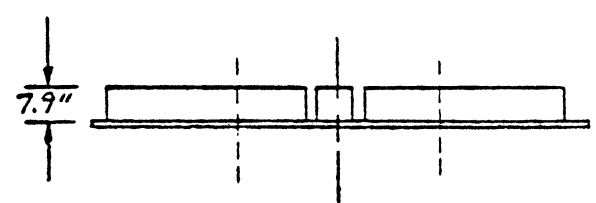
The solar array support structure connects the solar array subsystem to the support tube. It provides support for the two SEPS (Solar Electric Propulsion System) type solar array wings and the mechanisms for deploying and orientating the solar array. This system will give the solar array two degrees of freedom to maximize the time the array will be pointed toward the sun. The support structure is located on the front end of the support tube as shown in Figure 8.6. The support structure is made from 7178-T6 aluminum.

A main support beam will connect the solar array to the support tube. At the end, attached to the support tube, is located a motor and bearing assembly providing rotational positioning about the x axis. At the other end of the main support beam, is located a housing which provides the structural interfaces for the SEPS type solar array deployment canisters and bearing assembly. Also housed are the drive motors required for rotation of the array about the y axis.

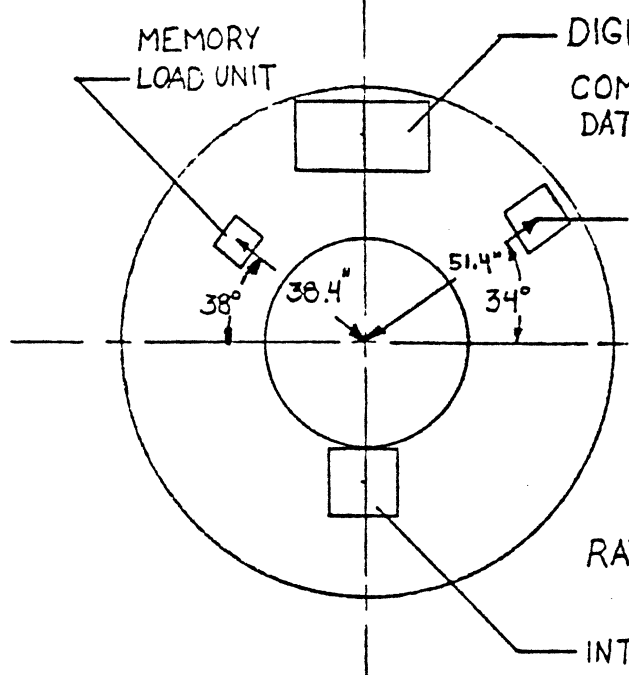
The deployment mechanism is similar to the solar array system under development in the SEPS technology program. This deployment system utilizes a tri-truss structure made of flexible fiberglass longerons to support the solar panels. In a deployed mode, the longerons provide the necessary support through longeron tension. Retraction and storage is achieved by collapsing one longeron and rolling the collapsed truss into the canister supported by the main support beam (as shown in Figure 8.7). Sizing of deployment mechanism components is determined by the needed solar array area. For the 23.9 ft x 236.7 ft (7.28 m x 72.15 m) solar array, an 83 in (2.11 m) long 39.4 in (1 m) diameter storage canister and four 30 watt drive motor are necessary.



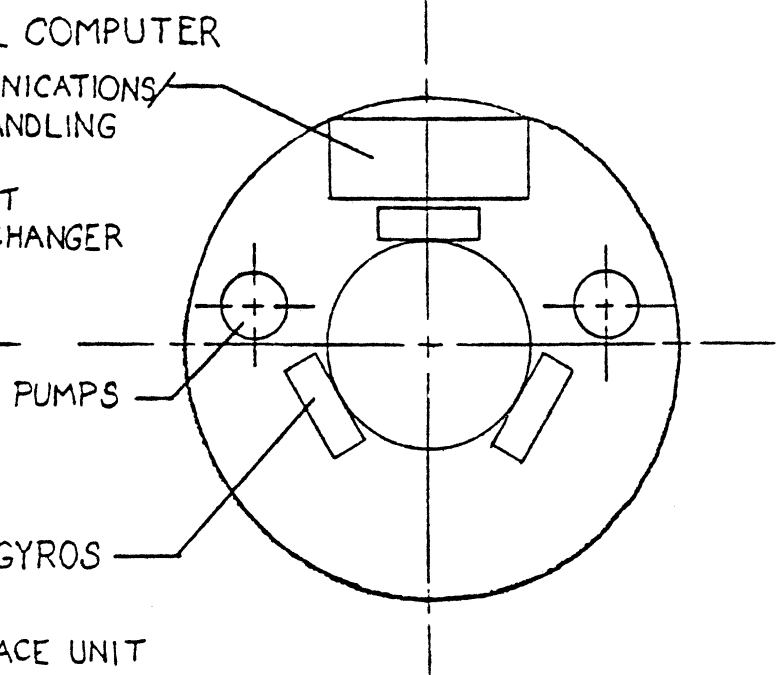
8.5A



8.5B



8.5D



8.5C

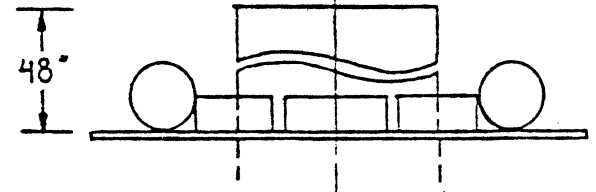
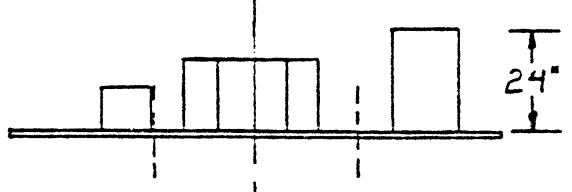


FIGURE 8.5

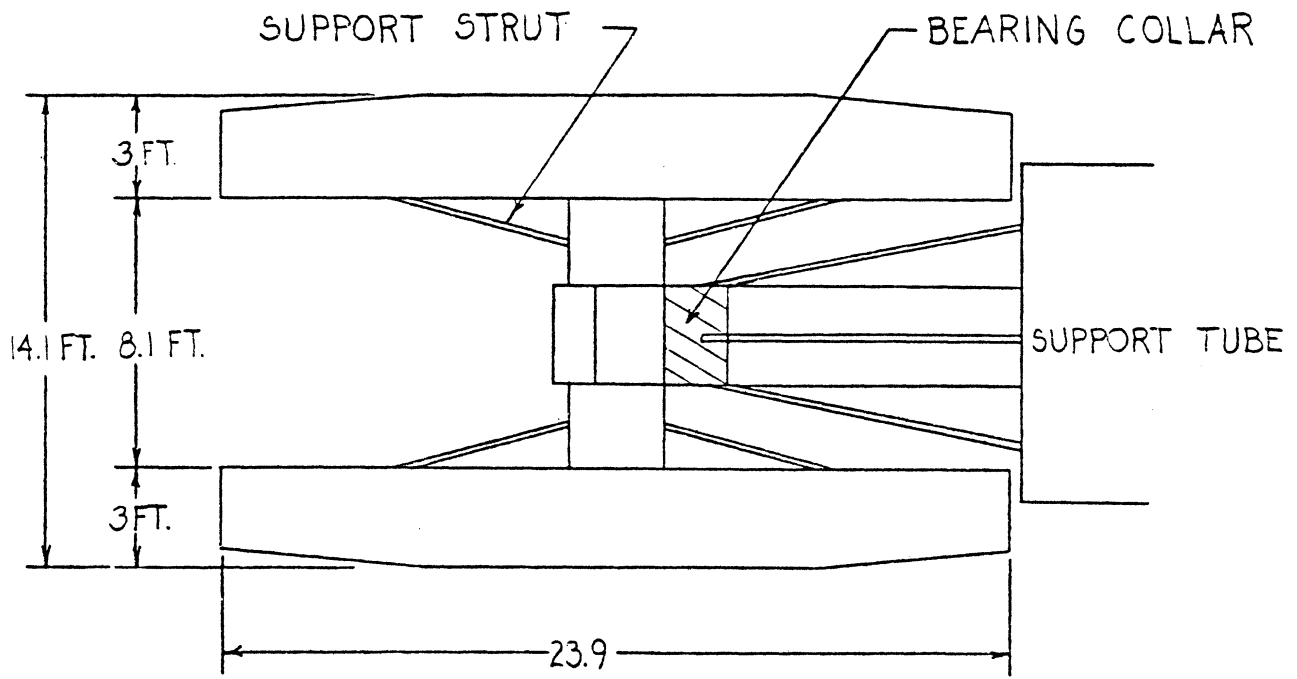


FIGURE 8.6 SOLAR ARRAY SUPPORT STRUCTURE

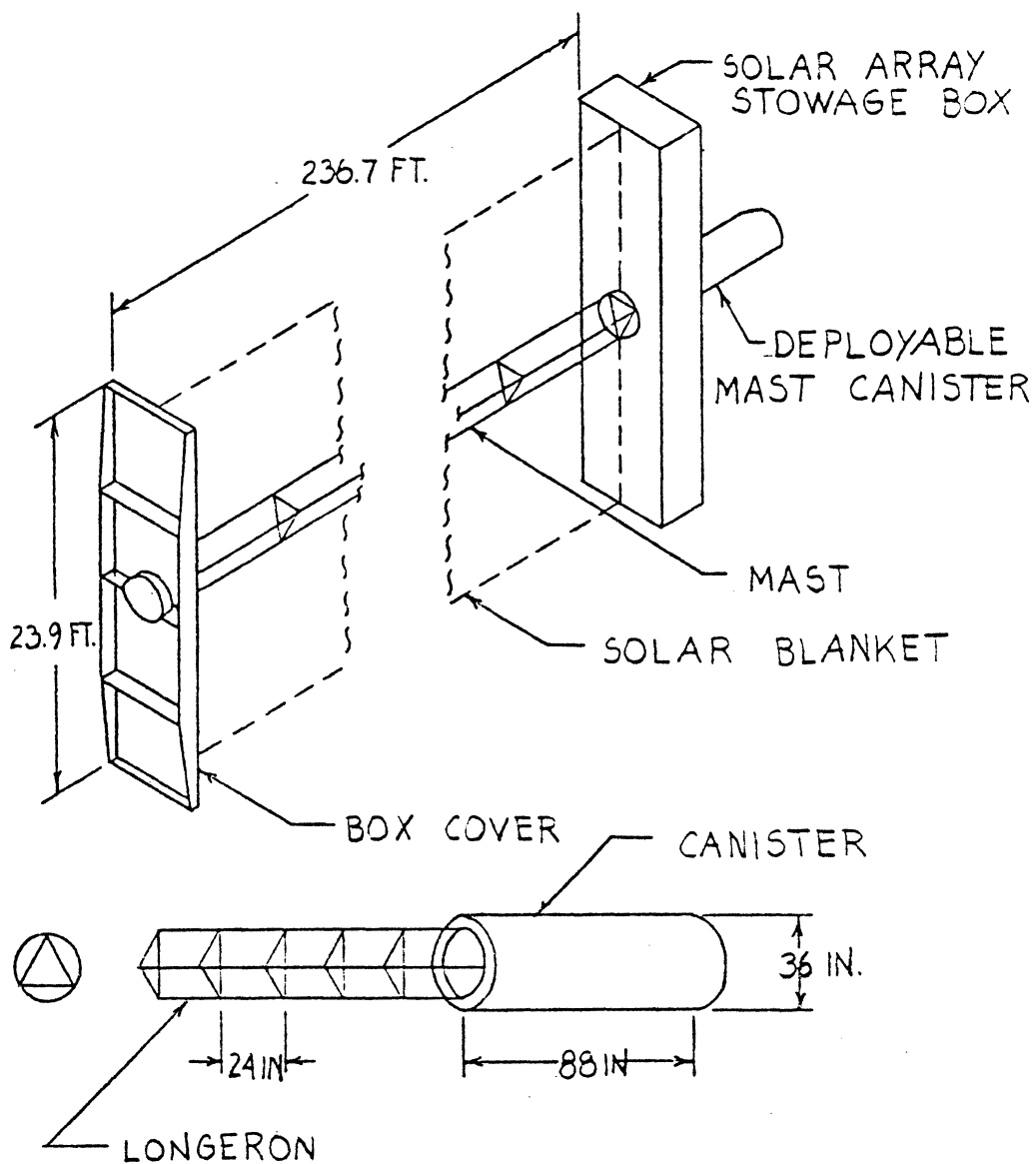


FIGURE 8.7 SOLAR ARRAY DESIGN



## 8.6 HEAT REJECTION SYSTEM

The structure of the radiators is design to maximize the amount of heat rejected to space while simplifying the required EVA to make the system operational.

The total system is comprised of 48 panels attached at the top and two sides on the support tube. At each location, three panels are placed in grooved slots with the appropriate connecting ports. Rather than simply joining these to the surface on the skin, these slots provide extra "clamped stiffness" to the panels. After the first three are in place and attached to the satellite tube, the other panels are joined to these (see Figure 8.8).

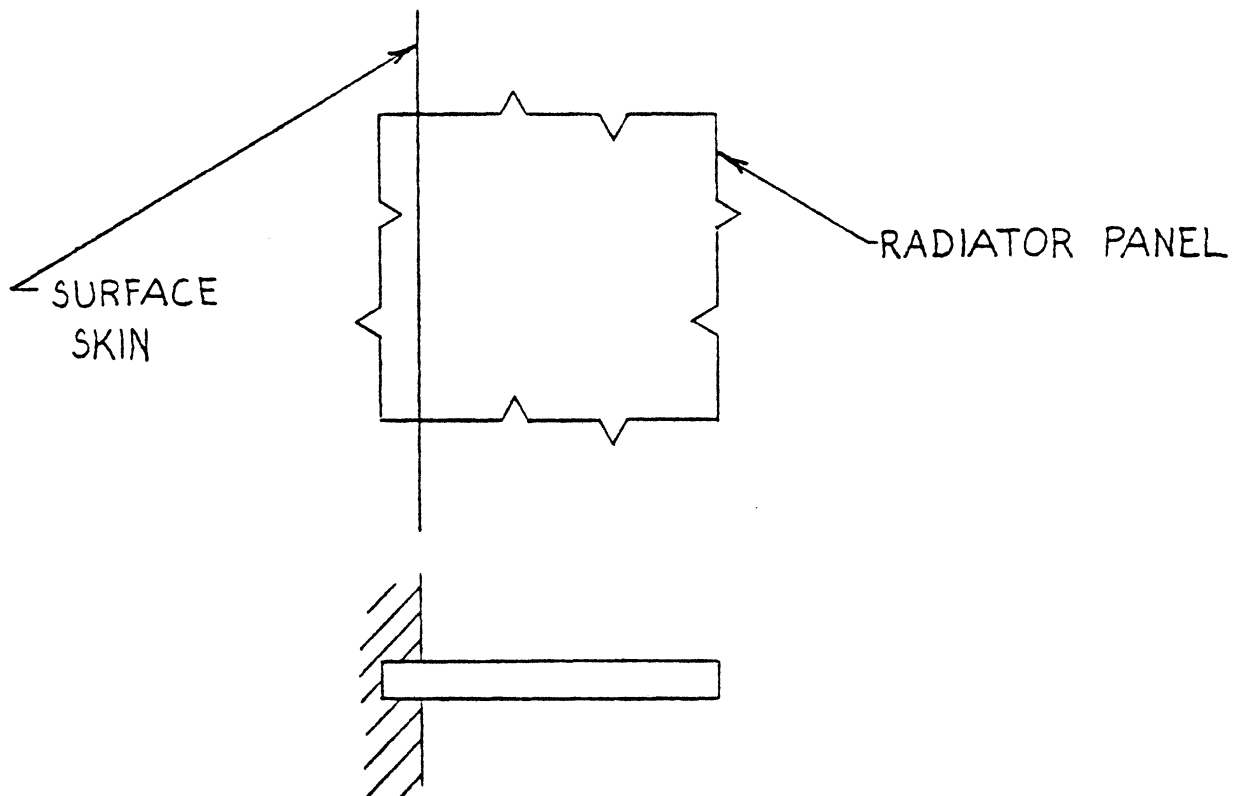


FIGURE 8.8 PANEL MOUNTING

The simplicity of the EVA is due to the basic construction of the individual panels. For launch, the stored position of the panels in the bay is chosen from available volume, while retaining symmetry about the x-axis. Placement in the Orbiter bay is shown in Figure 8.2. This positioning does not significantly effect the C. G. At each location, 12 panels are stored in a secure casing which attaches to pins on the Orbiter bay sides. This casing holds all 12 panels in a structurally stable arrangement.

## 8.7 ACCESS AND DOCKING

### 8.7.1 Access

The annular plates allow for entry and sufficient movement through the satellite interior for EVA repair purposes or removal of internal equipment. For access to the interior, a hatch is located on the satellite surface. The dimensions of the hatch are 4 ft x 4 ft (1.22 m x 1.22 m). A slide-release door is used instead of a hinged door, as it is free of obstructions. This allows for ease in opening (see Figure 8.9).

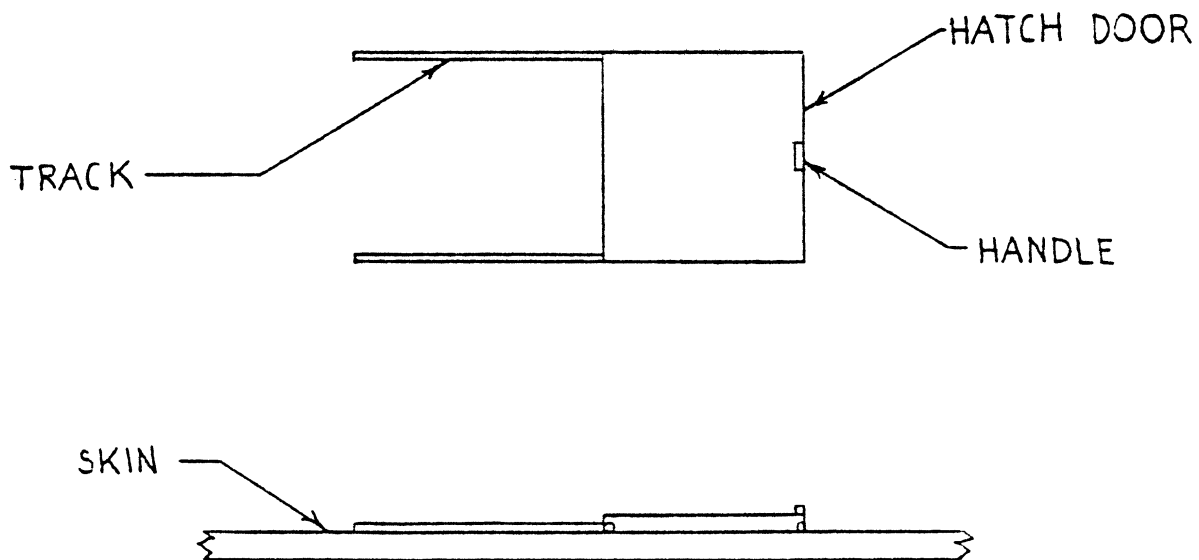


FIGURE 8.9 HATCH DOOR

### 8.7.2 Docking

Docking to the shuttle must be done with precision. The universal docking unit, similar to that used on the Apollo-Soyuz mission, is attached to the propulsion support structure. The docking location was chosen so as to allow the solar panels full freedom of rotation without hitting the Orbiter nose (see Figure 8.10).

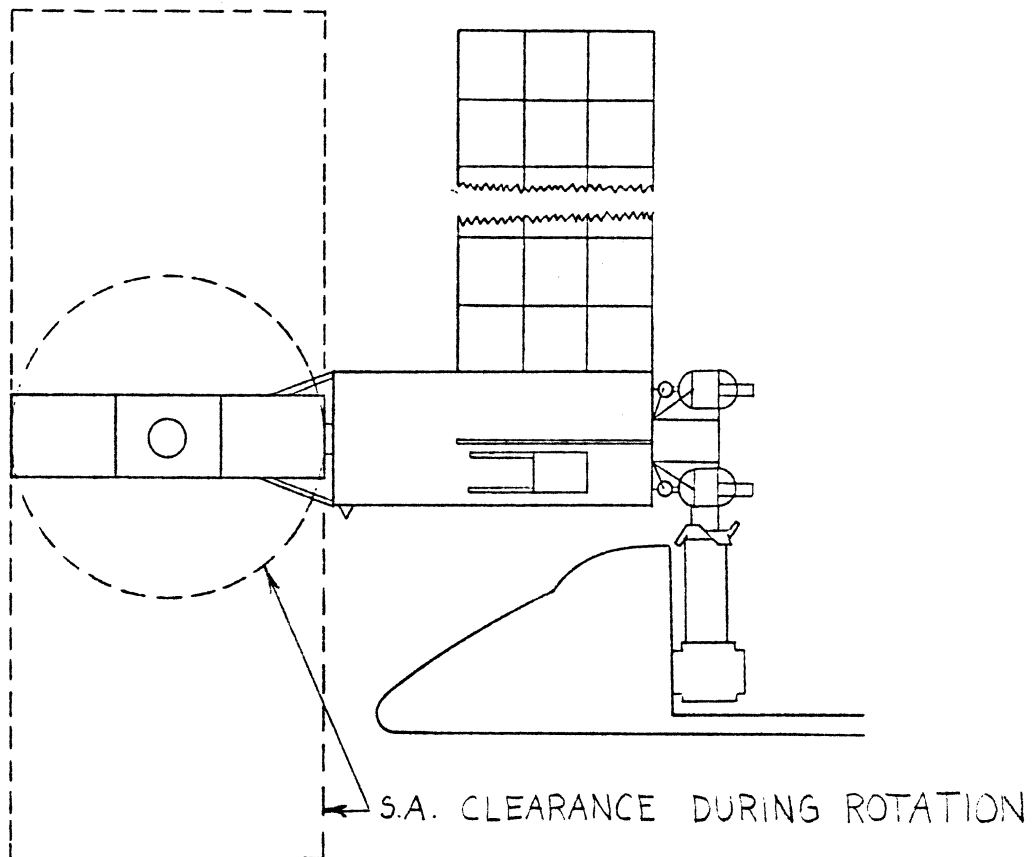


FIGURE 8.10 OASIS DOCKING CONFIGURATION

The docking port will have no EVA access to the satellite, but will transfer all power cables and coolant pipes to the Orbiter.

### 8.8 PROPULSION SUBSTRUCTURE

The support structure for the propulsion unit is an octagonal configuration with an open bottom for the docking unit (see Figure 8.11). Sliding tracks are incorporated into the design to secure the tanks. These allow for easy replacement of the tanks and follow our modular design basis.

Four propulsion tanks are located on every other side, leaving four sides open. The bottom cannot be used due to the docking unit. Therefore, the top remains open for structural symmetry. The 8 ft (2.44 m) long propulsion tanks are easily removable by EVA.

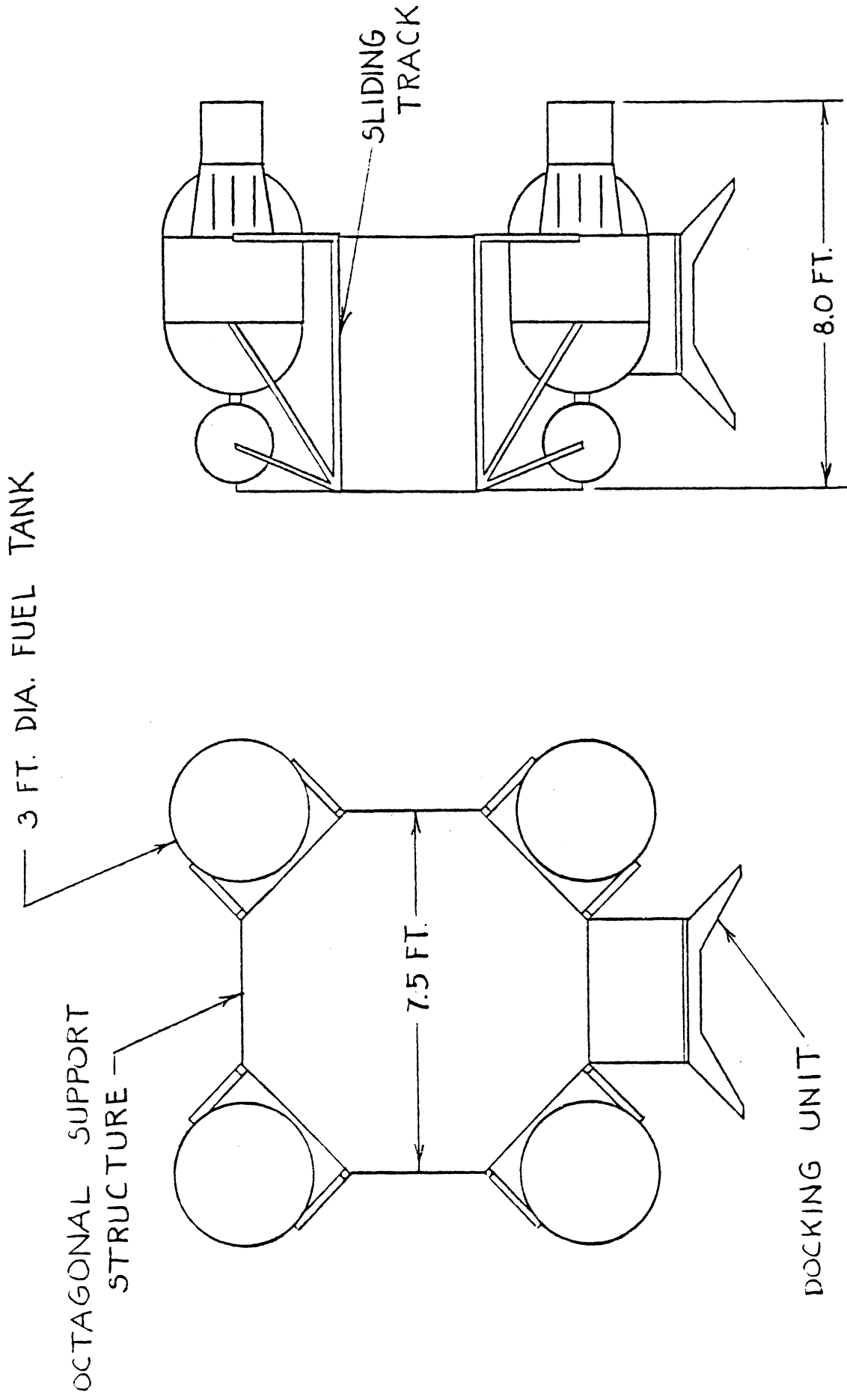


FIGURE 8.11 PROPULSION UNIT

### 8.9 COMPONENT WEIGHT AND CENTER OF GRAVITY

Item	Quantity	Total Weight lbs (N)	X-cg ft (m)	Y-cg ft (m)	Z-cg ft (m)
Main Structure	1	1801 (8014)	38.9 (11.9)	0.0 (0.0)	0.0 (0.0)
Docking Port	1	930 (4139)	55.4 (16.9)	0.0 (0.0)	-6.0 (-1.8)
SEPS Cannister	2	700 (3115)	14.5 ( 4.4)	0.0 (0.0)	0.0 (0.0)
Propulsion Support Structure	1	800 (3560)	55.4 (16.9)	0.0 (0.0)	0.0 (0.0)
Equipment Platforms	8	1379 (6137)			
Batteries	20	13600 (60520)			
Battery Chargers	20	800 (3560)			
Regulators	24	1488 (6622)			
Communications and Data Handling	1	270 (1202)	41.9 (12.8)	0.0 (0.0)	3.8 (1.2)
Thermal Radiator Modules	48	312 (1388)			
Insulation	-	55 ( 245)	-----	-----	-----
Coolant Pumps	2	124 ( 552)	41.9 (12.8)	0.0 (0.0)	.8 ( .2)
Cold Plates	-	520 (2314)	-----	-----	-----
Pressure Regulator	1	10 ( 45)	-----	-----	-----
Flow Control Assembly	1	17 ( 76)	-----	-----	-----
Interface Heat Exchanger	1	14 ( 62)	46.9 (14.3)	-3.6 (-1.1)	2.4 ( .7)
Momentum Wheels	6	2840 (12638)			
Rate Gyros	9	104 ( 463)	49.4 (15.1)	0.0 (0.0)	-3.5 (-1.1)
Digital Computers	2	200 ( 890)	41.9 (12.8)	0.0 (0.0)	0.0 (0.0)
			46.9 (14.3)	0.0 (0.0)	4.1 (1.3)

See Figure 8.5

Mounted Separately in Bay

8.9 COMPONENT WEIGHT AND CENTER OF GRAVITY (Cont'd)

Item	Quantity	Total Weight lbs (N)	X-cg ft (m)	Y-cg ft (m)	Z-cg ft (m)
Interface Unit	1	105 ( 467)	46.9 (14.3)	0.0 (0.0)	-2.7 (-.8)
Memory Load Unit	1	20 ( 89)	46.9 (14.3)	2.5 (0.8)	2.0 (0.6)
Solar Array	2	4172 (18565)	14.5 ( 4.4)	0.0 (0.0)	0.0 (0.0)
Fuel Tanks	4	7528 (33500)	55.4 (16.9)	0.0 (0.0)	0.0 (0.0)
Totals		37844 (168406)	38.1 (11.6)	0.0 (0.0)	0.0 (0.0)

## 8.10 AREAS OF FUTURE STUDY

Improvements in the designed system are possible by implementation of various alternatives.

Decreasing the size of the solar cell system would result in decreasing the needed bay volume. As it now stands, the volume for the present solar array occupies 40% of the Orbiter bay volume. Much research was done on dual-fold circular solar arrays. The deployment arrangement optimizes the cell area by incorporating the deployment mechanism into the solar array. Since this array type is still under development, proof of its feasibility was not available. However, when compared with bulky solar arrays, it does look like a promising alternative in the future (see Figure 8.12).

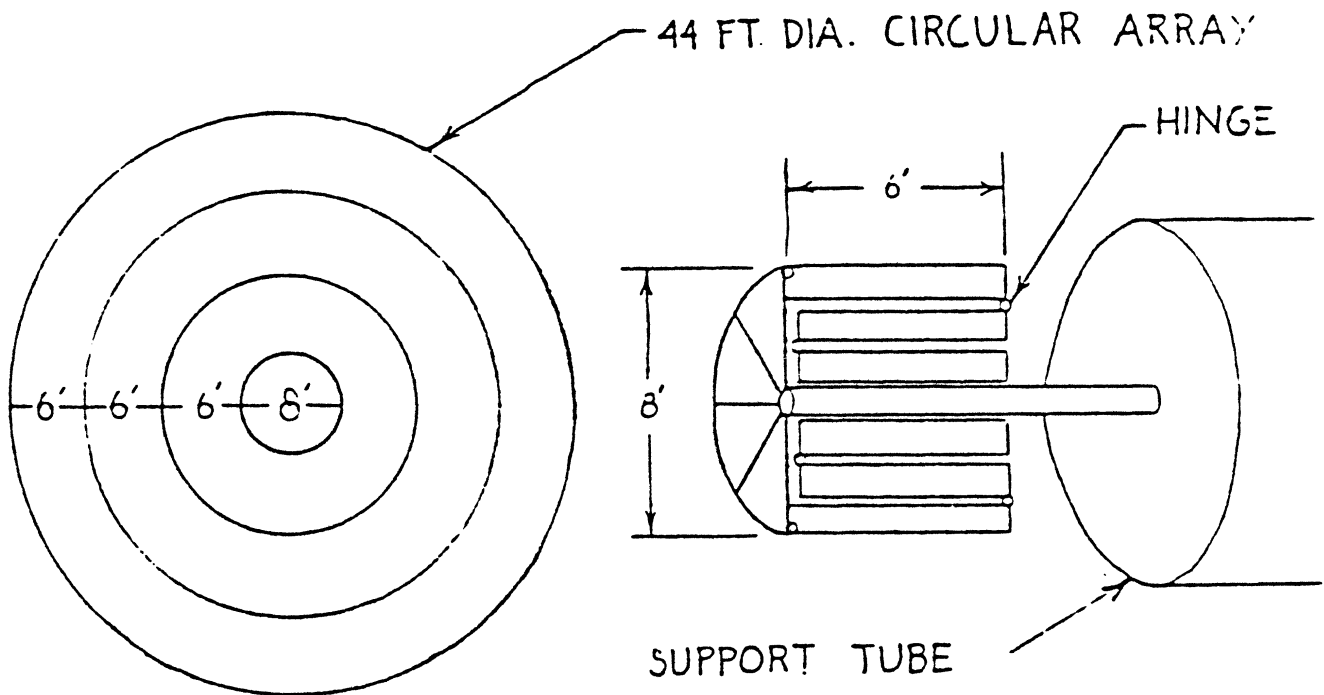


FIGURE 8.12 CIRCULAR ARRAY DESIGN

The docking mechanism could be modified to allow EVA access to the satellite from the orbiter. This transfer port is being investigated by NASA; and their system can accommodate this. However, their system does not have large power lines using most of the available crawl space. A futuristic docking port should be able to handle both human transfer and all necessary service umbilicals from the satellite.

Increasing the solar panel area is another way to improve the satellite. With larger arrays, we would have more power produced. Structurally, more study and testing must be done to improve the deployment mechanism and booms to support the added mass.

#### 8.11 REFERENCES

1. Baker, E. H. , Koualeusky, L. , Rish, F. L. , Structural Analysis of Shells, McGraw Hill Book Company, New York, N. Y. , 1972.
2. Dean, William S. , V. P. and Program Manager Shuttle System Int. , Rockwell International Corp. , "Space Shuttle Interface Control Document Level II," U. S. Government Printing Office, Washington, 1978.
3. Denton, Steven, Marshall Space Flight Center, Huntsville, Alabama, personal communication, March 1978.
4. Osgood, Carl S. , Spacecraft Structures, Prentice Hall, Englewood Cliffs, New Jersey, 1966.
5. "25 KW Power Module Preliminary Definition," NASA Marshall Space Flight Center, Alabama, September 1977.
6. Preiswerk, Peter, Astro Research Corp, Santa Barbara, California, personal communication, March 1978.
7. Rauschenbach, H. S. , Solar Cell Array Design Handbook, Vol. 1, Jet Propulsion Laboratory, Pasadena, California, October 1976.
8. Sammuals, Ronald, Astro Research Corp. , Santa Barbara, California, personal communication, March 1978.
9. Scott, Richard A. , The University of Michigan, Applied Mechanics and Engineering Science, Ann Arbor, Michigan, personal communications, February 1978.
10. Sikarskie, David L. , Aerospace Engineering 314 Class Notes, The University of Michigan, Ann Arbor, Michigan, 1975.
11. Sikarskie, David L. , Aerospace Engineering 515 Class Notes, The University of Michigan, Ann Arbor, Michigan, 1977.
12. Sikarskie, David L. , The University of Michigan, personal communications, February 1978.



13. Stanek, Floyd J. , Stress Analysis of Circular Plates and Cylindrical Shells, Dorrance and Company, Philadelphia, Pennsylvania, 1970.
14. Timoshenko, S. , Theory of Elastic Stability, McGraw Hill Book Company, Inc. , New York, N. Y. , 1st ed. , 1936.

## COMMUNICATIONS AND DATA HANDLING

## 9.1 INTRODUCTION

The Communications and Data Handling (C&DH) subsystem of Project OASIS serves as the overall command center for the entire satellite. The function of this subsystem is to:

- (1) Provide a telemetry link to a ground command facility
- (2) Provide a command uplink
- (3) Provide a tracking link with a ground command facility
- (4) Collect and record information from other subsystems of the spacecraft and transmit it to a ground command facility.
- (5) Detect and decode all command data and distribute it to various subsystems.

The C&DH module consists of several different components, each one performing specific functions in order to accomplish the duties of the entire subsystem. This chapter discusses the advantages of using the NASA Standard C&DH module, the functions of its various components, the existing and future ground communication facilities, and the OASIS tracking method.

## 9.2 SUMMARY

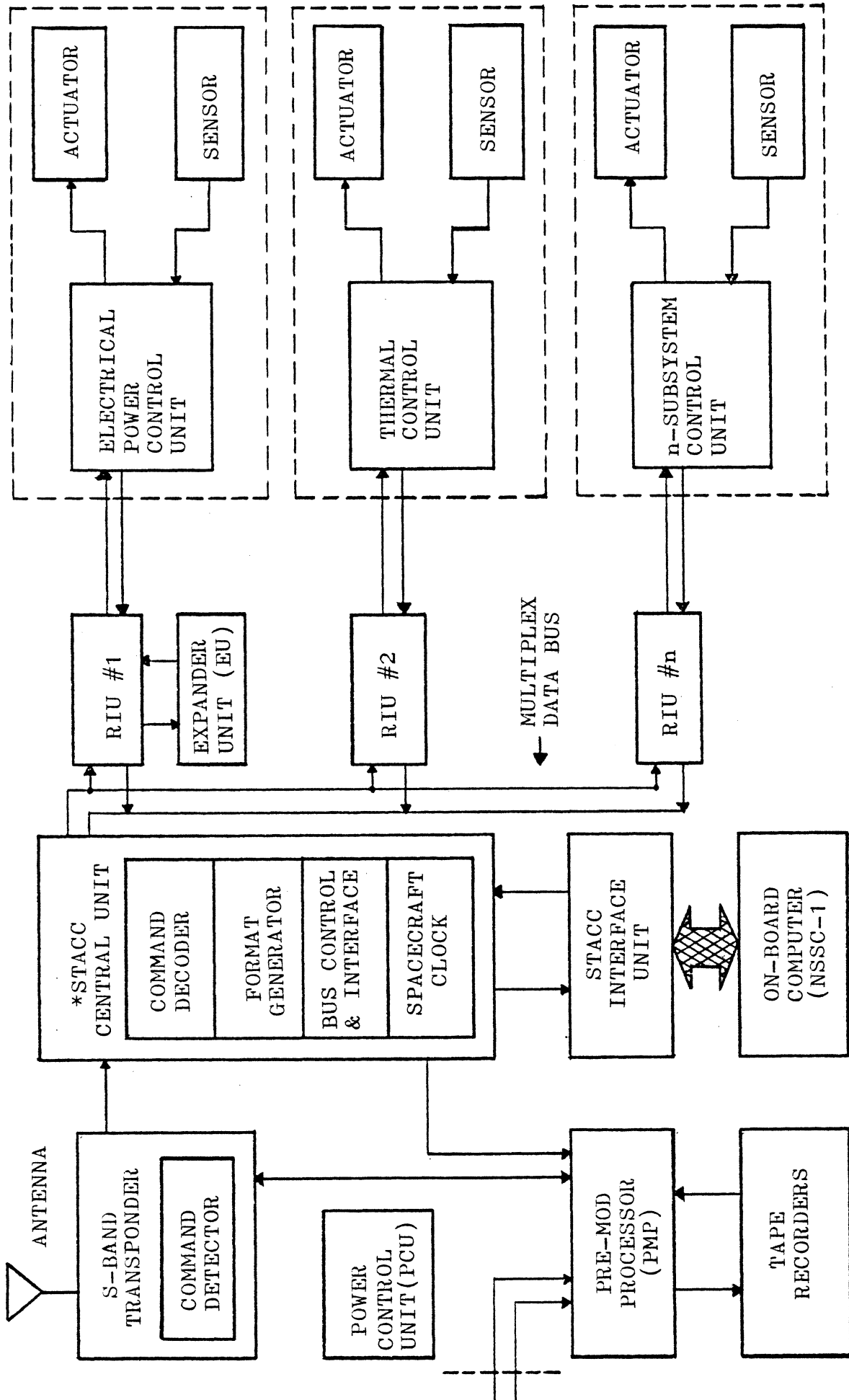
To accomplish the five tasks listed in Section 9.1 Project OASIS will utilize the NASA Standard C&DH module. This module is a fully integrated and self-sufficient package highly adaptable to the OASIS mission. The module offers several advantages over other similar systems due to its versatility, availability and relatively low cost.

The OASIS C&DH subsystem transmits in the S-band which allows compatible communication links with the Tracking and Data Relay Satellite System (TDRSS) and the Satellite Tracking and Data Network (STDN). Commands to OASIS can originate from a ground facility via TDRSS/STDN, or the Space Shuttle Orbiter. In addition, the on-board computer can operate OASIS in an autonomous condition.

All housekeeping telemetry will be either transmitted immediately or recorded and then dumped to a ground facility on every orbit.

Figure 9.1

# C&DH SUBSYSTEM BLOCK DIAGRAM



REDUNDANT COMPONENTS NOT SHOWN  
 \*STANDARD TELEMETRY & COMMAND COMPONENTS  
 \*\*EXTERNALLY GENERATED DATA SOURCES

### 9.3 ADVANTAGES OF UTILIZING THE NASA STANDARD C&DH SUBSYSTEM

Performance, versatility and adaptability, together with availability and economic values constitute the advantages of using the C&DH subsystem of the Multimission Modular Spacecraft (MMS).

#### 9.3.1 Performance

The C&DH module provides a fully redundant configuration of space-proven components and assembly techniques. Since the on-board computer can evaluate telemetry from remote subsystems, the possibility of up to 72 hours of independent operation of the satellite is available. Also, the modular construction allows for in orbit repairs or replacement of components.

#### 9.3.2 Versatility and Adaptability

Due to the foresight in the design of the C&DH module, adaptation to an individual mission is accomplished without great difficulty. The system can be easily expanded with the addition of general purpose remote interface units, remote interface expander units, tape recorders, and other mission unique equipment. Another feature of the system is that the computer, which offers both timed and decision-directed command and telemetry formats, can be reprogrammed in orbit.

#### 9.3.3 Availability and Economic Values

Since the MMS is planned to be used for a number of future missions, the C&DH system is now readily available. This eliminates the need for major development expenditures and new hardware design, which results in a relatively low cost of production. The C&DH module assembly procedures, testing and quality control have all been precisely organized to assure delivery within 16 months from the time the order is placed. For breakdown of production time and cost refer to Appendix G.1.

### 9.4 C&DH SUBSYSTEM DESCRIPTION

The C&DH module is composed of command detection, decoding, and routing equipment; telemetry collection, formatting, and processing equipment; and timing and computation units (see block diagram on previous page). In addition, the performance of these components is monitored by a fully self-contained housekeeping system. For a list of all basic Housekeeping Data Inputs and Commands refer to Appendix G.2.

The Standard Telemetry and Command Components (STACC) of the C&DH module operate on the concept of remote multiplexing of telemetry data and remote distribution of commands. Command and telemetry data are

routed to and from other spacecrafts and other OASIS subsystems by means of a duplex serial digital multiplex data bus. For emergencies or malfunctions of individual components, redundancy is implemented in the basic subsystem through the use of standby spare units. These techniques minimize system failures, and permit in orbit repair and replacement of components.

The following subsections discuss the function of individual C&DH components.

#### 9.4.1 Antennas

OASIS uses omnidirectional antennas for transmission and reception of data. In order to provide for fail-safe redundancy, two unified S-band (USB) antennas are mounted on the fuselage of OASIS. For position of antennas refer to page 81.

Omnidirectional USB antennas were chosen because of the following criteria:

- (1) Compatability with other spacecraft (TDRSS, Orbiter, etc).
- (2) Lower price as compared to high gain antennas
- (3) As opposed to highly directive antennas, omnidirectional antennas do not require a high degree of accuracy in positioning the spacecraft.

#### 9.4.2 Transponder

The transponder consists of antenna transfer switches, radio frequency (RF) loads, and interconnecting 1/4" (0.635 cm) O.D. semirigid coaxial cable assemblies. It is mounted so as to reduce power amplifier transistor junction temperatures, and RF losses. In addition to providing the RF link for telemetry and command, the transponder provides turn around ranging, compatible with the STDN/TDRSS data network. Its own housekeeping telemetry is routed to the Data Handling System (DHS) via a remote interface unit (RIV). Down-link telemetry is received from the DHS through a pre-modulator processor (PMP) for transmission. Command and control for the transponder are also routed via the internal RIU. OASIS transponder operates in the S-band, transmitting at a frequency of 2.23 GHz. It receives at a frequency of 2.05 GHz. At these frequencies and with the power available, 5 watts, the OASIS communication system will handle approximately 2.6 KBPS forward and 1.0 KBPS return via TDRSS single access channels. Data rates will be higher should direct communications with the STDY ground stations be established.

OASIS operating frequencies were chosen because:

- (1) They are compatible with the TDRSS & STDN USB transponders.
- (2) They allow transmission at the desired data rate.
- (3) They allow tracking using pseudo-random codes.
- (4) Combined background noise is minimum in the S-band frequency range.

#### 9.4.3 STACC Central Unit (CU)

The CU is the heart of the C&DH subsystem. It has eight major functions:

- . Command verification
- . Command decoding
- . Command distribution control
- . Telemetry format generation and control
- . Multiplex data bus control
- . Control and Timing of Data Exchange with the on-board computer
- . Spacecraft clock and timing control
- . Diversity error free command selection.

The eight functions are complimented by several advantages such as high thruput rates, high reliability and no single point failures possible in the redundant configuration.

#### 9.4.4 STACC Standard Interface for Computer (STINT)

The function of the STACC STINT is to provide the necessary interfaces for the exchange of information between the on-board NASA standard spacecraft computer (NSSC) and the STACC CU, the STACC RIU, and the pre-modulator processor (PMP). The STINT has the following capabilities:

- . Distribution of stored commands
- . Control of NSSC by ground command
- . Telemetry format control by the NSSC
- . Acquisition of Data for NSSC use
- . NSSC access to all transmitted telemetry data
- . Exchange of data between NSSC and RIU's.
- . Memory loading under software or hardware control
- . Memory readout under software or hardware control.

#### 9.4.5 NASA Standard Spacecraft Computer (NSSC)

The NSSC performs data computation within the C&DH subsystem. It consists of four memory modules (MM) which have a capability for 8K, 18 bit words each; and two central processing modules. With the addition of four memory units more, the capacity of the system can be enlarged to accommodate 64K, 18 bit words.

The NSSC performs the following functions:

- . Stores commands for execution
- . Provides command verification and fault detection
- . Provides flexible telemetry format control
- . Controls autonomous spacecraft operations
- . Performs limit check to monitor system health and safety
- . Generates summary messages
- . Performs attitude control law computations
- . Controls solar array pointing
- . Performs orbital maneuvering computations
- . Controls attitude and propulsion subsystems for orbital maneuvering.

#### 9.4.6 Pre-Modulator Processor (PMP)

The PMP is the principal component for the conditioning of the data signal. In this unit, data is encoded, conditioned and multiplexed and then routed to the transponder. This data can be accepted in the following forms:

- (1) Real time telemetry data formatted by the CU.
- (2) Stored data from the NSSC through the STINT.
- (3) Taped data from the tape recorders.
- (4) External data such as from a payload or orbiter.

#### 9.4.7 Remote Interface Units (RIU) and Expander Units (EU)

The RIU's of the C&DH serve two primary functions:

- . To distribute commands from the CU to the appropriate subsystems
- . To accept telemetry data from various subsystems and routes it to the CU.

To accomplish the task of communicating with the CU the RIU uses the multiplex data bus which is a type of party line system. The multiplex data bus contains two main communication lines. The supervisory line sends commands to the RIU from the central unit. The reply line sends messages to the CU from the RIU.

The C&DH subsystem uses several RIU's, each responsible for communications with a particular OASIS subsystem. All commands exiting the CU are accepted by every RIU. Each RIU then recognizes its own unique commands and proceeds to perform one of three possible functions.

- . Decode and distribute discrete and 16 bit serial commands
- . Accept, condition, format and transmit up to 64 channels of telemetry data
- . Provide up to 8 switched ground returns for analog data.

RIUs have three modes of operation, off, standby or active. Normally the RIU will operate in standby for power saving reasons and will switch to active when receiving commands or transmitting telemetry data. Up to 31 RIUs can be interfaced with one CU.

Expander units (EU) are attached to a host RIU to increase its multiplex capability. Each EU operates in the same mode as the host RIU and provides it with sixty-four additional telemetry channels, eight ground returns, clocks and other functions. Up to seven EUs may be attached to a single RIU.

#### 9.4.8 Mission Unique Equipment

The following components were chosen to assist the C&DH subsystem. Except for the NSTR, these components are not shown in the C&DH block diagram.

(1) NASA standard tape recorder (NSTR). The component is package in two parts: a transport unit (TU) and an electronic unit (ELU). The NSTR receives processed data from the PMP and provides  $9 \times 10^8$  bits of storage.

(2) Four additional memories for the NSSC (previously mentioned in Section 9.4.5).

(3) Global Positioning System (GPS) terminal. This terminal is used by the C&DH subsystem to provide accurate location of OASIS via GPS.

#### 9.4.9 Power Control Unit (PCU)

The PCU draws power from the main spacecraft unregulated +28 volt bus and distributes it among the components within the C&DH subsystem, while protecting the bus from shorts in the C&DH's components. The PCU also provides three regulated power lines to the two computers, their memory units, and the STINT. The PCU is programmed to shut down the computer in the event of improper computer operations or faulty line voltages. Finally, the PCU provides relay driving signals to the RF transfer switches and redundant switched lines to the mission unique equipment.

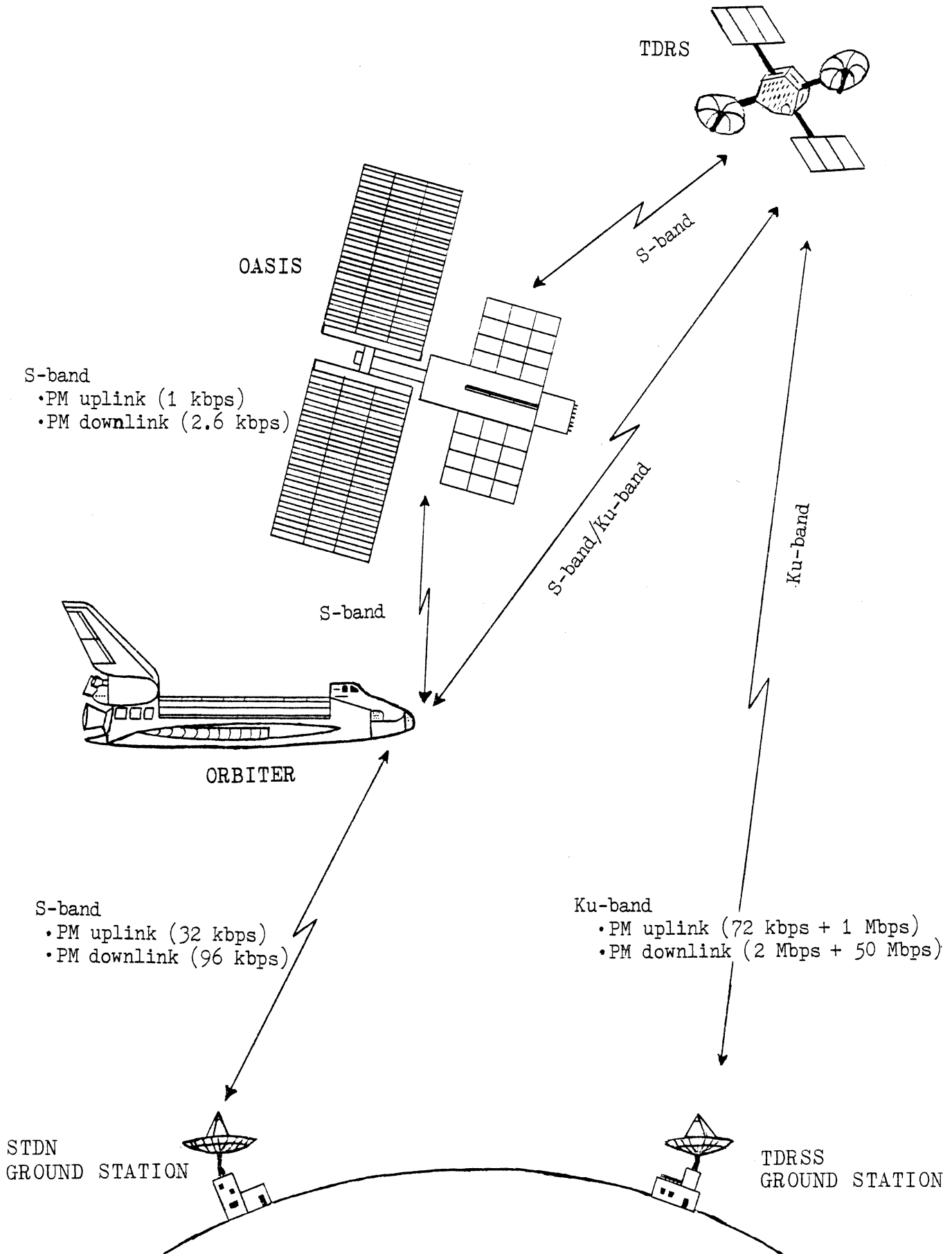
The power consumption of each individual C&DH component can be located in Appendix G.3.

### 9.5 GROUND COMMUNICATION SYSTEMS

The OASIS communications system is compatible with the Satellite Tracking and Data Network (STDN) and the Tracking and Data Relay Satellite System (TDRSS).



Figure 9.2  
 OASIS COMMUNICATION AND TRACKING LINKS



The TDRSS system is being developed for shared use by NASA and Western Union in the 1980's, (see Table 9.1). It consists of three geosynchronous satellites plus an in orbit spare which will relay data between orbiting user satellites and a ground station located in White Sands, New Mexico. The system provides simultaneous data relay service for up to 32 users with data rates ranging from 100 BPS to 300 MBPS. At the White Sands Station, the data relayed by the TDRS will be handed over to NASA's communication interface (NASCOM), which will distribute it to other NASA installations.

For most of OASIS communications with the ground, the TDRSS will handle all tracking, telemetry and control data links. If necessary, however, communication links with STDN ground stations could also be established so that housekeeping, command, and tracking functions can be handled directly from a STDN station.

Finally, all communications with OASIS will be handled through the space shuttle orbiter when the module is docked with the Orbiter. In this mode, all links will be established through hard wire methods.

Table 9.1 TDRS Launching Schedule

TDRS #	Shuttle Mission #	Date of Launch
A	8	July 80
B	10	Nov 80
C	12	Jan 81
D	15	May 81

## 9.6 TRACKING

The OASIS ranging system will be based on pseudo-random codes. In this method, a long code is transmitted and repeated by the C&DH subsystem of OASIS, allowing accurate range measurements. Range rate will be found by measuring the Doppler shift of the transponder carrier signal. Angles will be measured by antenna pointing.

## 9.7 REFERENCES

1. Balakrishnan, A. V., Space Communications, New York, McGraw Hill Book Company Inc., 1963.
2. Fairchild-Spacetac Company, NASA Standard Communications and Data Handling Subsystem, Germantown, Maryland, 1977.

3. Filipowsky, R. F. and E. I. Muehldorf, Space Communication Systems, Englewood, New Jersey, Prentice Hall International, Inc. , 1965.
4. Krassner, G. N. and J. V. Michaels, Introduction to Space Communication Systems, New York, McGraw Hill Book Company, Inc. , 1964.
5. Newman, D. B. , Space Vehicle Electronics, Princeton, New Jersey, D. van Nostrand Company, Inc. , 1964.
6. "25 kw Power Module Preliminary Definition," NASA, Marshall Space Flight Center, Alabama, September 1977.
7. "Project MERMAIDS", The University of Michigan, Department of Aerospace Engineering, Ann Arbor, April 1975.
8. "Project RODAN," The University of Michigan, Department of Aerospace Engineering, Ann Arbor, December 1973.
9. "Project SCANNAR," The University of Michigan, Department of Aerospace Engineering, Ann Arbor, April 1970.
10. "Project SPIDAR," The University of Michigan, Department of Aerospace Engineering, Ann Arbor, April 1974.
11. Tischer, F. J. , Basic Theory of Space Communications, Princeton, New Jersey, D. van Nostrand Company, Inc. 1965.
12. TRW Inc. TDRSS Fact Sheet, Redondo Beach, California, 1977.
13. Western Union News Bureau, News: Space Shuttle will Launch Western Union TDRSS Satellite; Upper Saddle River, New Jersey, August 1977.

PROGRAM COST AND DEVELOPMENT

10.1 INTRODUCTION

This chapter concludes the study of Project OASIS with a discussion of the cost analysis and a project development schedule.

10.2 SUMMARY AND CONCLUSIONS

10.2.1 Program Cost Breakdown

The net program cost for OASIS was estimated at 300.3 million in 1978 dollars. This figure includes the cost of fabricating and evaluating a test model and two operational spacecraft. One spacecraft is launched into orbit while the other serves as a backup. The total cost for Project OASIS is the sum of the following phases:

<u>Phase</u>	<u>Cost</u> <u>(Millions)</u>	<u>Per Cent</u> <u>of Net Program Cost</u>
Development, Design, Test & Evaluation (DDT&E)	137.5	43.6%
Fabrication & Evaluation (F/E)	132.4	41.9%
Operations & Support (O/S)	45.8	14.5%
Total	\$315.7	100.0%

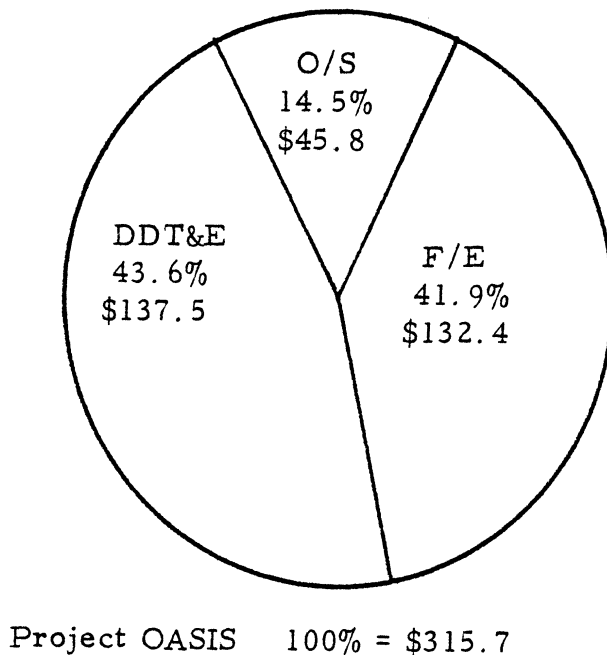


Figure 10.1 Project OASIS Cost (Millions in 1978 Dollars)

### 10.2.2 Project Scheduling

Based on the OASIS scheduling study, the initial operating date could be attained as early as 1983.

## 10.3 DISCUSSION

### 10.3.1 Program Cost Analysis

#### a) DDT&E Costs

The costs associated with using existing Apollo Telescope Mount (ATM) flight-qualified hardware were evaluated in terms of the costs of production and modification for OASIS requirements. This approach offers a low development cost and minimal technological risk.

The DDT&E cost accounts for 43.6% of the project expense.

Table 10.1 DDT&E Cost Breakdown

<u>Item</u>	<u>Cost (Millions)</u>	<u>Per Cent</u>
. Management	6.9	5.0
. Engineering Design & Dev. (ED&D)	61.9	45.0
. System Engineering & Integration (SE&I)	22.0	16.0
. Spacecraft Testing & Evaluation	22.0	16.0
. Ground Support Equipment (GSE)	15.1	11.0
. Ground Test Hardware (GTH)	9.6	7.0
Total	\$137.5	100%
	(100%)	

#### b) Cost of Fabrication & Evaluation

Direct estimates were used to predict the cost of each component throughout the study whenever there was sufficient information. This information was obtained from manufacturer's data.

The cost of fabrication and evaluation accounts for 41.9% of the project expense.

Table 10.2 Cost Breakdown of Manufacture and Testing

<u>Item</u>	<u>Cost (Millions)</u>	<u>Per Cent</u>
. Management	6.0	4.5
. Test Model	20.0	15.2
. Hardware Production Cost		
- electrical power system	20.0	
-thermal control system	1.5	
-propulsion system	1.0	
-attitude control system	7.7	
-structure	2.5	
-comm & data handling system	2.2	
	<u>34.9</u>	
x 2 spacecraft	69.8	52.7
. System Engineering & Integration	<u>36.6</u>	<u>27.6</u>
Total	\$132.4	100%
	(100%)	

A detailed cost breakdown of each subsystem is displayed in Table 10.3.

Table 10.3 Subsystem Cost Analysis

<u>Item</u>	<u>Cost (Millions)</u>
Electrical Power	
. Solar cells	18.72
. Charges	.20
. Batteries	.80
. Regulators*	.24
. S/A distributor*	.003
. Distributor*	.006
subtotal	<u>20.0</u>
Thermal Control	
. Radiators*	.65
. Insulation	.07
. Plumbing*	.13
. Heat exchanger	.20
. Pumps	.13
. Cold plates	.33
subtotal	<u>1.5</u>
Propulsion	
. One propulsion unit*	.26
x 4 unit	<u>1.0</u>
subtotal	<u>1.0</u>

Attitude Control	
. Momentum wheels*	4.2
. Sun sensors, star tracker, Earth sensor*	.04
. Rate gyro*	3.15
. Digital flight computer*	.1
. Interfaces*	.1
. Memory load unit*	.1
subtotal	<u>7.7</u>

The production cost for the attitude control system is the only cost associated with this system since the components are identical to those used in the ATM.

Structure	
. Docking mechanism*	1.5
. Seps cannister	.75
. Material for structure	.01
. Manpower	.25
subtotal	<u>2.5</u>

Comm. & Data Handling	
. Antennas	0.2
. MMS, C&DH	1.5
. Mission unique equipment (tape recorders, etc)	0.5
subtotal	<u>2.2</u>

Total Cost	<u>\$34.9</u>
------------	---------------

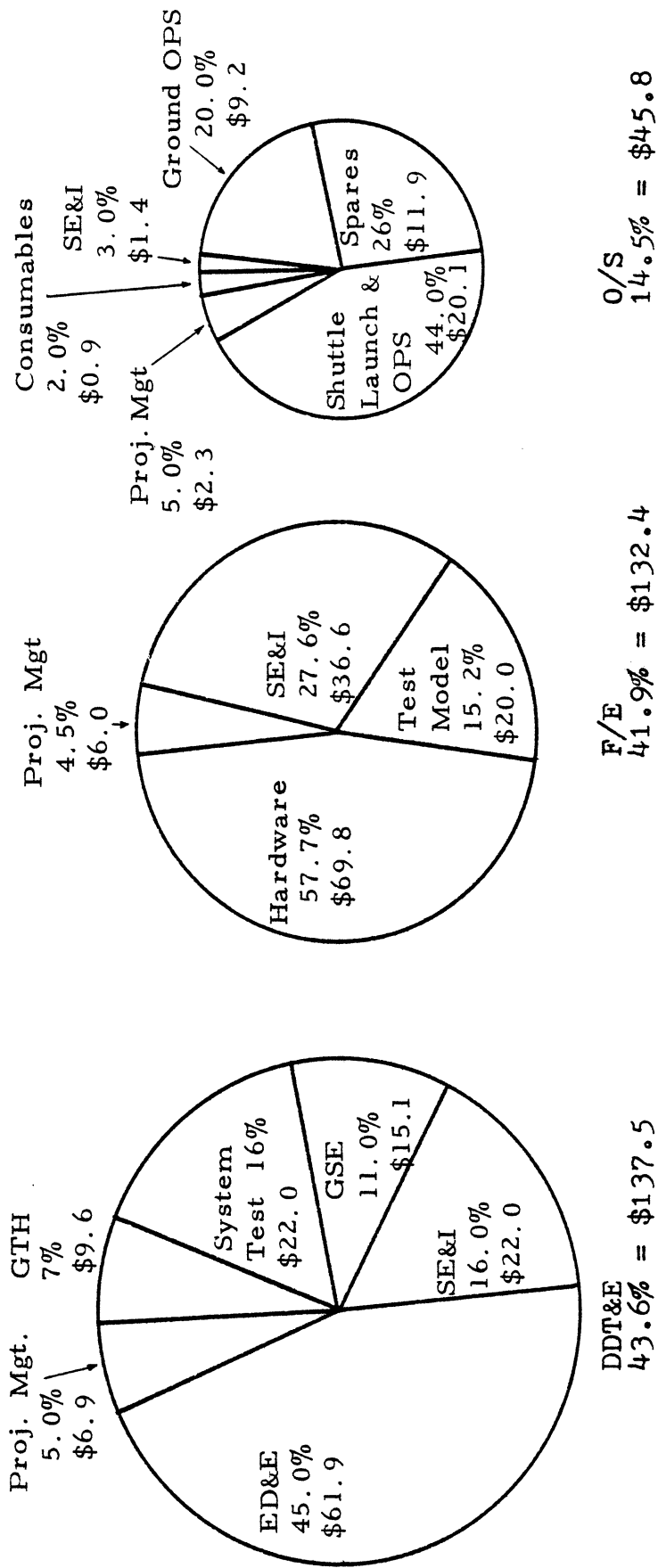
\* Existing components

---

### c) Operations & Support (O/S) Costs

In evaluating O/S costs, an operational, on-orbit lifetime of 5 years is assumed.

The O/S cost accounts for 14.5% of the total project cost.



Project OASIS  
 100% = \$315.7  
 Figure 10.2 Project Costs by Phase (Millions of 1978 Dollars)



Table 10.3 O/S Cost Breakdown (for 5 years)

Item	Cost (Millions)	Per Cent
. Management	2.3	5.0
. Consumables	0.9	2.0
. System Engineering & Integration	1.4	3.0
. Spares	11.9	26.0
. Ground Operation	9.2	20.0
. Shuttle Launch & Flight Operations	<u>20.1</u>	<u>44.0</u>
Total	\$ 45.8	100%
	(100%)	

A summary of these estimates is represented in Figure 10.2.

### 10.3.2 Project Development Plan

The initial operating date for OASIS was estimated in 1983. Based on the Project Planning Scheme, the program will go through four phases.

#### Phase A--Preliminary Analysis

This report is the result of the preliminary analysis which includes:

- . feasibility study
- . technical requirements
- . recommendations
- . preliminary cost estimates & gross scheduling

#### Phase B--Concept Definition

This phase would be performed by several contractors selected by NASA. It includes evaluation of the following:

- . defining mission & system requirements
- . refining the selection of alternative concepts
- . preliminary design
- . preliminary manufacturing & testing requirements
- . performance-trade studies
- . cost & scheduling
- . define management & human approach

The Phase B study reports will be submitted to NASA and the contract will be awarded to the winner by NASA if the budget is approved by congress.

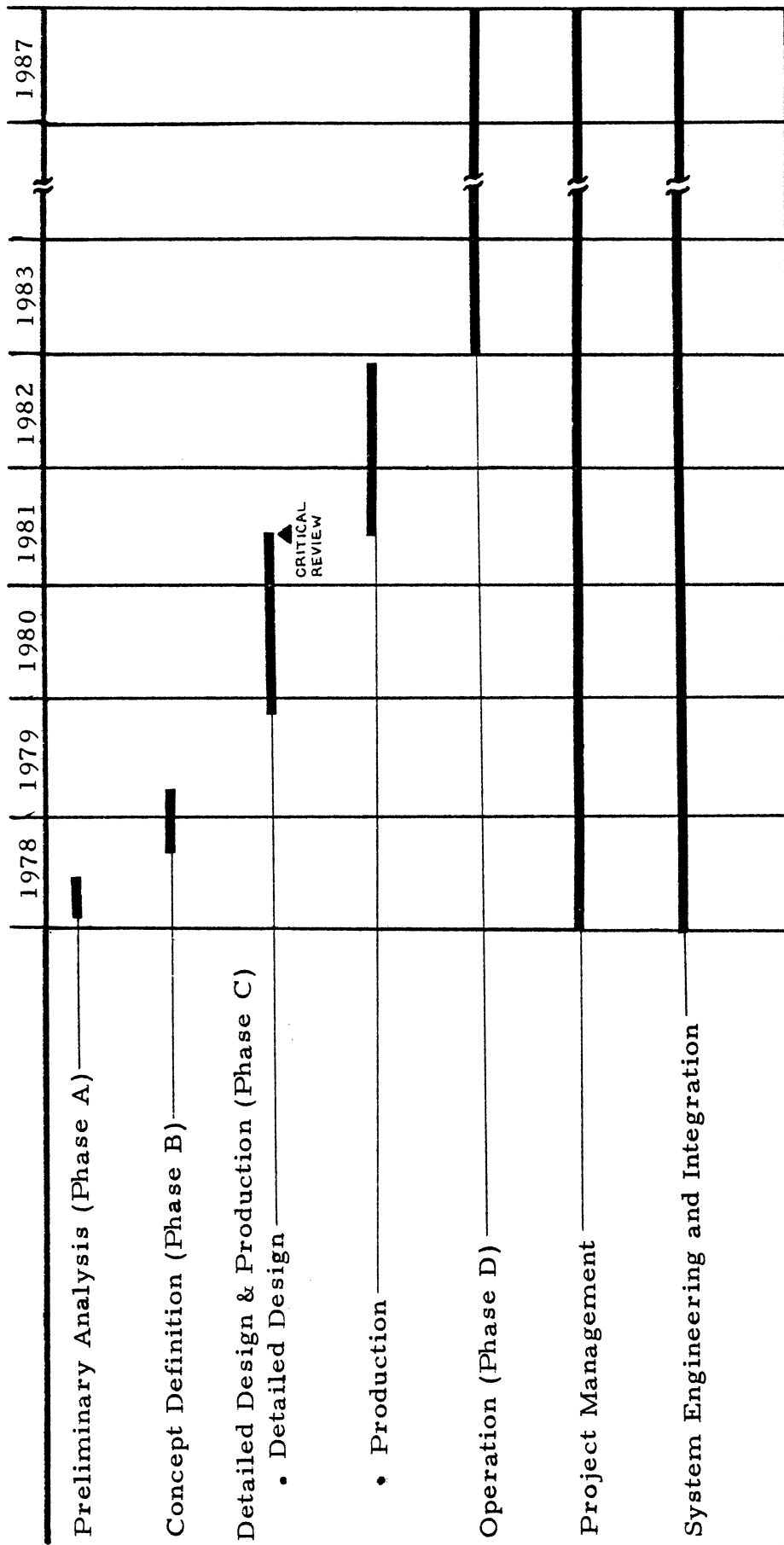


Figure 10.3 OASIS Project Schedule

## Phase C--Detailed Design & Production

The beginning part of Phase C includes:

- . preliminary design review
- . detailed definition of requirements & specifications
- . detailed estimation of cost

Upon the completion of these studies the contractor will freeze the design, go through the critical design review followed by:

- . construction of a model for vibration, thermal, vacuum & radiation environment testing
- . construction of flight models
- . acceptance test
- . mission planning with subsequent crew training, development of pertinent flight procedures

## Phase D--Operation

This phase includes:

- . launch & support operations
- . flight operations
- . maintenance & refurbishment operation.

A typical time schedule for Project OASIS is shown in Figure 10.3.

## 10.4 REFERENCES

1. Manned Orbital System Concepts Study, Book 4, McDonnell Douglas Astronautics Company-West, September 1975.
2. "Solar Power Satellite, Concept Evaluation, Vol. 1, summary", NASA USC, July 1977.
3. Space Planners Guide, USAF, Air Force System Commands, July 1965, pp VIII-VII27.
4. Smith, William: personal communication, March 23, 1978.

## APPENDIX A

### A. 1 TEMPERATURE ANALYSIS

The steady-state operating temperature of the solar array wings for the sunlit period is found as follows:

First, these assumptions were made:

- 1) the process is isothermal
- 2) no interaction between neighboring cells
- 3) neglect thermal conduction in connecting wires
- 4) the emitting areas on front and back of the panels are equal
- 5) the earth albedo is neglected (this causes the resulting  $T_{op}$  to be lower than normal)

The governing equation is:

$$T_{op} = \left[ \frac{\alpha_{SE} S}{\sigma(\epsilon_{HF} + \epsilon_{HB})} \right]^{\frac{1}{4}} \quad (\text{Reference 14})$$

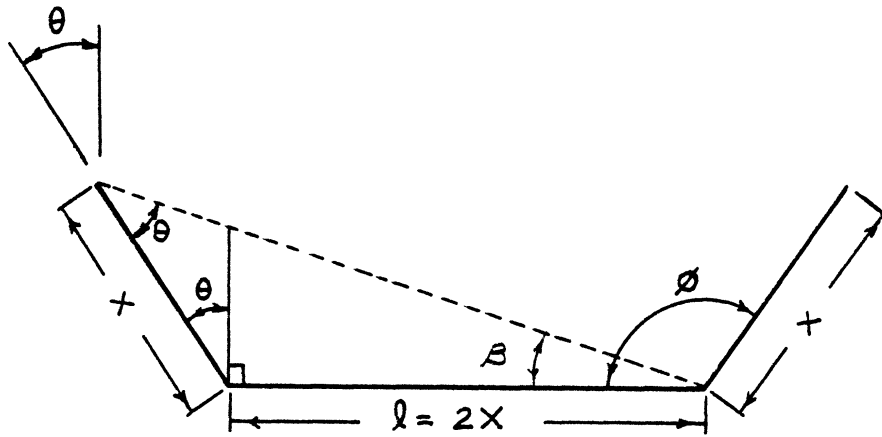
where

$\alpha_{SE}$ = effective solar absorption (worst case)	0.81
$S$ = solar constant	2.15 kW/m <sup>2</sup>
$\epsilon_{HF}$ = hemispherical emittance (front)	0.82
$\epsilon_{HB}$ = hemispherical emittance (back)	0.90
$\sigma$ = Stefan-Boltzman constant	5.67 x 10 <sup>-8</sup> $\frac{w}{m^2 \text{ } ^\circ K}$

$T_{op} = \left[ \frac{(0.81)(2.15 \times 10^3 \frac{watts}{m^2})}{(5.67 \times 10^{-8} \text{ watts } (0.82 + 0.9) \frac{m^2 K^4}{m^2})} \right]^{\frac{1}{4}}$	$= 365.5^\circ K$ $= 92.5^\circ C$ $= 198.6^\circ F$
--	--

## A.2 SOLAR ARRAY CONCENTRATORS



SIDE VIEW OF SUB-BLANKET

$$(l \tan \beta) \cos \theta = \frac{x}{2} \quad (1)$$

$$\beta + \phi + \theta = 180^\circ \quad l = 2x \quad \theta + 90^\circ = \phi$$

$$\beta + 2\phi - 90^\circ = 180^\circ \quad \cos \theta = \sin \phi \quad (2)$$

$$\cos (\beta + 2\phi) = \cos 270^\circ = 0$$

$$\tan \beta = \frac{1}{\tan 2\phi} \quad (3)$$

Substituting (3) and (2) into (1) results in

$$\frac{l \sin \phi}{\tan \phi} = \frac{x}{2}$$

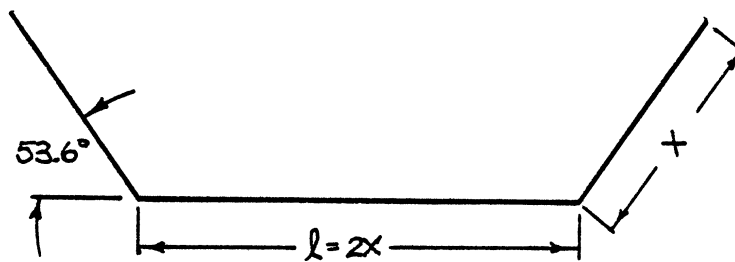
$$l \frac{(\cos^2 \phi - \sin^2 \phi)}{2 \cos \phi} = \frac{x}{2}$$

$$\cos^2 \phi - 1/4 \cos \phi - 1/2 = 0$$

using the quadratic equation the results

$$\phi = 126.38^{\circ}$$

Note: The other solution does not apply.



SIDE VIEW OF SUB-BLANKET

$$\frac{\text{Power}}{\text{Area}} \text{ from sun} \equiv \frac{1.35 \text{ kW}}{\text{m}^2}$$

$$(2 LX) (\cos (53.62^{\circ})) (1.35 \text{ kW/m}^2)$$

The above equation is the energy diverted from both reflectors to the cell bed.

The "new" power/area incident on the solar cells is as follows.

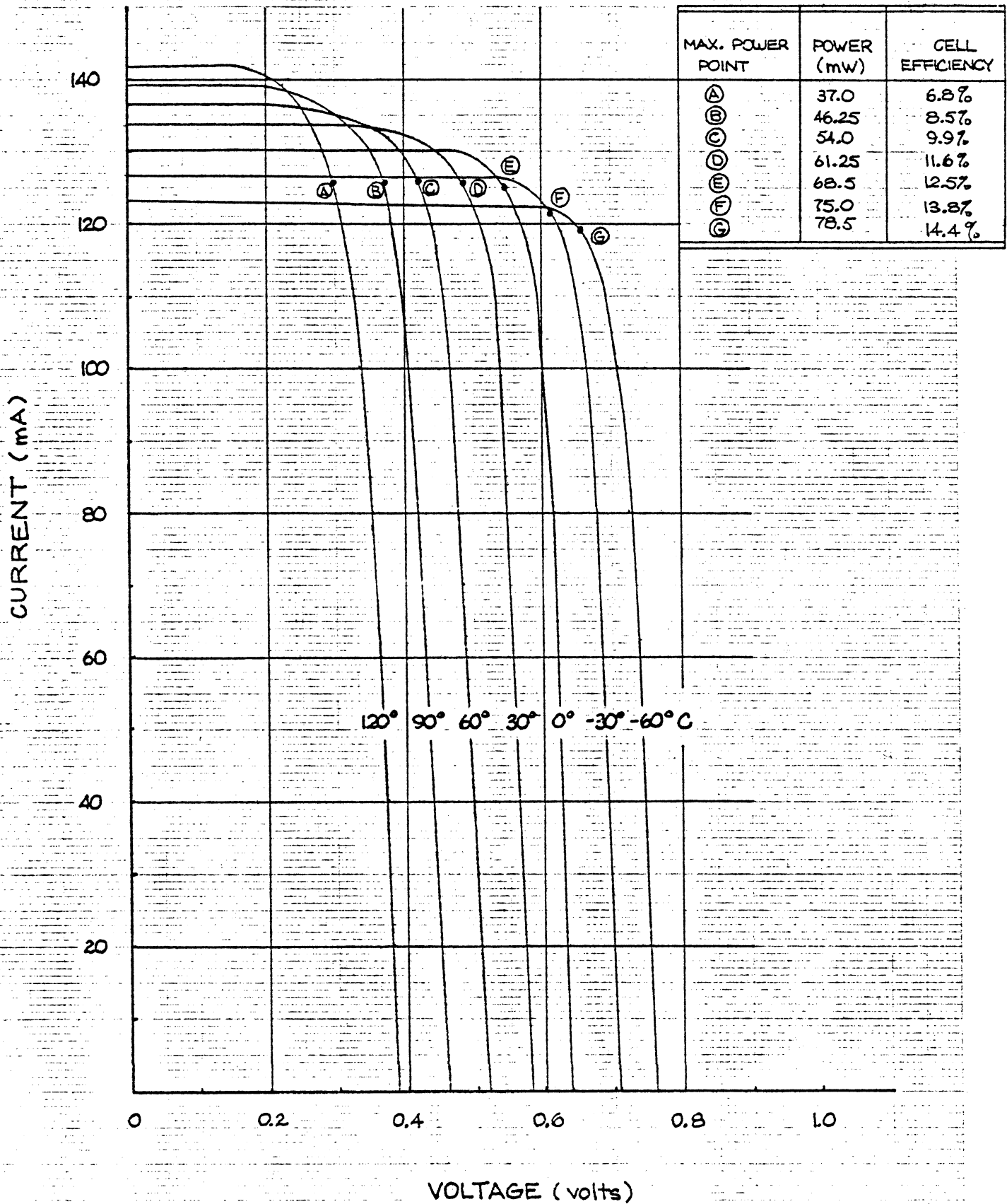
$$\cos (53.62^{\circ}) (1.35 \text{ kW/m}^2) + 1.35 \text{ kW/m}^2$$

$$(.8 + 1.35) \text{ kW/m}^2$$

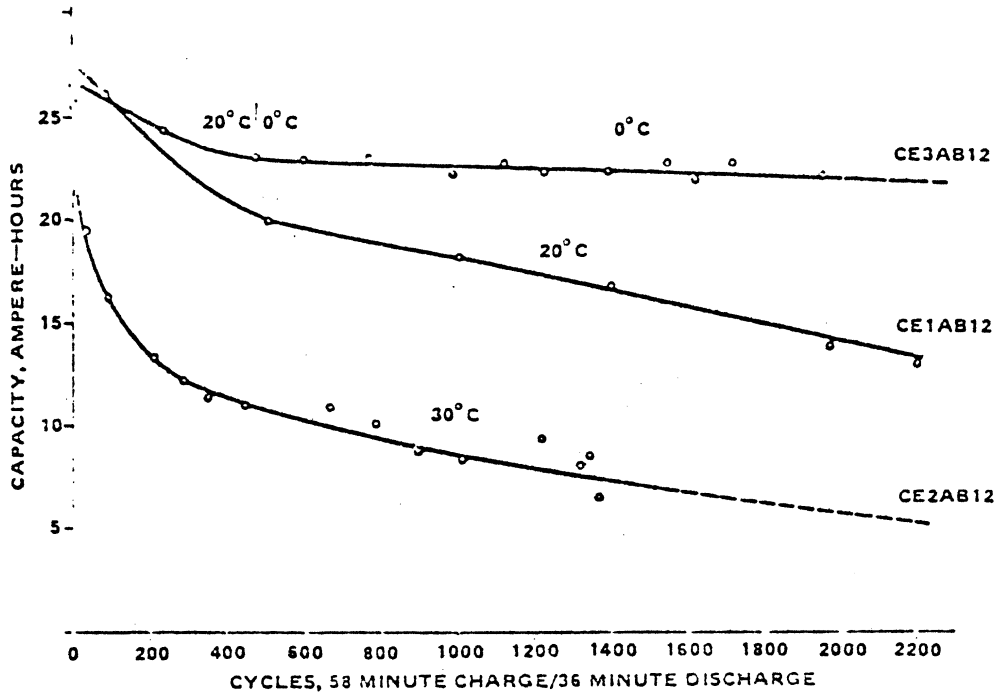
$$2.15 \text{ kW/m}^2$$

A.3 VOLTAGE - CURRENT CHARACTERISTICS vs. CELL TEMPERATURE (°C)  
 FOR 2 x 2 cm 2 ohm-cm N/P SOLAR CELL

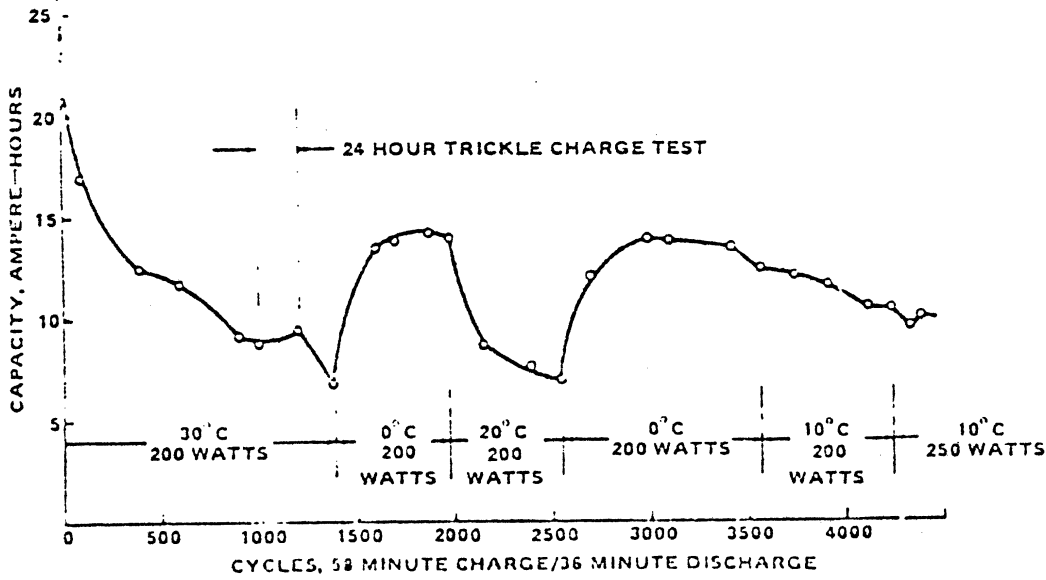
SILICON THICKNESS : .014 inch ACTIVE AREA : 3.9 cm<sup>2</sup>  
 SUNLIGHT SIMULATOR : 140 mW/cm<sup>2</sup>



A.4 ATM BATTERY TEST DATA (Reference 10)



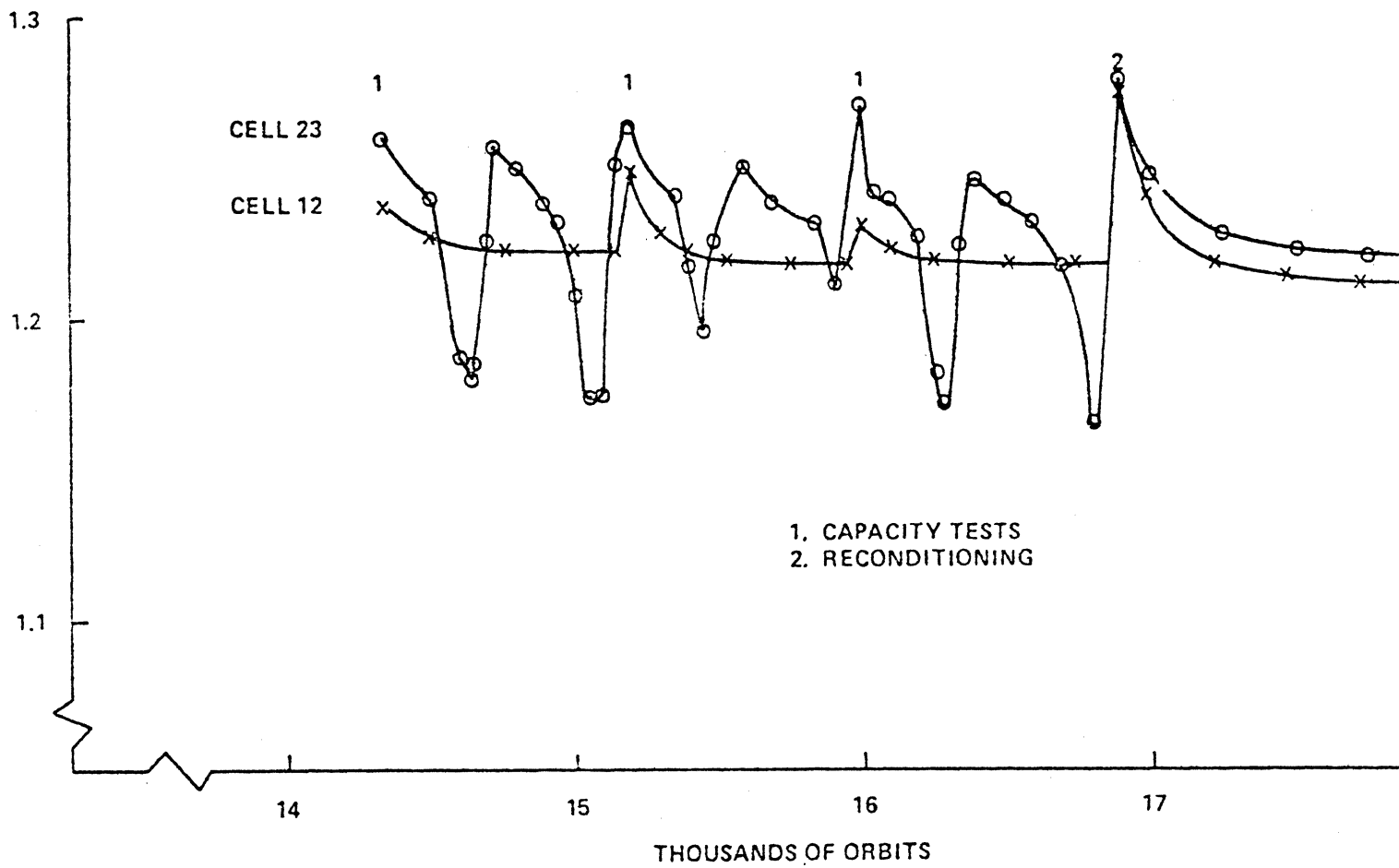
CAPACITY DEGRADES WITH INCREASED TEMPERATURES



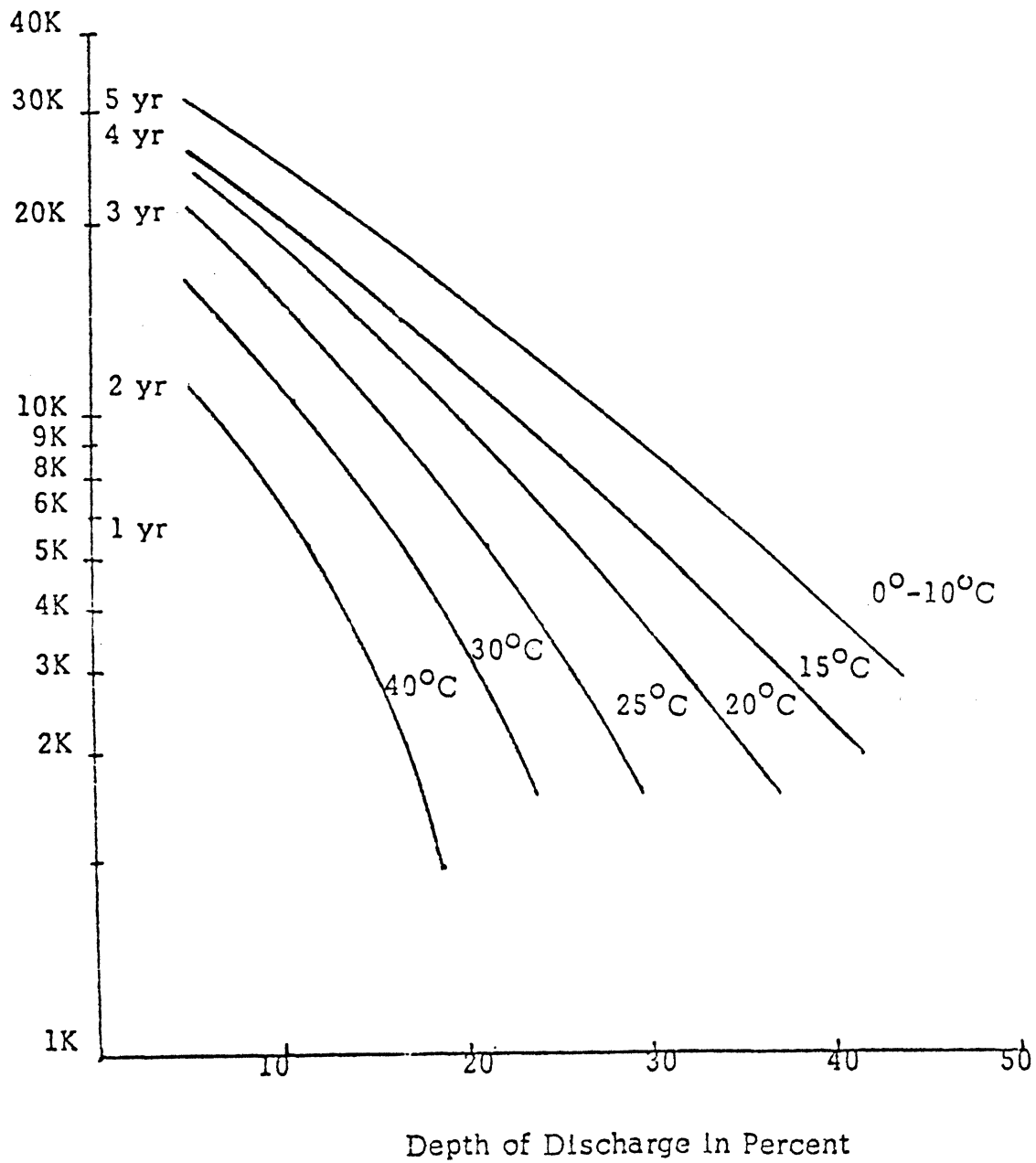
PARTIAL CAPACITY RECOVERY WITH BATTERY RECONDITIONING



A.4 (Continued) (Reference 7)



### A.5 Ni-Cd BATTERY LIFE CHARACTERISTICS (Reference 10)



## APPENDIX B

### B.1 TEMPERATURE ANALYSIS (References 1, 3)

#### a. Definitions of Terms

T	Temperature (Absolute)
$A_s$	Area of Radiators Facing Sun
$A_s^{(R)}$	Area of Body Facing Sun
$A_e^{(B)}$	Area of Radiators Facing Earth
$A_s^{(R)}$	Area of Body Facing Earth
$A^{(R)}$	Total Area of Radiators
$G_s$	Solar Constant (for Earth Orbit $130 \text{ w/ft}^2$ , $442 \text{ BTU/hr ft}^2$ )
E	Earth Emission ( $22 \text{ w/ft}^2$ , $75 \text{ BTU/hr ft}^2$ )
R	Earth Reflection (assuming albedo .80; $60 \text{ w/ft}^2$ , $200 \text{ BTU/hr ft}^2$ )
$\sigma$	Stefan-Boltzman Constant ( $5.07 \times 10^{-10} \text{ w/ft}^2 \text{ } ^\circ\text{R}^4$ , $0.1714 \times 10^{-8} \text{ BTU/hr ft}^2 \text{ } ^\circ\text{R}^4$ )
$q_i$	Internal Heat
$q_s$	Absorbed Solar Emission ( $[A_s a_B + A_s^{(R)} a_R] G_s$ )
$q_e$	Absorbed Earth Emission ( $[A_e^{(B)} a_B + A_e^{(R)} a_R] E$ )
$q_r$	Absorbed Earth Reflection ( $[A_e^{(B)} a_B + A_e^{(R)} a_R] R$ )
$q_E$	Heat Emitted ( $A_e T^4$ )
$a_B$	Average Absorptivity of Body (S-13-G White Paint, .2)
$a_R$	Average Absorptivity of Radiator (.11)
e	Average Emissivity (.76)

#### b. Equations

Assuming that the heat absorbed from the solar panels and the heat radiated and conducted from the various parts of the satellite is zero then the heat equation is:

$$q_E = q_s + q_e + q_r + q_i$$

which becomes

$$A\sigma eT^4 = G_s (A_{s(B)} a_B + A_{s(R)} a_R) + E(A_{e(B)} a_B + A_{e(R)} a_R) \\ + R (A_{e(B)} a_B + A_{e(R)} a_R) + q_i$$

Solve for T

$$T = \left[ \frac{G_s}{A\sigma e} (A_{s(B)} a_B + A_{s(R)} a_R) + \frac{E}{A\sigma e} (A_{e(B)} a_B + A_{e(R)} a_R) + \right. \\ \left. + \frac{R}{A\sigma e} (A_{e(B)} a_B + A_{e(R)} a_R) + \frac{q_i}{A\sigma e} \right]^{\frac{1}{4}} \quad (B.1)$$

Solve for  $q_i$

$$q_i = A\sigma eT^4 - G_s (A_{s(B)} a_B + A_{s(R)} a_R) - E(A_{e(B)} a_B + A_{e(R)} a_R) \\ - R (A_{e(B)} a_B + A_{e(R)} a_R) \quad (B.2)$$

### c. Results

Two cases of satellite orientation were analyzed; the worst case and the normal case. For the worst case it is assumed that the Sun shines on 3 radiators, 1/4 of the body and one end of the body; and the Earth shines on 3 radiators, 1/2 of the body and one end of the body. Therefore

$$A_{s(R)} = 900 \text{ ft}^2 \\ A_{e(R)} = 900 \text{ ft}^2 \\ A_{s(B)} = 200 \text{ ft}^2 + 80 \text{ ft}^2 = 280 \text{ ft}^2 \\ A_{e(B)} = 400 \text{ ft}^2 + 80 \text{ ft}^2 = 480 \text{ ft}^2$$

for the worst case.

The normal case assumes 2 radiators, 1/2 the body and one end are oriented toward the Sun and the same amount of area toward the Earth. Therefore

$$\begin{aligned} A_s &= 600 \text{ ft}^2 \\ A_e(R) &= 600 \text{ ft}^2 \\ A_s(B) &= 480 \text{ ft}^2 \\ A_e(B) &= 480 \text{ ft}^2 \end{aligned}$$

for the normal case.

Equation B. 1 for the worst case becomes

$$T = [3.91 \times 10^{10} \text{ } ^\circ\text{R}^4 + 1.08 \times 10^6 \frac{\text{ } ^\circ\text{R}^4}{\text{w}} q_i]^{1/4} \quad (\text{B. 3})$$

The results are listed in Table B. 1 for various heat loads ( $q_i$ ).

Equation B. 2 for the worst case becomes

$$q_i = 9.25 \times 10^{-7} \text{ w/} ^\circ\text{R}^4 T^4 - 3.61 \times 10^4 \text{ w.} \quad \text{B. 4}$$

The results are listed in Table B. 2 for various temperatures.

Equation B. 1 for the normal case is

$$T = [3.71 \times 10^{10} \text{ } ^\circ\text{R}^4 + 1.08 \times 10^6 \text{ } ^\circ\text{R}^4/\text{w } q_i]^{1/4} \quad \text{B. 5}$$

and Equation B. 2 is

$$q_i = 9.25 \times 10^{-7} \text{ w/} ^\circ\text{R}^4 T^4 - 3.43 \times 10^4 \text{ w} \quad \text{B. 6}$$

The results are listed in Tables B. 3 and B. 4 respectively.

Table B.1 Worst Case Surface Temperatures for Specified Heat Load

$q_i$ Heat Load (kW)	Temperature	
	$^{\circ}\text{F}$	$^{\circ}\text{C}$
0	-15.38	-26.32
1	-12.34	-24.63
14	22.55	-5.65
25	47.55	8.38
50	92.45	33.58

Table B.2 Worst Case, Heat Load for Specified Surface Temperature

Surface Temperature		Heat Load kW
$^{\circ}\text{F}$	$^{\circ}\text{C}$	
32.0	0	18.0
57.2	14	30.0
104.0	40	57.4

Table B.3 Normal Case, Surface Temperatures for Specified Heat Load

Heat Load kW	Surface Temperature	
	$^{\circ}\text{F}$	$^{\circ}\text{C}$
0	-21.0	-29.5
1	-17.9	-27.7
14	18.2	-7.7
25	43.3	6.3
50	89.6	32.0

Table B.4 Normal Case, Heat Load for Specified Surface Temperature

Surface Temperature		Heat Load kW
$^{\circ}\text{F}$	$^{\circ}\text{C}$	
32.0	0.0	19.8
57.2	14.0	31.8
104.0	40.0	59.2

## B. 2 COMPONENT OPERATING TEMPERATURES (Reference 5)

Attitude Control	0° F to 135° F	-18° C to 57° C
Communications	-4° to 167°	-20° to 75°
Batteries	41° to 59°	5° to 15°
Solar Panels	-290° to 392°	-179° to 200°
Radiator Surface	-202° to 248°	-130° to 120°
Bearings	-75° to 150°	-59° to 66°
Freon	-211° to ...	-135° to ...

### B. 2. 1 System Specifications

#### a. Radiator (Reference 6)

Thickness	1 in (2.5 cm)
Composition	5056-H39 Aluminum Honeycomb .001 in (.0025 cm) Hexagon Diameter .19 in (.475 cm)
Pipes (29 per Panel)	1 in (2.5 cm) and .19 in (.475 cm)
Face Sheet	2024-T81 Aluminum .01 in (.025 cm)
Overall Density	3 lb/ft <sup>3</sup> (50 kg/m <sup>3</sup> )
Solar Absorptance	a = .11
Hemispherical Emittance	e = .76
Weight	6.6 lb/section (3 kg/section)

#### b. Pumps (Reference 4)

Weight with Accumulator	63 lb (28.2 kg) each
Flow Rate	2500-300 lb/hr (1136-1364 kg/hr) each
Power Consumption	.4 kW each

#### c. Paint

Solar Absorptance	S-13-G White a = .2
Hemispherical Emittance	e = .9

## APPENDIX C

### C.1 EQUATIONS

#### Rocket Equation

$$\Delta V = g_o I_{sp} \ln R$$

$$R = \frac{W_i}{W_i - W_p}$$

#### Maximum Acceleration

$$n_{\max} = \frac{F_{\max}}{(m g_o)_{\min}}$$

#### Burning Time

$$t_B = \frac{I_{sp} W_p}{F}$$

$\Delta V$  = change in velocity

$g_o$  = acceleration of gravity

$I_{sp}$  = specific impulse of propulsion system

$W_i$  = initial weight of engine prior to maneuver

$W_p$  = weight of propellant used in maneuver

$n_{\max}$  = maximum acceleration

$F_{\max}$  = maximum thrust of system

$(m g_o)_{\min}$  = minimum weight possible of system

$t_B$  = burning time of maneuver



### Weight of Propulsion Unit Components

<u>Component</u>	<u>Unit Weight - lbs (Kgf)</u>	<u>Quantity</u>	<u>Total Weight - lbs (Kgf)</u>
Pressure Tank	54.8 (24.8)	1	54.8 (24.8)
Propellant Tank	93.6 (42.4)	1	93.6 (42.4)
Helium Filters	1.0 (0.5)	2	2.0 (0.9)
Propellant Filters	1.8 (0.8)	3	5.5 (2.5)
Latching Valve (Pressurant-Isolation Valves)	0.9 (0.4)	2	1.8 (0.8)
Latching Valve (Propellant-Isolation Valves)	3.7 (1.7)	2	7.4 (3.4)
Rocket Engine Modules	15.2 (6.9)	12	182.4 (82.5)
Pressure Regulator	5.0 (2.3)	2	10.0 (5.6)
Check Valve	1.0 (0.5)	1	1.0 (0.5)
Propellant Management Device	15.0 (6.8)	1	15.0 (6.8)
Fill Valve (Pressurant)	0.3 (0.1)	1	0.3 (0.1)
Fill Valve (Propellant)	0.3 (0.1)	1	0.3 (0.1)
Dump Valve	10.0 (5.6)	1	<u>10.0 (5.6)</u>
Total unit weight (empty)			382.1 (172.9)
<u>Weight of Propellant and Pressurant</u>			1500 (678.7)
Total unit weight (fully fueled)			1882.1 (851.6)
Total weight of 4-unit system			7528.1 (3406.4)

## APPENDIX D

Earth's gravitational parameter

$$\mu = 1.40766 \times 10^{16} \text{ ft}^3/\text{sec}^2 \quad (3.9860 \times 10^{14} \text{ m}^3/\text{sec}^2)$$

Earth's radius

$$R_e = 20.9029 \times 10^6 \text{ ft} \quad (6371.1 \times 10^3 \text{ m})$$

Drag weight parameter,  $C_D A/w$

$C_D$  = drag coefficient  
 $A$  = projected area  
 $w$  = weight

Phasing maneuver

$$V_{lc_L} = \sqrt{\mu/R_e + h_2} \qquad V_{lc_H} = \sqrt{\mu/R_e + h_2 + \delta}$$

$$T_t = \frac{\pi}{\sqrt{\mu}} \left( \frac{2 R_e + h_1 + h_2 + \delta}{2} \right)^{3/2}$$

Terminal phase maneuver

$$\dot{x}_d(0) = \frac{\delta[-14(1 - \cos wT) - (1 - 6wT) \sin wT]}{T[3 \sin wT - 8/wT(1 - \cos wT)]}$$

$$\dot{y}_d(0) = \frac{\delta[(3 wT \cos wT - 4 \sin wT) + 2(1 - \cos wT)]}{T[3 \sin wT - 8/wT(1 - \cos wT)]}$$

angular rate of OASIS

$$w = \frac{V_{lc_H}}{(R_e + h_2 + \delta)} \quad \text{rad/sec}$$

$T$  = time allowed for terminal phase maneuver

APPENDIX E

Equipment List

Design Source	Component	# of Units	Weight lb (Kg)	Power (watts)	Volume ft <sup>3</sup> (m <sup>3</sup> )
ATM	Momentum Wheel	6	2840(1291)	1.21 (900)	162 (4.6)
ATM	Sun Sensor	2	6 (2.73)	- (2)	12 (.36)
ATM	Rate Gyros	9	104 (47.3)	.24 (180)	3 (.09)
ATM	Digital Computer	2	200 (90.9)	.22 (165)	5.1 (.15)
ATM	Interface Unit	1	105 (97.7)	.02 (105)	2.6 (.01)
ATM	Memory Load Unit	1	20 (9.1)	.04 (33)	.5 (.02)
	Total		3375 (1534)	1.72 (1285)	173.2 (5.2)

OASIS

$$I_x = 2.5 \times 10^6 \text{ slug ft}^2$$

$$I_y = 1.63 \times 10^5 \text{ slug ft}^2$$

$$I_z = 7.67 \times 10^5 \text{ slug ft}^2$$

## Gravity Gradient

The gravity gradient torque can be expressed as (Reference 6)

$$\vec{T}_g = 3\Omega^2 [r] [I] \vec{r} \quad (1)$$

where  $\Omega$  is the orbital rate,  $\vec{r}$  is a unit vector parallel to the radius vector from the earth center to the vehicle center of mass,  $[I]$  is the moment of inertias in the vehicle axes, and  $[r]$  is defined as

$$[r] = \begin{bmatrix} -r_z & r_y \\ r_z & -r_x \\ -r_y & r_x & 0 \end{bmatrix}$$

When expressing the torque in the principal axes system, equation (1) becomes

$$T_g = 3\Omega^2 [\vec{r}_{p_r}] [\epsilon]^T [I_p] [\epsilon] \vec{r}_{p_r} \quad (2)$$

where  $[I_p]$  is the principal of inertias matrix, and  $[\epsilon]$  is the transformation matrix from the principal reference system to the principal axes system. The principal reference system is a rotation of the principal axes through the  $[\epsilon]$  angles.

Equation (2) can also be written in the form

$$\vec{T}_g = \vec{T}_{gn} + \vec{T}_{gd}$$

which separates the gravity gradient torque into two components.  $\vec{T}_{gn}$  is a nominal part which is not a function of the  $\epsilon$  angles and  $\vec{T}_{gd}$  is the controllable part which depends on the  $[\epsilon]$  angles. The  $\vec{T}_{gd}$  component will be the part used for desaturation.

Through the integration of the matrix elements of  $\vec{T}_{gd}$ , the angular momentum desaturated,  $[H_d]$ , is obtained as a function of the angles  $[\epsilon]$ . By inverting the resulting matrix equations the angles  $[\epsilon]$  can be obtained as a function of the desaturated angular momentum of the momentum sheels  $[H_d]$ . Therefore once having sampled the accumulated angular momentum of the wheels  $[H_{acc}]$  and setting

$$[H_d = -[H_{acc}]]$$

the necessary maneuvering angles  $\epsilon$  can be computed. Commanding the vehicle to make the maneuvers using the momentum wheels, they will return to the unsaturated position.

For a detailed derivation of the equations involved, Reference 6 should be consulted.

## APPENDIX F STRUCTURES

The symbols used in the following calculations are defined below:

A	= cross sectional area
d	= distance from satellite center of gravity to bottom of the satellite
E <sup>c. g.</sup>	= modulus of elasticity
G	= maximum payload accelerations in g's
I	= area moment of inertia
ℓ	= member length
M	= applied bending moment
r	= average radius
r <sub>a</sub>	= inner radius
r <sub>i</sub>	= outer radius
S <sup>o</sup>	= safety factor
σ	= applied stress
σ <sub>a</sub>	= bending stress
σ <sub>b</sub>	= applied compressive normal stress
σ <sub>c</sub>	= critical buckling stress
σ <sub>cr</sub>	= compressive yield stress
t <sup>y</sup>	= wall thickness
μ	= Poisson's ratio
W	= satellite weight

### 1. Support Tube

The design criterion for the support tube is to prevent it's failure in the buckling mode. For purposes of analysis it is assumed to be a cylindrical shell carrying an axial load. From the text, Theory of Elastic Stability, by Timoshenko and Gere, the correct formula for the buckling of such a member depends upon the relative magnitudes of the terms

$$\frac{\pi r_a^2}{\ell} \quad \frac{2 r_a}{t} d(1 - \mu^2)$$

If the first is greater than the second, the Euler strip formula may be used; if vice versa, an imperical formula developed by L. H. Donnell may be used.

$$r_a = 59.906 \text{ in (1.52 m)} \quad t = 0.1875 \text{ in (4.8 mm)}$$

$$\ell^a = 300 \text{ in (7.62 m)} \quad \mu = 0.33$$

$$\frac{\pi r_a^2}{l} = 37.58 \quad \frac{2r}{t} a^3 (1 - \mu^2) = 1708.23$$

Thus Donnell's formula is used;

$$\sigma_{cr} = E \frac{.6 \left(\frac{t}{r}\right) - 10^{-7} \frac{r}{t} a}{1 + .004 \frac{E}{\sigma_y}}$$

$$E = 10^7 \text{ psi}$$

$$\sigma_y = 70,000 \text{ psi}$$

$$t = 0.1875 \text{ in}$$

$$r_a = 59.906$$

$$\sigma_{cr} = (10^7) \frac{(.6)(.1875) - (10^{-7}) \left(\frac{59.906}{.1875}\right)}{1 + .004 \left(\frac{10^7}{70,000}\right)}$$

$$\sigma_{cr} = 11,747 \text{ psi} \quad (80.99 \times 10^6 \text{ Pascals})$$

The total applied compressive stress is due to the axial acceleration, and a bending contribution due to the lateral acceleration.

$$\sigma_a = \sigma_c + \sigma_b$$

$$\sigma_a = \frac{WG}{A} + \frac{Mr_a}{I}$$

$$W = 37,844 \text{ lbs (17,166 kg)}$$

$$d_{c.g.} = 255.48 \text{ in (6.49 m)}$$

$$G = 45$$

$$r_o = 60 \text{ in (1.52 m)} \quad r_i = 59.8125 \text{ in (1.51 m)}$$

$$A = \pi(r_o^2 - r_i^2) = \pi(60^2 - 59.8125^2)$$

$$\underline{A = 70.58 \text{ in}^2 \text{ (.0455 m}^2\text{)}}$$

$$M = W d_{c.g.} = (37,844)(255.48)$$

$$\underline{M = 9,668,385 \text{ in-lb}}$$

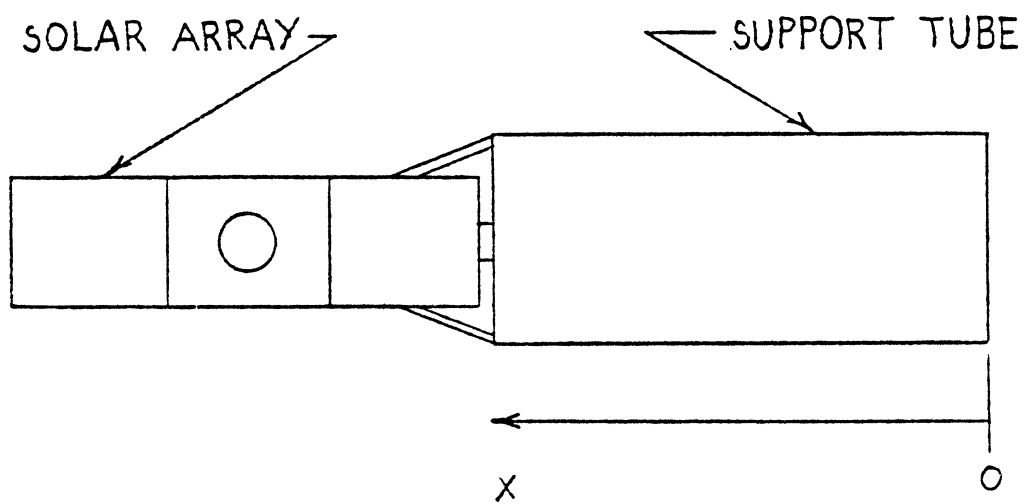


FIGURE 8.13 REFERENCE FOR C.G.



$$I = \frac{\pi}{4} [r_o^4 - r_i^4] = \frac{\pi}{4} [60^4 - 59.8125^4]$$

$$I = \underline{126,639 \text{ in}^4} \quad (.0527 \text{ m}^4)$$

$$\sigma_a = \frac{(37,844)(4.5)}{(70.58)} + \frac{(9,668,385)(59.906)}{(126,639)}$$

$$\sigma_a = 6986 \text{ psi} \quad (48.17 \times 10^6 \text{ Pascals})$$

The safety factor for the support tube is defined as:  $s = \frac{\sigma_{cr}}{\sigma_a} = \frac{11,747}{6,986}$

$$S = 1.68$$

## 2. Center of Gravity

The center of gravity of the satellite, in the y and z directions, is in the center of the support tube. In the axial, x-direction, the center of gravity is found by using the end of the support tube as a reference.

# OASIS COMPONENT C.G. LOCATIONS

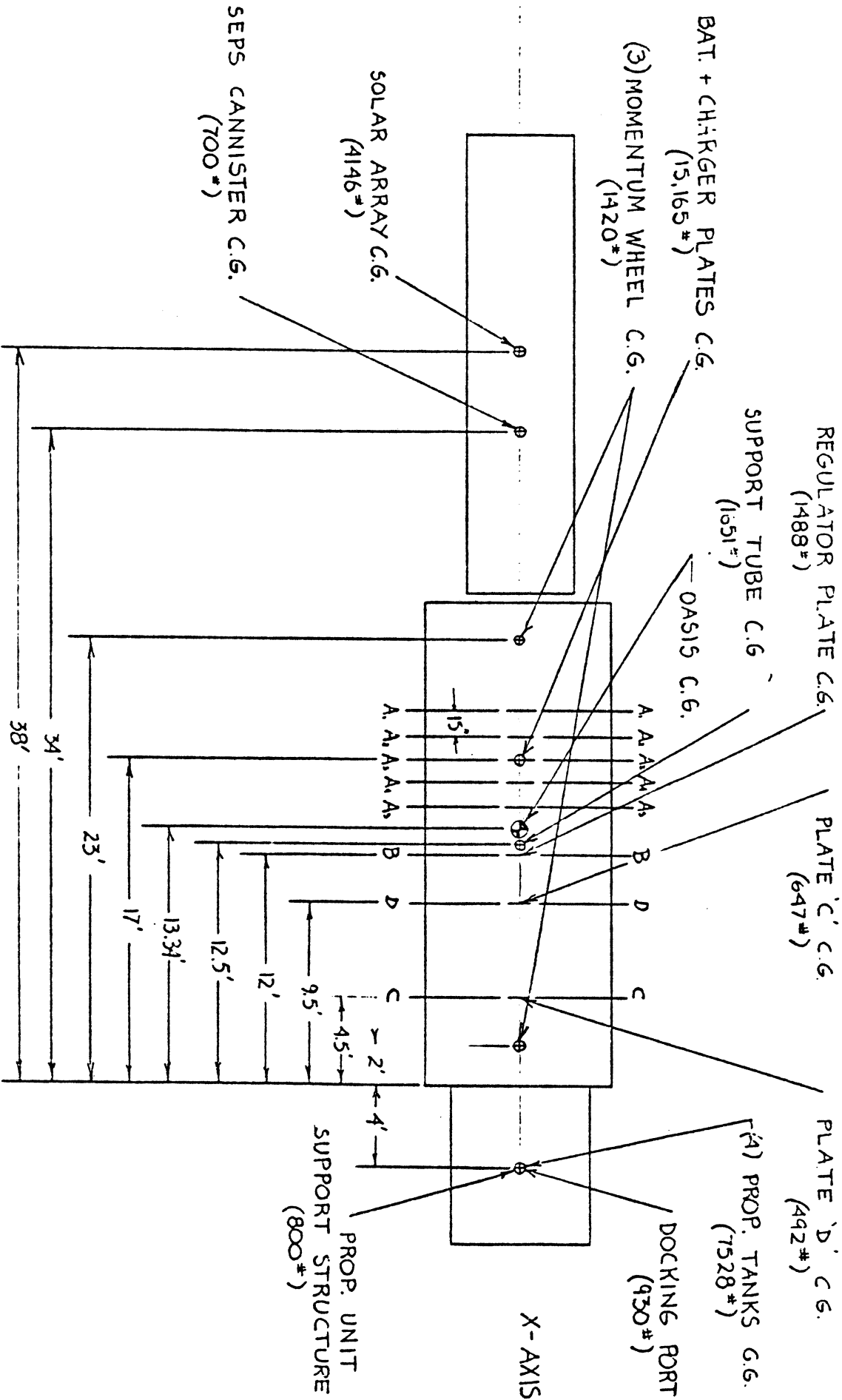


FIGURE 8.14 OASIS COMPONENT C.G. LOCATIONS

$X_{c.g.}$  = center of gravity of the satellite as measured from the end of the support tube

$W_i$  = weight of individual satellite component (lbs)

$l_i$  = distance of component c. g. from reference point (ft)

$$X_{c.g.} = \frac{\sum_{i=1}^n W_i l_i}{\sum_{i=1}^n W_i}$$

$$X_{c.g.} = \frac{(38')(4146\#) + (34')(700\#) + (23')(1420\#) + (12.5')(1651\#) + (2.0')(1420\#) - (4')(800\#) - (4')(930\#) - (4')(7528\#) + (17')(15,165\#) + (12')(1641\#) + (9.5')(647\#) + (4.5')(492\#) + (100\#)(24.5')}{4146\# + 700\# + 1420\# + 1651\# + 1420\# + 800\# + 930\# + 7528\# + 15,165\# + 100\# + 1641\# + 647\# + 492\#}$$

$$X_{c.g.} = 13.34 \text{ ft (4.07 m)}$$

Knowing that the satellite will be placed 7 inches from the rear of the Orbiter bay, and that the propulsion unit is 8 feet long, we can determine the position of the satellite center of gravity from the front of the cargo bay,  $X'_{c.g.}$ .

$$X'_{c.g.} = 60 \text{ ft} - [13.34 \text{ ft} + 8 \text{ ft} + .58 \text{ ft}]$$

$$X'_{c.g.} = 380.08 \text{ ft} \quad (11.61 \text{ m}) \quad \text{See Figure 8.14.}$$

From Figure 8.1 it can be seen that OASIS' center of gravity lies well within the payload longitudinal c. g. constraints of the Orbiter. With a payload of 37,844 lbs (17,166 kg) the envelope is 33 ft - 44.5 ft (10.06 m - 13.56 m).

### 3. Internal Plate Analysis

#### A. Determining Regulator Platform Thickness

The loading on the platform which will hold the regulators is assumed to be distributed along the outer edge of the plate. The loading will be between 43 inches and 60 inches radius. This is the approximate area covered by the 24 regulators.

Using the total load of these regulators distributed over the plate area described above, what thickness will give a safety factor of 1.4?

$$\text{Safety Factor (SF)} = \frac{\text{Critical Stress}}{\text{Applied Stress}} = \frac{\sigma_{cr}}{\sigma_a}$$

$$\sigma_{cr} = 70000 \text{ psi for T6 Aluminum } (4.83 \times 10^8 \text{ N/m}^2)$$

$$\text{Loading on plate} = \frac{\text{Total Weight}}{\text{Area}}$$

$$\text{Total Weight} = 24 \text{ reg.} \times \frac{62 \text{ lbs}}{\text{regulator}} = 1488 \text{ lbs } (6622 \text{ N})$$

$$\text{Area} = \pi(60 \text{ in})^2 - \pi(43 \text{ in})^2 = 5500 \text{ in}^2 \text{ } (3.55 \text{ m}^2)$$

$$\text{Loading} = \frac{1488 \text{ lbs}}{5500 \text{ in}^2} = .27 \text{ psi} \times 4.5 \text{ (launch acceleration)}$$

$$\text{Loading} = 1.22 \text{ psi } (8415 \text{ N/m}^2)$$

Using the formulae in Stanek's book (see references) along with the loading value and area, the maximum applied stress is:

$$\sigma_a = \frac{3263 \text{ lbs}}{h^2} \quad \text{where } h = \text{plate thickness}$$

$$\text{S. F.} = 1.4 = \frac{70000 \text{ lbs/in}^2}{3263 \text{ lbs/h}^2}$$

Solving gives:

$$h_{\min} = 0.26 \text{ inches } (.66 \text{ cm})$$

This value is slightly non-conservative. Therefore, a platform thickness of 0.30 inches (.76 cm) will be used.

In addition, this platform can be used elsewhere throughout the structure to hold communications equipment, digital computers, etc., as shown in Figures 8.5C, 8.5D.

This equipment will generate lower applied stresses, thereby allowing use of this plate thickness while meeting the safety factor.

## B. Determining Battery/Charger Platform Thickness

The loading on the platform, which will hold the batteries and chargers, is assumed to be distributed along the outer edge of the plate. The loading will be between 51 inches and 60 inches radius. This is an approximate area covered by the four batteries and four chargers on each plate.

Using the total load of the batteries and chargers distributed over the plate area, what thickness will give a safety factor of 1.4?

$$\text{Loading on plate} = \frac{\text{Total Weight}}{\text{Area}}$$

$$\text{Total Weight} = 4(680 \text{ lbs}) + 4(40 \text{ lbs}) = 2280 \text{ lbs} (12816 \text{ N})$$

$$\text{Area} = \pi(60 \text{ in})^2 - \pi(51 \text{ in})^2 = 3138 \text{ in}^2 (2.02 \text{ m}^2)$$

$$\text{Loading pressure} = \frac{2880 \text{ lbs}}{3138 \text{ in}^2} = .92 \text{ psi} \times 4.5 (\text{launch accel.})$$

$$\text{Pressure} = 4.14 \text{ psi} (28550 \text{ N/m}^2)$$

Using Stanek's formulae (see references), the maximum applied stress is:

$$\sigma_a = \frac{21294 \text{ lbs}}{h^2}$$

For a safety factor = 1.4, the minimum thickness is:

$$1.4 = \frac{70000 \text{ lbs/in}^2}{21294 \text{ lbs/h}^2}$$

Solving gives:

$$h_{\min} = .65 \text{ inches} (1.65 \text{ cm})$$

The battery/charger platforms will be built using a thickness of .65 inches. Five of these plates must be built to provide platforms for the batteries and chargers, as shown in Figure 8.5A.

## 4. Solar Array Support Tube

The solar array is held in place by a 12 foot long, 3 foot wide support tube. How thick must this tube be to maintain a safety factor of 1.4?

The formulae used are the same as previously listed in the support tube section of the appendix.

$$S. F. = \frac{\sigma_{cr}}{\sigma_a}$$

$$\text{where } \sigma_{cr} = E \frac{.6(tr_a) - 10^{-7}(r_a/t)}{1 + .004 E/\sigma_y}$$

$$E = 10^7 \text{ psi}$$

$$\sigma_y = 70000 \text{ psi}$$

$$t = .08 \text{ inches}$$

$$r_a = 18 \text{ inches}$$

$$\text{Substituting gives } \sigma_{cr} = 16827 \text{ psi } (1.16 \times 10^8 \text{ N/m}^2)$$

$$\text{The applied stress is } \sigma_a = \frac{WG}{A} + \frac{Mr_a}{I}$$

$$W = 4872 \text{ lbs}$$

$$G = 4.5$$

$$A = 9.03 \text{ in}^2$$

$$M = 7.02 \times 10^5 \text{ in-lbs}$$

$$I = 1456 \text{ in}^4$$

$$r_a = 18 \text{ inches}$$

$$\text{Substituting gives } \sigma_a = 11106 \text{ psi } (7.66 \times 10^7 \text{ N/m}^2)$$

Using  $\sigma_{cr}$  and  $\sigma_a$ , a safety factor is found.

$$S. F. = \frac{16827 \text{ psi}}{11106 \text{ psi}} = 1.52$$

A thickness of the support tube = .08 inches (.20 cm) will provide the necessary margin of safety.

APPENDIX G

Appendix G. 1

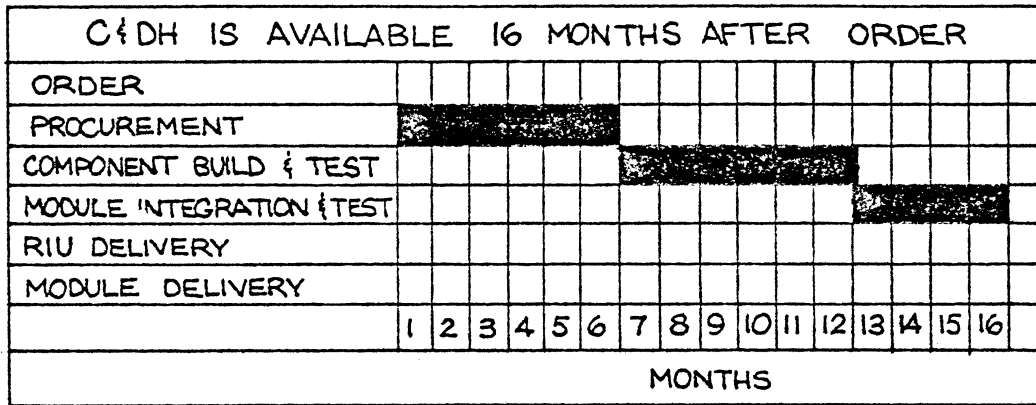


Figure G. 1 C&DH Module Availability

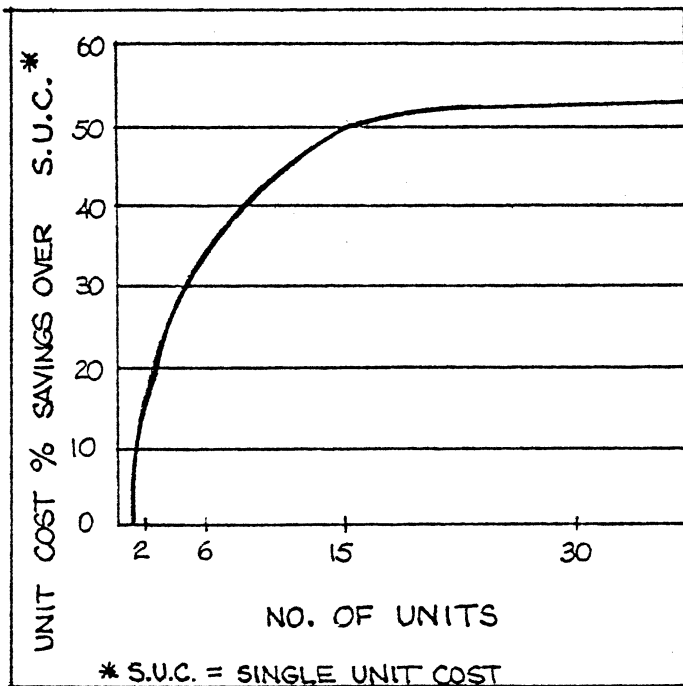


Figure G. 2 Percent Savings Over Single Unit Cost vs Number of Units Manufactured

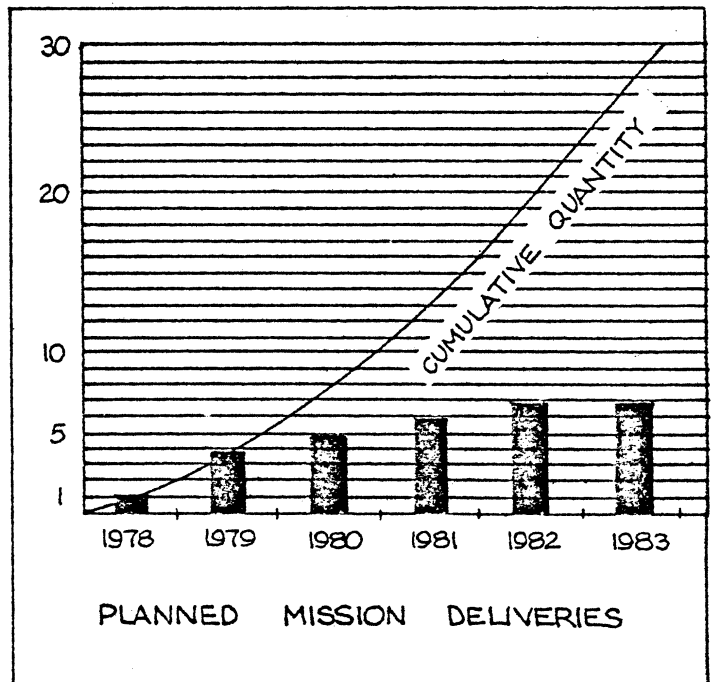


Figure G. 3 Planned Mission Deliveries Per Year from 1978 to 1983.

## G.2 HOUSEKEEPING DATA INPUTS AND COMMANDS

Subsystem	Housekeeping Data Inputs	Commands
Electric Power	Solar Array:	
	- temperature of panels	
	- voltage & current output	
	- position of deployment	-deploy or retract (A)(G)
	- position of 2-axis rotation	-change position (A)(G)
	- sun tracking sensors	-on/off (A)(G)
	Regulators: (24 units)	
	- voltage & current output	-on/off (A)(G)
	Charger/Battery Assemblies: (20 units)	
	- input voltage & current	-charge battery (A)
- battery voltage & current	-on/off battery (A)(G)	
- temperature of battery		
Distributers: (switching network)		
- voltage & current output of power buses (subsystems, payload, orbiter)	-on/off buses (A)(G)	
Thermal	- thermal control unit	on/off (A)(G)
	- temperatures of individual subsystem components	
	- coolant flow rates thru individual parts of the fluid network	
	- state of valves of the fluid network	-open/close (A)(G)
	- RPM of pump	-on/off (A)(G)
		-change RPMS (A)(G)
Propulsion	- pressure of helium tank	
	- pressure of hydrazine tank	
	- propellant flow rate	
	- state of latching valves (between helium and hydrazine tanks) (2 units)	-open/close (A)(G)
	- state of latching valves (between hydrazine tank and rocket motors) (2 units)	-open/close (A)(G)
- state of thruster valves (48 units)	-open/close (A)(G)	



Appendix G. 1

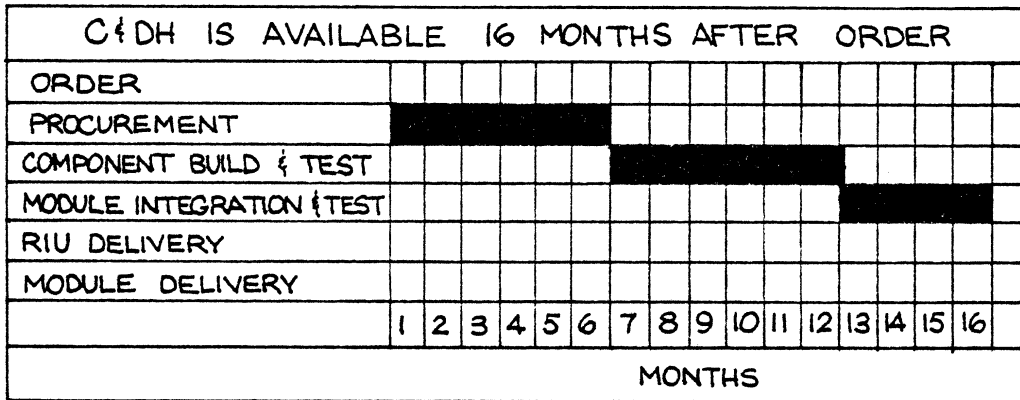


Figure G. 1 C&DH Module Availability

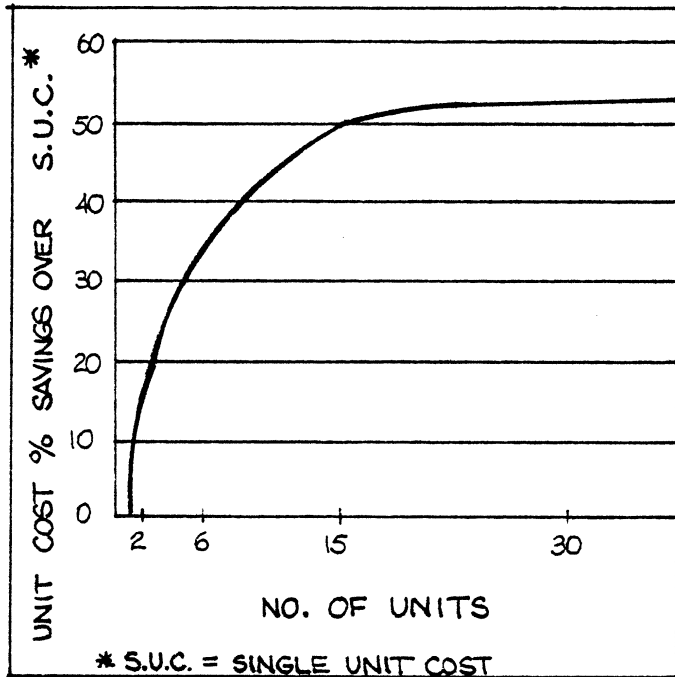


Figure G. 2 Percent Savings Over Single Unit Cost vs Number of Units Manufactured

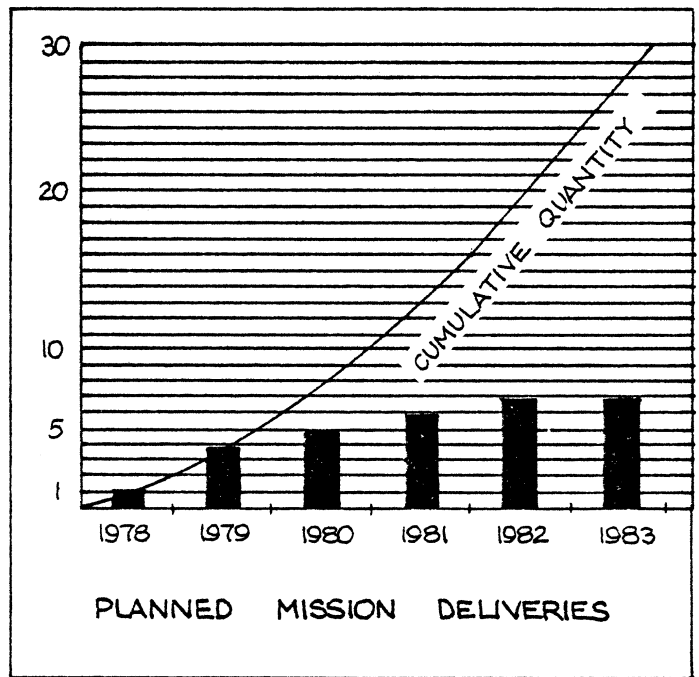


Figure G. 3 Planned Mission Deliveries Per Year from 1978 to 1983.

Attitude	- earth sensors	on/off	(A)
Control	- sun sensors	on/off	(A)
	- state of rate gyros (3 units)	on/off	(A)
	- state of rate integrating gyro	on/off	(A)
	- state of control moment motors (3 units)	on/off change direction of motor spin	(A)(G) (A)(G)
C&DH	- individual component malfunction	C&DH module on/off	(G)
	- spacecraft clock	on/off	(A)
	- individual component status (standby/active)	on/off	(A)(G)

Note: (A) - Automatic command transmitted by subsystem control unit or by C&DH subsystem.

(G) - Commands transmitted from ground control facility via TDRSS.

### G.3 POWER CONSUMPTION OF EACH COMPONENT

Component	Power Consumption
Transponder	2 watts standby 38 watts active
STACC CU	0.9 watts standby 10.9 watts active
STINT	2.5 watts active
NSSC	
CPU	5.5 watts active
Memory	0.35 watts standby 23 watts active
PMP	6 watts active
RIU & EU	1.08 watts (standby + 1% on time)
PCU	16.6 watts at full load

## ACKNOWLEDGMENTS

We would like to thank the following persons who generously gave their time and assistance to help make Project OASIS a success:

Mr. Kenneth Atchison - NASA, Goddard Space Flight Center  
Mr. James C. Beblavi - Martin Marietta  
Mr. Roy E. Currie - NASA, Marshall Space Flight Center  
Mr. Steven Denton - NASA, Marshall Space Flight Center  
Mr. Donald Dutcher - Western Union Space Communications  
Mr. James Foster, Vice President, Public Relations, Western Union Space Communications  
Prof. Donald T. Greenwood - Aerospace Engineering, University of Michigan  
Mr. William Huber - NASA, Marshall Space Flight Center  
Dr. C. W. Kauffman - Aerospace Engineering, University of Michigan  
Mr. Jack Keller - NASA, Lewis Research Center  
Mr. Hans Kennel - NASA, Marshall Space Flight Center  
Mr. Steven S. Myers - Space Systems Marketing Manager, Fairchild Industries Inc.  
Mr. P. D. Nicaise - NASA, Marshall Space Flight Center  
Dr. Farhad Nozari - Assistant Professor, Electrical and Computer Engineering, University of Michigan  
Mr. J. A. Oren - Vought Corporation  
Mr. Peter Preiswerk - Astro Research Corporation  
Mr. Ronald Sammuals - Astro Research Corporation  
Prof. Richard A. Scott - Applied Mechanics and Engineering Science, University of Michigan  
Mr. Francis Shissler - Western Union Space Communications  
Prof. David L. Sikarskie - Aerospace Engineering, University of Michigan  
Mr. William Smith - NASA, Washington, D. C.

We wish to extend deep appreciation to Prof. Harm Buning of the Aerospace Engineering Department at The University of Michigan, for his guidance throughout the project. We would also like to extend our deepest thanks to the Aerospace Engineering Departmental Secretaries especially to Caroline Rehberg for her efforts in the typing of this report and Ann Gee for her assistance throughout the semester.

UNIVERSITY OF MICHIGAN



**3 9015 03524 9757**